SYNTHESIS OF MAGNETITE NANOPARTICLES ON SUBSTRATE FOR WATER PURIFICATION

Thesis submitted in fulfillment for the requirement of the degree of

DOCTOR OF PHILOSOPHY

IN

MATERIALS SCIENCE

BY

SARITA
[Enrollment Number 126903]

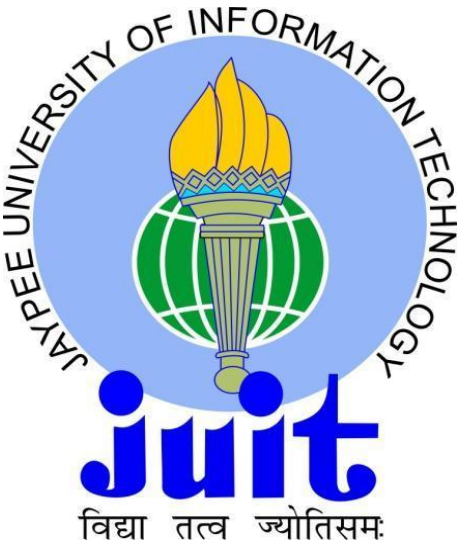

DEPARTMENT OF PHYSICS & MATERIALS SCIENCE

JAYPEE UNIVERSITY OF INFORMATION TECHNOLOGY
WAKNAGHAT, SOLAN-173234, H.P., INDIA

MARCH 2016

JAYPEE UNIVERSITY OF INFORMATION TECHNOLOGY
(Established by H.P. State Legislative vide Act No. 14 of 2002)
P.O. Waknaghat, Teh. Kandaghat, Distt. Solan – 173234 (H.P.) INDIA
Website : www.juit.ac.in
Phone No. (91) 07192-257999 (30 Lines)
Fax: +91-01792-245362

DECLARATION

I hereby declare that the work reported in the Ph.D. thesis entitled **"Synthesis of Magnetite Nanoparticles on Substrate for Water Purification"**, submitted at **Jaypee University of Information Technology, Waknaghat, India**, is an authentic record of my work carried out under the supervision of **Dr. Rajesh Kumar**. I have not submitted this work elsewhere for any other degree or diploma.

Sarita

Sarita
Department of Physics & Materials Science
Jaypee University of Information Technology
Waknaghat, Solan, H.P., India- 173234

Date: March 19, 2016

JAYPEE UNIVERSITY OF INFORMATION TECHNOLOGY
(Established by H.P. State Legislative vide Act No. 14 of 2002)
P.O. Waknaghat, Teh. Kandaghat, Distt. Solan – 173234 (H.P.) INDIA
Website : www.juit.ac.in
Phone No. +91-07192-257999 (30 Lines)
Fax: +91-01792-245362

CERTIFICATE

This is to certify that the work reported in the Ph.D. thesis entitled, **"Synthesis of Magnetite Nanoparticles on Substrate for Water Purification"**, which is being submitted by **Miss Sarita** for the award of degree of **Doctor of Philosophy** in **Materials Science** by the **Jaypee University of Information Technology, Waknaghat, India**, is the record of candidate's own work, carried out by her under my supervision. This work has not been submitted partially or wholly to any other University or Institute for the award of this or any other degree or diploma.

Dr. Rajesh Kumar
Assistant Professor
Department of Physics & Materials Science
Jaypee University of Information Technology
Waknaghat, Solan, H.P., India- 173234

Date: March 19, 2016

AKNOWLEDGEMENTS

O Mother Saraswati, I bow my head before you as a mark of respect, everyday. The knowledge of the Vedas, Vedangas and Vedantas is imbibed in you. You are the beholder of ultimate knowledge. Offering my Ph.D. Thesis, I submit myself before you, uttering the mantra, 'Om Oing Shree Shree Saraswattoyi Namoh Namah'.

I offer my sincerest gratitude to my Ph.D. supervisor ***Dr. Rajesh Kumar*** *for his expert guidance, constructive criticism, support and motivation throughout this work. Whatever I learnt in the field is because of him. His support throughout my research period was unimaginable. I am always thankful to him.*

I acknowledge my gratefulness to ***Prof. P.B. Barman****, Head of Department of Physics & Materials Science for his guidance, help, encouragement and cooperation throughout my research work. My words fail whenever I try to express my gratitude to him. He was always there just behind me as my father. Only because of his inspirations, suggestions and care I won the battle of troy (finishing Ph.D. thesis).*

I also want to thank my former advisor ***Dr. Susheel Kalia*** *for his support, help and motivation. He taught me how to convert a new thought into fruitful result.*

I insistently express my esteemed thanks to ***Prof. (Dr.) Samir Dev Gupta*** *(Director and Academic Head JUIT),* ***Brig. (Retd.) Balbir Singh*** *(Registrar JUIT),* ***Prof. (Dr.) S. C. Saxena*** *(Vice Chancellor JUIT) and* ***Prof. (Dr.) T.S. Lamba*** *(Dean JUIT) for providing opportunity to pursue my research work at Jaypee University of Information Technology, Waknaghat (H.P.).*

I owe my heartiest gratitude to ***Dr. Pankaj Sharma****,* ***Dr. Ragini Raj Singh****,* ***Dr. Vineet Sharma****,* ***Dr. Surajit Kumar Hazra****,* ***Dr. Sanjiv Kumar Tiwari, Dr. Dheeraj Sharma*** *and* ***Prof. Sunil Kumar Khah*** *for providing me assistance, moral support, suggestions and necessary facilities in the department during the course of my research work. I also thank all non-teaching staff for their support and kind help.*

I am also thankful to IIT Bombay, IIT Roorkie and JIIT Noida for providing me the facilities for characterizations.

I also express my gratitude to ***Department of Science and Technology (DST)****, Delhi, (Project number: FTP/PS-40/2011), India for providing research grant.*

Journey of Ph.D. is not always smooth sometimes it is bed of thorns but I am lucky to have seniors Pawan Kumar, Abhishek Kandwal, Jai Verdhan Chauhan, Rajinder Singh, Hitanshu Kumar and Richa Khohkra, who extended their support in all possible ways. I thank them for always being there to guide and encourage whenever the journey got tough. I am also privileged to have friends who always stood beside me. I extend my heartfelt thanks to my friends Ranjana dadhwal, Jyoti gautam and Shalu Sharma. I also thank my colleagues Dikshita Gupta, Swati Gupta, Rajinder Kumar, Bandana Bharti, Jonny Dhiman, Neha Kondal, Rohit Sharma, Prashant Thakur, Asha Sharma, Subhash Chand and Priyam Dhani.

My deepest gratitude goes to my lovely family for their motivation, continuous support, sacrifice and prayers. My father, ***Mr. Santosh Kumar*** *is the person who always supported me for my educational decisions since I was a child. My mother,* ***Mrs. Uma Devi*** *is the one who raised me with her endless love. My brothers* ***Sumit Kango*** *and* ***Sudhir Kumar*** *thanks to you for being supportive and caring. I would also like to thank my grandparents; Mrs. Sandhya Devi, Lt. Nand Lal Soni and Lt. Ramki Devi for their blessings.*

I also want to express my heartfelt gratitude to all those who have contributed directly or indirectly towards obtaining my doctorate degree and apologize if I have missed out anyone.

Sarita

TABLE OF CONTENTS

LIST OF FIGURES

LIST OF TABLES

CHAPTER 1

INTRODUCTION

1.1. IMPORTANCE OF WATER

Water is one of the very basic requirements for life, as we can survive without eating food for weeks but can survive only for few days without drinking water. In scientific terms, bulk or 55-60 % of the human body is made up of water. The water content of tissues of various body organs viz. brain is 74.8 %, lungs 79 %, kidneys 82.7 %, blood 83 %, intestine 74.5 %, heart 79.2 %, liver 74.8 %, muscle 75.6 %, skeleton 22 % and spleen 75.8 % [1]. In simple terms human body water needs replenishment and it can be achieved only by drinking clean water.

The earth's surface is composed of more than 70 % water, out of which about 97 % is salt water which is technically not suitable for human consumption; the other 2 % is glacier ice, which is very far away from the places where people live. The remaining 1 % is the fresh water which we use for drinking, washing, irrigation, industrial purposes and many more, but this 1 % water appearing crystal clear may not always be as clean as it appears [2]. Due to industrialization and urbanization of human society, release of heavy metal ions such as aluminium, arsenic, lead, mercury, chromium etc. pollutes the drinking water. Over the past few decades, the toxicity of water caused by discharge of these contaminants into natural water have become a global issue as these contaminants not only threat the aquatic life but also become a risk factor for human health through the food chain. Among these, arsenic (As) contamination of drinking water is a worldwide challenge as it causes many diseases such as lung, kidney, skin and bladder cancers, still births, heart attacks etc. [3-5].

As there is only 1 % fresh water available for human consumption or drinking, so there is a need to handle the water systems appropriately and to make this water free from contaminants. Water treatment plays an important role in making water free from contaminants. In this study, we have made an attempt to develop a material for water purification by removing hazardous arsenic from drinking water.

1.2. ARSENIC IN THE ENVIRONMENT

1.2.1. Arsenic chemistry

The word arsenic has been originated from the Greek word arsenikon which means potent i.e. king of all poisons [6]. Arsenic is a metalloid, fourth row, group fifteenth element with atomic number 33, atomic weight 74.9, specific gravity 5.73 and vapor pressure 1 mm-Hg at 372 ^{o}C. It is the twentieth most abundant element in earth's crust, fourteenth in seawater and twelfth in the human body [7]. Arsenic rarely exists in its free state as it has strong affinity to form bonds with other elements and species. It occurs naturally in earth's crust, rocks, soil,

water and air in combination with sulphur, oxygen and iron [8, 9]. It occurs in the environment in four oxidation states i.e. −3, 0, +3 and +5 depending upon environmental conditions [10, 11], often as sulfides or metal arsenides or arsenates [12]. In aqueous environment, arsenic exists predominantly as inorganic oxy-anions of trivalent arsenite (As(III)) or pentavalent arsenate (As(V) [13]. Trivalent arsenite (As(III)) species viz. $H_3AsO_3^0$, $H_2AsO_3^-$, $HAsO_3^{2-}$ and AsO_3^{3-} mostly occur in reducing anaerobic environments such as groundwater, while pentavalent arsenate (As(V)) species viz. H_3AsO_4, $H_2AsO_4^-$, $HAsO_4^{2-}$ and AsO_4^{3-} are dominant in oxygen rich aerobic environments such as surface water [14]. Although inorganic arsenic species are present in abundance, the presence of organic arsenic species, i.e. monomethylarsonic acid (MMA) and dimethylarsinic acid (DMA) has also been reported in natural water [15, 16]. The molecular configurations of arsenite and arsenate are shown in Fig. 1.1 (a) and (b), respectively [17]. As(III) has three pyramidal bonds and a lone pair of electron occupying the fourth arm of a tetrahedron as show in Fig. 1.1 (a).

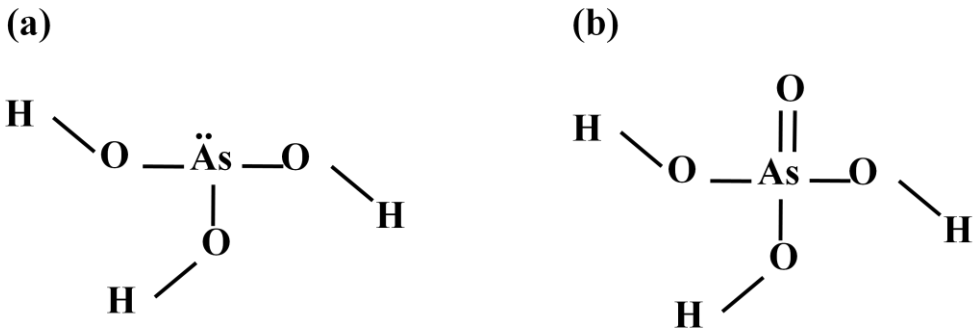

Figure 1.1: Molecular configuration of (a) arsenite and (b) arsenate [17].

On the other hand, As(V) forms regular tetrahedron by forming bond with oxygen ligands resulting in stable AsO_4^{3-} anion similar to PO_4^{3-} in structure (Fig. 1.1 (b)). The occurrence, distribution, mobility and speciation of arsenic in aqueous environment is based on the interplay of certain geochemical factors such as pH conditions, reduction-oxidation reactions, presence of other ionic species, aquatic chemistry, microbial activity and adsorption reactions. Among all these factors, oxidation reduction potential (Eh) and pH conditions are most important ones to control the arsenic speciation. In oxidizing environment, $H_2ASO_4^-$ species dominate at pH less than 6.9, while $HAsO_4^{2-}$ dominates at higher pH. On the other hand under reducing environmental conditions, the uncharged H_3AsO_4 species predominate at

pH less than 9.2 [18]. The effect of pH and oxidation reduction potential on arsenic chemistry is shown in Fig. 1.2 [11].

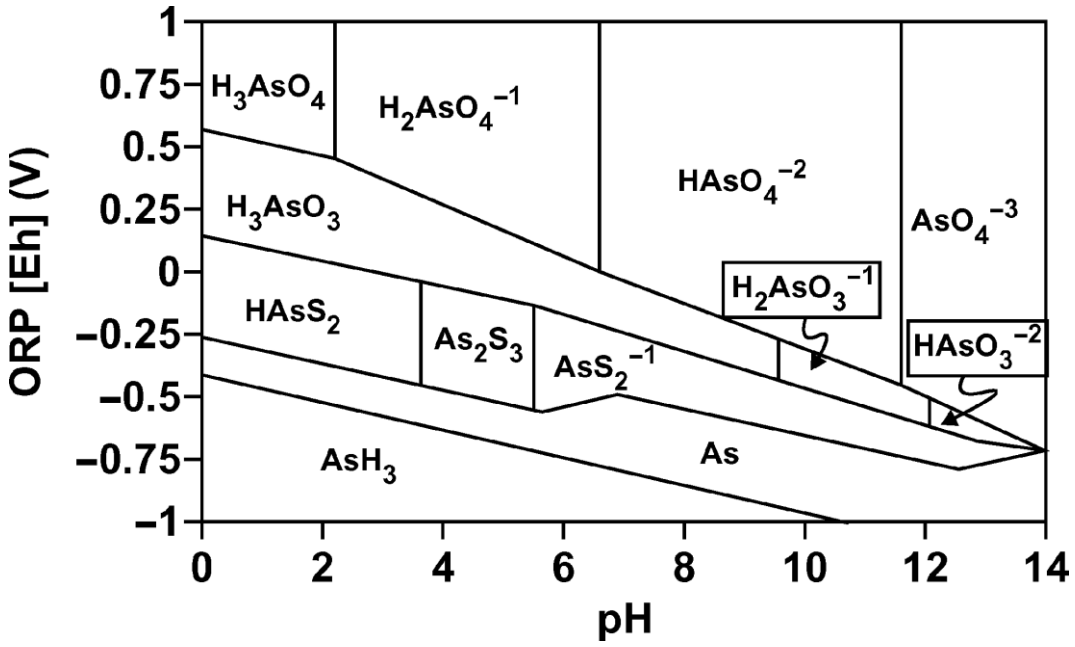

Figure 1.2: Behaviour of arsenic at various oxidation-reduction- (Eh) pH combinations. ORP = oxidation reduction potential; AsO_4 = arsenate compounds; AsO_3 = arsenite compounds; AsS_2 = arsenic disulfide compounds; As = elemental arsenic; and AsH_3 = arsine [11].

It has been reported in the literature that As(III) is pH independent in comparison to As(V) pH dependency [13]. Dissociation reactions and corresponding equilibrium constants of arsenious (H_3AsO_3) and arsenic (H_3AsO_4) acids are summarized in Table 1.1 [19].

Table 1.1: Dissociation constants of arsenate and arsenite [19].

Speciation	**Dissociation reactions**			**pKa**
Arsenate				
As(V)	H_3AsO_4	⇌	$H^+ + H_2AsO_4^-$	2.24
	$H_2AsO_4^-$	⇌	$H^+ + HAsO_4^{2-}$	6.69
	$HAsO_4^{2-}$	⇌	$H^+ + AsO_4^{3-}$	11.5
Arsenite	H_3AsO_3	⇌	$H^+ + H_2AsO_3^-$	9.2
As(III)	$H_2AsO_3^-$	⇌	$H^+ + HAsO_3^{2-}$	12.1
	$HAsO_3^{2-}$	⇌	$H^+ + AsO_3^{3-}$	13.4

1.2.2. Sources and occurrence of arsenic

Arsenic is introduced in the surface water and groundwater as a result of number of natural and anthropogenic sources. It cannot be destroyed; it can only be converted from one form to other form or combined with other elements to be converted into insoluble compounds [20]. Arsenic being a metalloid exhibits some metallic properties and co-exists in nature with other metals like Fe, Cu, Ni, Zn, etc., as sulphide or oxide ores. It exists naturally in more than 200 different mineral forms in the environment, out of which approximately 60 % are arsenates, 20 % sulphides (arsenopyrite, cobaltite, gersdorffite, orpiment, realgar) and sulfosalts (enargite and proustite) and the remaining 20 % includes arsenides, arsenites, oxides, silicates and elemental arsenic (As) [21, 22]. The most common arsenic minerals found in nature are arsenopyrite (FeAsS), realgar (As_4S_4), orpiment (As_2S_3), lollingite ($FeAs_2$), scorodite ($FeAsO_4.2H_2O$) and austenite ($CaZn(AsO_4)OH$). The sulphide minerals i.e. arsenopyrite, orpiment and realgar are mostly found in hydrothermal and magmatic deposits [23]. It has been reported that on an average 6 mg of As per kg is present naturally in the earth's crust. Coal minerals also have elevated concentrations of arsenic (1.5 mg As/kg) in the form of arsenite and arsenate [21, 24]. The desorption and dissolution of naturally occurring arsenic compounds by weathering of rocks and sediments, hydrothermal ore deposits, volcanic eruptions, geothermal activities, wind-blown dust, sea salt spray and forest fires are considered as principal natural sources of As distribution in ground water and environment [24-27]. The volcanic eruption releases 17,150 tons of arsenic and burning of wood in forest fires releases 125 to 3,345 tons of arsenic per year in the environment [21, 28, 29]. There are some anthropogenic sources which are also responsible for arsenic poisoning of groundwater. Arsenic containing compounds are widely used as herbicides, pesticides and fungicides in agriculture. These are also used to some extent as wood preservatives, in glass, alloys and electronics. Chromated copper arsenate (CCA) is widely used as wood preservative, copper acetoarsenite pigment and lead arsenate have long been used as pesticides and insecticides. The continuous use of these arsenic containing insecticides, pesticides and wood preservatives results in increased residual arsenic concentrations in soils and sediments upto 2 g As/kg. The mining, smelting of Cu, Au, Ni, Pb and Zn ores, processing of cotton and wool, seepages from hazardous waste sites, power generation by the burning of arsenic contaminated coal also causes the arsenic poisoning of water [30-35, 20]. In comparison to natural sources, these anthropogenic sources are much less responsible for arsenic poisoning of groundwater, but their contribution for groundwater contamination cannot be neglected.

Arsenic poisoning was identified in West Bengal and Bangladesh for the first time and then reported in Inner Mongolia, Vietnam and other areas of Asia [36-38]. Now arsenic poisoning has been reported in various countries of the world but the maximum concentration limit (MCL) of these countries differs due to their different socio-politico-economical contexts or unavailability of different treatment technologies [39]. Fig. 1.3 shows the 'As' contaminated parts of the world with their respective MCL value [40, 41, 13].

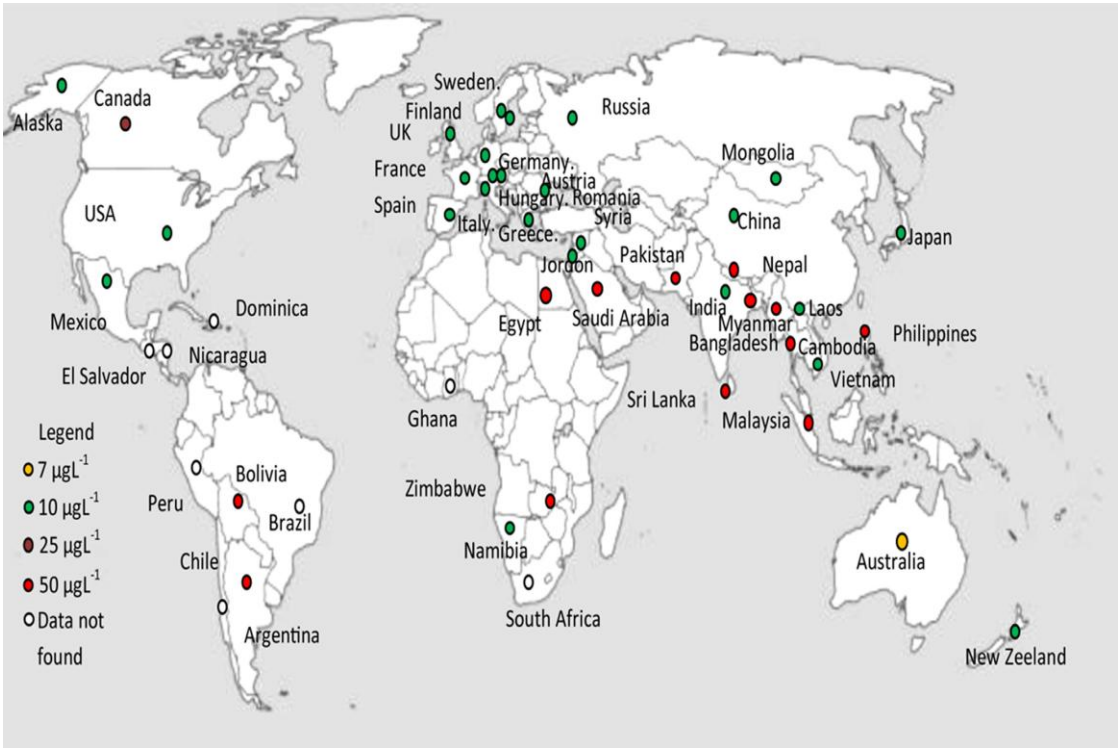

Figure 1.3: Arsenic contaminated countries and their respective MCL value [41].

1.2.3. Hazardous effects of arsenic

It is well known that arsenic is toxic for both plants and animals, and the toxic effects of arsenic decreases in the order of arsine > As(III) > As(V) > organic arsenic compounds > elemental arsenic [20]. Inorganic arsenic compounds are more toxic than organic arsenic compounds and inorganic As(III) is 25-60 times more toxic than inorganic As(V) [32]. There are various factors such as arsenic species, amount of arsenic, exposure time, nutritional status, methylation capacity, genetic conditions, bioavailability, and presence of co-carcinogenic factors such as sunlight exposure, cigarette smoking etc. on which arsenic toxicity generally depends [42-49]. Two types of effects of arsenic exposure on human health have been reported viz. acute and chronic. Acute arsenic poisoning effects occur immediately

after ingestion of high concentration of arsenic at one time, while chronic poisoning effects occur gradually with consumption of low concentration of arsenic for a long time period. International Agency for Research on Cancer (IARC), has classified arsenic as group 1 carcinogenic substance to human beings [50]. US Environmental Protection Agency (USEPA) also classified arsenic poisoning as a Class 'A' human carcinogen. Arsenic interferes with a number of essential biological activities such as action of enzymes, essential cations and transcriptional events in cells thus causing arsenic poisoning [51]. The common symptoms which arises as a result of acute arsenic poisoning are muscle pain, weakness, numbness, stomach pain, nausea, vomiting or diarrhoea (if one consume 0.3 to 30 mg/L arsenic at a time), and in severe cases seizures, coma, or even death can occur (at large oral dose of 60 mg/L) [52, 53]. The chronic arsenic poisoning symptoms starts to appear after few years of exposure, initially as skin ailments because skin is quite sensitive to arsenic. Hyperpigmentation and hypopigmentation can occur which shows dark and light spots respectively, then keratosis begins which hardens the skin on hands and feet causing skin lesions. Long term exposure of about 10 years results in skin cancer and about 20 to 30 years of exposure can cause internal body cancers such as lung, bladder and kidney and liver cancers [54]. The other effects of arsenic poisoning such as hypertension, peripheral vascular diseases, cardiac vascular diseases, respiratory diseases, diabetes mellitus, and malignancies have also been reported in the literature [55-59].

1.3. TECHNOLOGIES AND METHODS AVAILABLE FOR ARSENIC REMOVAL

In recent years, arsenic contamination of drinking water has become a global issue due to its toxicological and carcinogenic effects on humans as discussed in the above section. The maximum concentration limit of arsenic set by World Health Organization (WHO) for drinking water is 10 µg/L. Therefore, it is worldwide demand to develop effective technologies for arsenic removal to meet the standard. Although various technologies are available for arsenic removal but effective technologies are economically unaffordable at large scale. On the other hand, economically affordable and easily available technologies are not much effective to meet the quality of the treated water as per WHO standards [60]. In this section, we have given a brief description of some available technologies for arsenic removal. Fig. 1.4 shows the schematic of various existing technologies for arsenic removal.

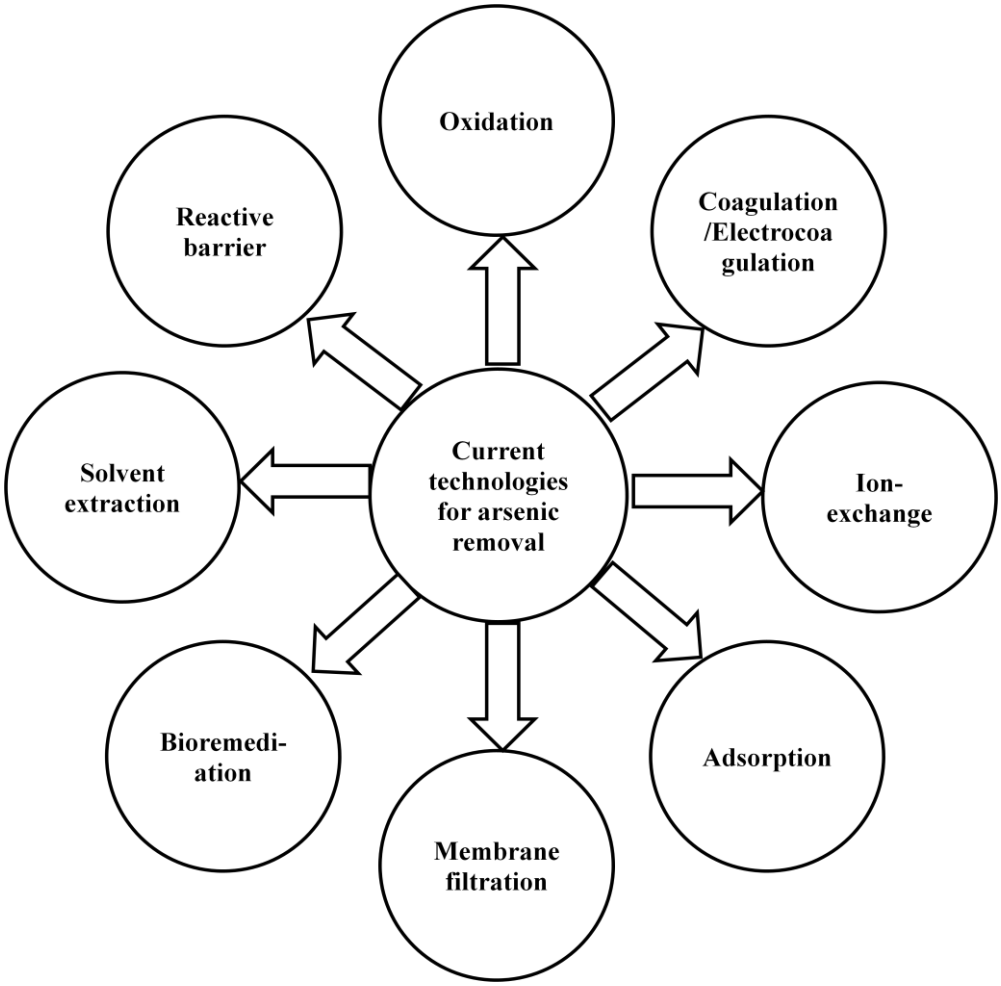

Figure 1.4: Schematic of various existing technologies for arsenic removal.

1.3.1. Oxidation/Precipitation

In aqueous environment, arsenic is mainly found in +3 (As(III)) and +5 (As(V)) oxidation states. Most of the arsenic treatment technologies are effective in removing As(V) but not As(III) due to the uncharged behaviour of As(III) at low pH values [61]. Therefore, it is essential to convert soluble As(III) to As(V) by oxidation followed by precipitation of As(V) as arsenic sulphide, calcium arsenate or ferric arsenate [62-66]. There are number of oxidants viz. ozone, freely available chlorine, Cl_2O, FeO_4^{2-}, H_2O_2, hypochlorite, potassium permanganate, Fenton's reagent (H_2O_2/Fe^{2+}), MnO_2 coated nanostructured capsules for the oxidation of As(III) to As(V) [67-86]. The oxidation followed by adsorption is also found to be effective for arsenic removal as As(V) adsorbs more efficiently than As(III) on the solid surfaces [62, 87].

The photochemical and photocatalytic oxidation of As(III) has also been reported in the literature [70, 85, 88-92]. It has been found that UV irradiation in the presence of oxygen,

increases the oxidation rate of As(III) in water [77, 93]. García et al. [94] explored solar oxidation (SORAS) process in which he utilizes sunlight irradiation of arsenic contaminated water in PET- or other UV-A transparent bottles for arsenic removal. In this process arsenic removal takes place in two steps. In the first step, As(III) photochemicaly oxidized to As(V) and then adsorbs to iron(hydr)oxides surface. In the second step, Fe(III)(hydr)oxides formed from naturally present iron with the adsorbed As(V) settled down at the bottom of the container and the clear water in the supernatant can be decanted. In Bangladesh, iron is naturally present in groundwater; therefore SORAS could be useful to reduce arsenic contents in water at virtually no cost. Thus this method can potentially be used at household level for treatment of small quantities of drinking water. It has been reported by Yang et al. and Bissen et al. [95, 96] that photocatalytic oxidation can be efficient for oxidation of As(III) to As(V). To achieve high arsenic removal efficiency by oxidation method, an adequate selection of oxidants in relation with aquatic chemistry and water composition is essential. Moreover, oxidation alone is not considered as an effective method for arsenic removal as it removes only a part of arsenic.

1.3.2. Coagulation/Electro-coagulation

The coagulation method is one of the conventional methods used for removal of suspended and dissolved solids including arsenic from the drinking water. In this method, chemical coagulants such as alum (hydrated potassium aluminium sulphate), iron and manganese salts are added into large volumes of water for arsenic removal. Among these iron coagulants have proved to be more effective for arsenic removal [63, 97-100]. This method involves the aggregation of fine particles in water into coagulate due to strong reduction in the absolute values of zeta potentials of the particles resulted by addition of coagulants. Then there is precipitation of arsenic ions with the ferric or aluminium ions on coagulates, and finally they are concentrated in the coagulates. The arsenic-borne coagulates are then separated from water through filtration. The rate of coagulation is mainly affected by pH, coagulant dosage, turbidity, natural organic matter, other competing ions in solution and temperature. The use of ferric iron coagulants for treatment of arsenic contaminated deep-well water in Taiwan was reported even in the late 1960s [101]. This method has been proved much more effective for As(V) removal as compared to As(III) removal. Hence, it is essential to convert As(III) to As(V) by pre-oxidation step. Moreover, coagulation method is usually associated with treatment and disposal problem of the resulting waste sludge [102]. Therefore,

electrocoagulation (EC) method is typically used instead of coagulation method to reduce the sludge production. In this method aluminium or iron, when dissolved electrolytically, supports the coagulation process and decreases the amount of sludge. This method proved to be effective in removing arsenic from water as compared to coagulation method [102-106].

1.3.3. Adsorption

Adsorption is a process in which substances from either gas or a liquid solution bind to the surface of a solid. The substances which are separated from one phase and accumulated or concentrated at the surface of another are called adsorbate. The solid material which adsorbs adsorbate on its surface is called adsorbent. The reverse processes in which the adsorbate detaches from the surface of a solid to a gas or a liquid is called desorption [107]. There are two types of adsorption processes which mainly takes place viz. physical adsorption and chemical adsorption. In physical adsorption, there are weak chemical interactions such as Van der Waals forces of attraction or hydrogen bonding between the adsorbate and adsorbent. Therefore, physical adsorption does not cause any major chemical changes in the chemical structure of adsorbent and adsorbate as a result of adsorption. As the adsorbate molecules can adsorb on each other via Van der Waals or hydrogen bonding forces, multilayers are formed frequently in case of physical adsorption. In chemical adsorption, there is covalent chemical bonding between the adsorbate and a specific adsorption site of the adsorbent due to which there is an upper limit to the quantity that may adsorb on the surface resulting in monolayer covering of the surface. The chemical adsorption generally has higher enthalpy and slower kinetics of adsorption as compared to physical adsorption [107, 108]. The adsorption method has widely been used for the treatment of arsenic contaminated groundwater.

This technology is effective to remove both As(III) and As(V) below MCL value set by WHO i.e. 10 µg/L, but its effectiveness is sensitive to a variety of other contaminants present in polluted water. There are number of adsorbents viz. magnetite (Fe_3O_4), goethite, zero valent iron-reduced graphite oxide, ferrihydrite, Mn-substituted Fe oxyhydroxide, granular ferric hydroxide, Ce(IV)-doped Fe oxide, natural hematite and natural siderite, activated alumina, iron oxide coated cement, iron oxide coated sand, indigenous filters and cartridges etc. which have been reported in the literature for arsenic removal through adsorption technique [5, 109-118]. The adsorption media is usually packed into a column and as the arsenic contaminated water is passed through the column, arsenic gets adsorbed and we get

arsenic free water in the effluent. When adsorption sites become saturated, the column should be regenerated or disposed of and replaced with new adsorption media.

1.3.4. Ion exchange

Ion exchange method has also been widely used for the arsenic removal from water [118, 119]. This method is considered as special form of adsorption in which reversible interchange of ions between the solid and liquid phases occurs without causing permanent change in the structure of solid. While other forms of adsorption involve stronger bonds therefore they are less easily reversed. It is a physical-chemical process in which metal ions are swapped between a solution phase and solid resin phase. The solid resin is typically an elastic three-dimensional hydrocarbon network to which a large number of ionisable groups are bounded electrostatically. These groups are exchanged with metal ions of similar charge in solution that have a stronger exchange affinity (i.e., selectivity) for the resin.

Chloride is proposed as one of ion-exchange resins to remove the As(V), as shown in the following equation [120].

$$R\text{-}[N(CH_3)_3]^+Cl^- + H_2AsO_4^- \Leftrightarrow R\text{-}[N(CH_3)_3]^+H_2AsO_4^- + Cl^- \qquad (1.1)$$

The resins can be regenerated by using sodium chloride solutions. Metal hydroxides can also be used for As(V) removal. However, these resins are insensitive to pH in the range 6.5-9.0 [121, 122].

1.3.5. Membrane filtration process

Membrane filtration processes also used as a promising technology for water purification by removing a wide range of contaminants including arsenic. This technology is able to remove arsenic below 50 µg/L and in some cases below MCL value of 10 µg/L. The effectiveness of this technology is also sensitive to a variety of contaminants and their characteristics present in the contaminated water. There are four different kinds of pressure driven membrane filtration processes viz. microfiltration (MF), ultrafiltration (UF), nanofiltration (NF) and reverse osmosis (RO), reported in the literature for remediation of arsenic contaminated water. All the four processes are characterized by pore size of the membrane or the particles size that can pass through the membrane and selectivity of the membranes increases with increasing driving pressure [123]. As MF and UF require low pressure (0-100 psi), therefore the contaminants are separated by mechanical sieving. These membranes can remove only particulate form of arsenic from water and not the dissolved arsenic, because the dissolved

arsenic size is much small to pass through the pores of such membranes. Therefore, the arsenic removal efficiency of these membranes depends on the size distribution of arsenic bearing particles in water. Many researchers enhance the arsenic removal efficiency of these membranes by making some modifications [124-126].

On the other hand, NF and RO require relatively high pressure (50-150 psi), therefore the contaminants are separated via chemical diffusion across the permeable membrane [123, 40, 121, 122]. These membranes can remove dissolved arsenic from water to a particular level provided the feed water contains a very low amount of suspended solids [127]. It has been reported by Waypa et al. that NF and RO membranes removed both As(III) and As(V) effectively upto 99 % from water [128]. This shows that size exclusion is responsible for arsenic removal and not the charge interaction. RO membrane with extremely small pores i.e. < 0.001 µm is the oldest and effective technology available for water desalination and arsenic removal from small water systems [129]. This shows a very high rejection upto 99 % of low molecular mass compounds [130]. Moreover, a number of researchers reported that these membranes shows a high rejection for As(V) in comparison to As(III) and this is the most important drawback of RO [131, 132].

1.3.6. Bioremediation

There are certain plants and micro-organisms which have been used by researchers for arsenic removal. This type of remediation of arsenic by using plants and microorganisms is termed as bioremediation of arsenic. These biological methods are categorized as either phytoremediation utilizing plants to remove the elemental contamination, or biological treatments utilizing micro-organisms. In case of phytoremediation, various plant species viz. poplar, cottonwood, sunflower, Indian mustard, maize, grasses (ryegrass and prairie) are used to either stabilize or remove arsenic from groundwater through phytostabilization and phytoextraction. There are certain hyper-accumulating ferns which accumulate high concentrations of arsenic in their aerial tissues [133]. Chinese brake fern *Pteris vittata* is the first reported arsenic hyperaccumulator, which can accumulate 12–64 mg As/kg in its fronds from soils containing 0.5–7.5 mg As/kg, and up to 22,630 mg As/kg from a soil amended with 1500 mg As/kg [134]. A number of other fern species including *Agrostis tenuis*, *Agrostis stolonifera*, *Pityrogramma calomelanos*, *Pteris cretica*, *Pteris longifolia* and *Pteris umbrosa*, have also been reported to hyperaccumulate the arsenic [133]. These plants are able to tolerate high concentrations of As(V) but not As(III).

Similarly a variety of microorganisms viz. *Sphaerotilus*, *Leptothrix ochracea*, *Gallionellaferruginea*, *Thiobacillus acidophilus*, *Acidithiobacillus ferrooxidans*, *Escherichia coli* were utilized by various researchers for the biological removal of arsenic [135-138]. Two types of microbiological interactions i.e. microbial oxidation of As(III) to As(V) followed by precipitation, and bio- accumulation of arsenic by microbial biomass, have been reported for arsenic removal by Parknikar et al. [139]. Bioremediation is more effective for As(V) removal rather than for As(III) removal.

1.3.7. Other methods

There are number of other methods including solvent extraction, reactive barrier, lime softening, foam flotation etc. for the arsenic removal. In solvent extraction, a substance is extracted from one liquid phase to another liquid phase based on the relative solubility of compounds in two different immiscible liquids, such as water and an organic solvent. The extractant, diluents and valency of arsenic in water affects the efficiency of extraction. It has been reported that the aromatic diluents such as toluene are preferable diluents for arsenic removal. Many researchers have used this method for water purification [140-143]. The main problems associated with this method are arsenic removal below MCL value and disposal of by-products.

In reactive barrier method, a reactive material zone termed as permeable reactive barrier (PRB) contains a reactive material for arsenic removal [144-146]. In a typical PRB design, there is excavation and backfilling of continuous trench of reactive material such as iron, limestone, calcium phosphate-based minerals, activated carbon, compost, zeolites etc. The reactive material is selected on the basis of target contaminants. In this method, there is involvement of a "funnel and gate" system, which uses low-permeability walls to direct contaminated groundwater towards a permeable reactive barrier treatment zone. In most of field-scale PRB systems, zero-valent iron is used as a reactive media for the remediation of chlorinated organic, metal and radionuclide contamination [147].

Arsenic removal by lime softening process is somewhat similar to the coagulation method. In this method hydrolyzed lime ($Ca(OH)_2$) react with carbonic acid to form calcium carbonate, which acts as a arsenic adsorbent. This method is effective for arsenic removal in case of very hard water especially at pH > 10.5 [63]. It has been reported that only 40-70 % As(V) was removed from water having an initial arsenic concentration of 0.1 to 20 mg/L at pH values 9.0 to 10.0. An increase in arsenic removal efficiency was obtained when lime softening was

followed by the coagulation using an iron salt. In this method, a high As(V) removal efficiency of 95 % was obtained for pH from 10.6 to 11.4 at an initial arsenic concentration of 12 mg/L [63, 148-150]. This method is not effective for extremely low arsenic concentrations. Moreover, this method is costly and therefore is not suitable for small systems.

The use of adsorbing colloid floatation (ACF) method has also been reported for removal of low arsenic concentrations in water [151-154]. This method is considered as an analytical method for simultaneous removal of germanium, arsenic and boric acid [155-157]. In this method, a coagulant viz. goethite, iron(III) sulphate, alum or ferric hydroxide is added to produce a floc and arsenic is adsorbed on these flocs and co-precipitated with them followed by collection of these flocs by addition of surfactant [158-161]. It has been found that 99.5 % arsenic was removed by using colloidal ferric hydroxide as a co-precipitant and sodium dodecyl sulphate as a collector at pH 4.0 to 5.0 [151]. However this method is non-selective for arsenic removal.

1.3.8. Comparison between different methods of arsenic removal

The various technologies for arsenic removal as discussed above have certain advantages and disadvantages of their own. Table 1.2 shows a comparative account of arsenic removal efficiency and water losses for various technologies operated under normal conditions as reported in the literature. Among all the methods, adsorption is considered as more effective because of low treatment cost, high arsenic removal efficiency and minimum water loss as compared to other technologies. Further in adsorption method, iron based adsorbents such as magnetite, maghemite etc. have proved to be more effective with high arsenic removal efficiency (upto 99 %) and minimum water loss of 1-2 % only [9, 121].

Table 1.2: Comparison between treatment efficiencies of different arsenic removal methods and corresponding water loss [9, 121].

Treatment process	As removal efficiency	Water loss
Oxidation and Filtration		
Greensand	50-90 %	< 2 %
Biological oxidation	> 95 %	< 2 %
Co-precipitation		
Enhanced lime softening	90 %	1-2 %
Enhanced Coagulation/Filtration		
With alum	< 90 %	1-2 %
With ferric chloride	95 %	1-2 %
Coagulation assisted microfiltration	90 %	5 %
Adsorption		
Activated alumina	95 %	1-2 %
Iron based sorbents	upto 99 %	1-2 %
Ion exchange	95 %	1-2 %
Membrane Technology		
Reverse osmosis	> 95 %	15-20 %

Looking to the higher arsenic removal efficiency, in the present work we have used magnetite nanoparticles (iron based sorbents) as the adsorbent for arsenic removal.

1.4. MAGNETITE NANOPARTICLES

1.4.1. Synthesis of magnetite nanoparticles

There are several methods reported in the literature for the synthesis of magnetite nanoparticles. Fig. 1.5 represents schematic of some widely used synthesis methods such as co-precipitation, sol-gel, hydrothermal, microemulsion, thermal decomposition, sonochemical and electrochemical etc. for magnetite nanoparticles [162-175]. We have adopted co-precipitation method for the synthesis of magnetite nanoparticles on sand surface.

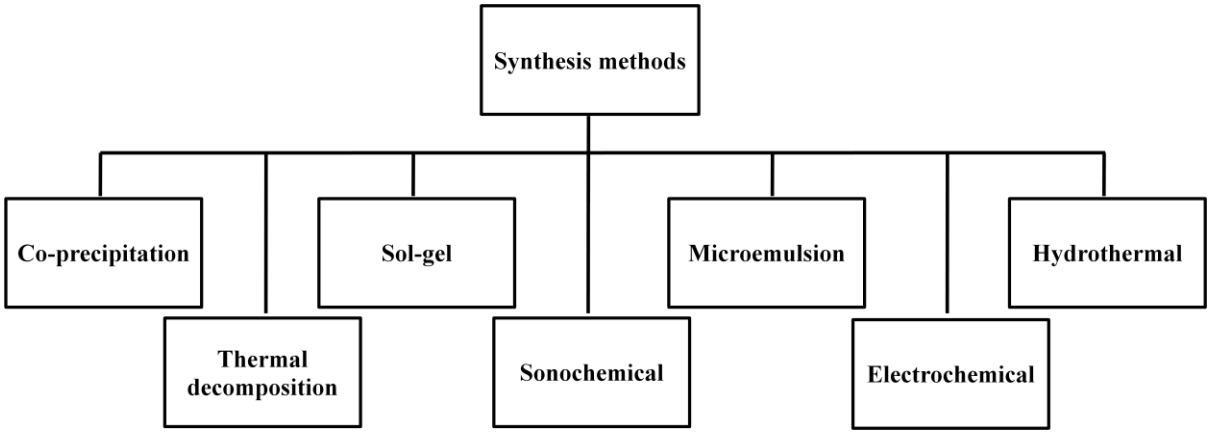

Figure 1.5: Methods for synthesis of magnetite nanoparticles.

1.5. APPLICATIONS OF MAGNETITE NANOPARTICLES AS AN ADSORBENT FOR ARSENIC REMOVAL FROM WATER

Many studies have been reported in the literature for the arsenic removal by magnetite nanoparticles. It is well known that being an iron oxide, surface hydroxyl groups are the reactive functional groups of magnetite nanoparticles. The double pair of electrons with a dissociable hydrogen atom enables magnetite nanoparticles to react with ions in solution and to form the surface complexes. Arsenic can form three types of complexes with iron oxides viz. bidentate mononuclear, bidentate binuclear and monodentate mononuclear as shown in Fig. 1.6 [176]. We have shown only the coordination of arsenate with iron oxide in this figure.

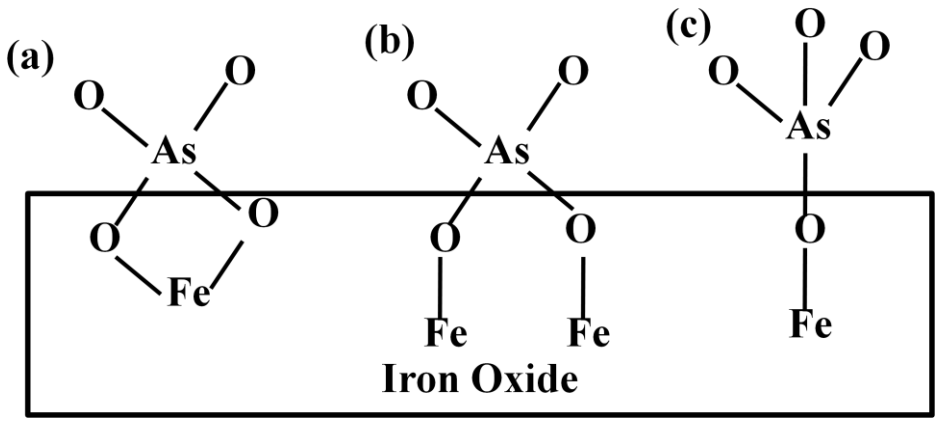

Figure 1.6: Schematic representation of different complexes of arsenic that may form on the iron oxide surface; (a) bidentate mononuclear (b) bidentate binuclear (c) monodentate mononuclear [176].

There are two types of studies reported in the literature for arsenic removal using magnetite nanoparticles, i.e. batch study and column study. In batch experiment usually adsorbent is

added in a series of flasks containing known amount of arsenic solution. Then these flasks are kept on an incubator shaker at a fixed temperature and speed for a time until equilibrium is attained. After attaining the equilibrium, the solution is filtered for arsenic analysis. The adsorbent can be regenerated for further use. A wide range of batch studies have been reported for arsenic removal by magnetite nanoparticles. On the other hand in column studies, an adsorbent is packed as a fixed bed in a column for arsenic removal from water by adsorption. The influent with known arsenic concentration is pumped through the column containing adsorbent where the arsenic get adsorbed on the adsorbent surface and the effluent free from arsenic passes out of the column. When the adsorbent get exhausted, the arsenic concentration in the effluent starts rising. At this point, the adsorption process is usually stopped and the adsorbent is either regenerated or replaced/disposed [108]. There are very few studies reported in the literature for arsenic removal by using magnetite nanoparticles and other iron oxides in columns as compared to batch studies.

Khodabakhshi et al. [177] synthesized magnetite nanoparticles by sol-gel method and studied the potential of these nanoparticles for As (III) removal from synthetic industrial wastewater. They found that 82 % of As(III) was removed within 20 min of contact time and adsorption data fitted well in Freundlich isotherm model. The As(III) adsorption capacity of Fe_3O_4 nanoparticles was found to be 23.8 mg/g at pH 7.0. The newly synthesized sub-4-nanometer magnetite nanoparticles were used for arsenic removal under aerobic and anaerobic conditions. Magnetite nanoparticles exhibited As(III) and As(V) adsorption capacity of 168.8 mg/g and 206.9 mg/g, respectively under anaerobic conditions, and 108.6 mg/g and 138.1 mg/g, respectively under aerobic conditions [178]. Stefusova et al. [179] carried out the synthesis of magnetite nanoparticles by co-precipitation of Fe(II) and Fe(III) under alkaline conditions for arsenic removal from water. They performed various batch studies for arsenic removal and reported that the maximum adsorption capacity of these magnetite nanoparticles was 46.7 mg/g at pH 3.5. They have also studied desorption of arsenic loaded on magnetite nanoparticles under various experimental conditions which is beneficial for regeneration of adsorbent for real life application.

The use of commercially available magnetite nanoparticles for arsenic removal has also been reported in the literature. Turk et al. [180] used commercially available magnetite nanoparticles purchased from Sigma Aldrich as adsorbent for arsenic removal. The authors have investigated the potential of these nanoparticles for As(V) removal by varying various experimental parameters viz. effect of initial solution pH (3.0-12.0), contact time (15–180

min), adsorbent dosage (0.05–5 µg/L), and effect of initial As(V) concentration (100–2,000 µg/L). The batch adsorption kinetics data was described by pseudo-second-order kinetic model and batch adsorption isotherm data was fitted well in Langmuir and Freundlich isotherm models. It was found that magnetite nanoparticles reduced As(V) concentration below MCL value set by WHO. Chowdhury and Yanful [181] studied the potential of commercially synthesized 20 nm magnetite nanoparticles for arsenic removal from synthetic as well as natural groundwater. The maximum As(III) and As(V) adsorption capacity was found to be 3.69 mg/g and 3.71 mg/g, respectively at an initial concentration of 1.5 mg/L of both arsenic species at pH 2.0 from synthetic water.

Various studies have also been reported in the literature on use of complex magnetite nanosystems for arsenic removal. Chandra et al. [182] synthesized magnetite-reduced graphene oxide composites with magnetite nanoparticles (size about 10 nm) for arsenic removal. The synthesized composites have shown a high binding capacity for both As(III) and As(V), with 99.9 % arsenic removal as compared to bare magnetite nanoparticles. Thus the synthesized composite is practically beneficial for arsenic removal from water due to high binding capacity. An et al. [183] synthesized starch-bridged magnetite nanoparticles of high specific surface area for the arsenic removal. The authors reported that 99 % of arsenic was removed using 0.49 wt % concentration of synthesized starch solution and further addition of starch (> 0.049 wt %) decreases arsenic removal efficiency. The authors also reported that the presence of high concentration of NaCl in water does not effects arsenic removal efficiency and this is the main advantage of starch-bridged magnetite nanoparticles. Zheng et al. [184] developed a zirconium-based magnetic adsorbent ($ZrO(OH)_2 \cdot 1.6Fe_3O_4 \cdot 2.5H_2O$) by co-precipitation method for arsenic removal. The results shows that lower pH i.e. 2.6 to 3.3 is favourable for As(V) adsoption and maximum adsorption capacity of 45.6 mg/g is achieved which is much higher than many reported adsorbents. Magnetite nanoparticles (commercially prepared, laboratory synthesized or magnetite nanoparticles in various forms) have also been utilized for arsenic removal in various other studies [185-192].

Shipley et al. [193] carried out column studies for arsenic removal by using commercially available 19.3 nm magnetite nanoparticles. In this study, the authors packed a column with 1.5 and 15 wt % magnetite nanoparticles and Lula soil, respectively. Then arsenic contaminated aqueous solutions passed through the column. They carried out arsenic removal experiments with 1.5 wt % magnetite nanoparticles at flow rate of 1.5 and 6 mL/h with initial As(III) and As(V) concentrations of 100 µg/L. In this case, arsenic release occurred after 400

PV and 100 % arsenic release was achieved. They also conducted a long term study with 15 wt % magnetite nanoparticles at flow rate of 0.3 mL/h with an initial As(V) concentration of 100 µg/L. They found a negligible As(V) concentration for 3559.6 pore volumes (PVs) (132.1 d), and the As(V) concentration reached about 20 % after 9884.1 PV (207.9 d). They have calculated a retardation factor of about 6742, which indicates strong adsorption of arsenic to the magnetite nanoparticles in the column. An increase in arsenic adsorption was also observed after flow interruption. Column studies for arsenic removal has been reported in the literature using iron oxide adsorbents other than magnetite viz. iron oxide coated sand, iron oxide coated cement.

1.6. FACTORS AFFECTING ARSENIC REMOVAL EFFICIENCY

1.6.1. Effect of initial solution pH

Solution pH can affect both chemical speciation of arsenic (pKa values for H_3AsO_4 are 2.2, 7.0 and 11.5) and surface charge of the adsorbent. This is because the proton concentration in water strongly modifies the redox potential of sorbates and sorbents which enhances dissolution of the adsorbent material and thus affects the chemical speciation of adsorbates and surface charge of adsorbent. Thus pH is considered as an important factor in adsorption based water treatment processes [194]. In general, it has been widely observed that As(V) adsorption is pH dependent, while As(III) adsorption is independent of pH over a wide range. This is due to the different charges of As(III) (non-ionic over wide range of pH) and As(V) (anionic). Moreover, the pH point of zero charge (pH_{pzc}) is also an important factor above which the adsorbent surface is negatively charge and below pH_{pzc} the adsorbent surface is positively charged. Therefore, when pH value is below point of zero charge ($pH < pH_{pzc}$) then the positively charged surface of adsorbent adsorbs negatively charged As(V) significantly as compared to uncharged As(III). This is the reason that at lower pH such as 4.0 As(V) usually has higher adsorption as compared to As(III). When pH value is above point of zero charge ($pH > pH_{pzc}$) then the surface of the adsorbent acquires negative charge due to more OH^- groups on the surface of adsorbent that generally result in decreased As(V) adsorption due to electrostatic repulsion between negatively charged As(V) species and negatively charged adsorbent surface sites. On the other hand, pH independency of As(III) adsorption can be explained in terms of high pKa value of As(III) (i.e., pKa, 9.2). As(III) is mostly present as a non-ionic species at low pH values and therefore adsorption of this non-ionic form of As(III)

to adsorbent surface did not change with pH. There are a number of studies reported in the literature on the effect of pH on As(III) and As(V) removal efficiency.

Yean et al. [195] investigated the effect of pH on adsorption capacities of As(III) and As(V) by magnetite nanoparticles of size 20 nm and 300 nm. They found that increase in pH did not cause any change in As(III) adsorption capacity while the maximum adsorption capacities of As(V) for 20 and 300 nm magnetite decreased with increase in pH. Dixit and Hering [196] observed that As(III) adsorption efficiency by magnetite increases at pH values less than 9.0 while the adsorption efficiency decreases with further increase in pH. Khodabakhshi et al. [177] also reported that with increase in pH from 3.0 to 7.0, As(III) removal efficiency of magnetite nanoparticles increases from 59 % to 82 % and decreases to 39 % as the pH was increased to 9.0. Chowdhury and Yanful [185] also observed that As(III) and As(V) adsorption decreases with increase in pH. They observed that As(III) removal efficiency deceases sharply above pH 9.0 and As(V) removal efficiency was less than 10 % at pH above 10.0. Similar results have been reported by Turk et al. [180], Chandra et al. [182], Zhang et al. [187], Shipley et al. [197] and Hai et al. [198]. Chunming and Puls [199] investigated the influence of pH on As(V) removal efficiency by using eight commercially available magnetite particles and observed that As(V) adsorption was more favourable below pH 5.6 – 6.8.

1.6.2. Effect of contact time

The contact time between adsorbate and adsorbent is also an important factor which influences adsorption processes. Many investigators have studied the effect of contact time on arsenic removal efficiency by using different magnetite nanosystems and reported different equilibrium time. The equilibrium time is the time after which no more adsorption of arsenic occurs on adsorbent surface. The equilibrium at different contact times have been achieved due to different nature of the systems used.

Chowdhury and Yanful [185] studied the effect of contact time on As(III) and As(V) removal by using mixed magnetite-maghemite nanoparticles at initial arsenic concentrations of 1 and 2 mg/L. The equilibrium for different initial arsenic concentrations was achieved in almost 3 hrs of contact time between adsorbate and adsorbent at pH 6.5. The authors found that initially within 10 min of contact time, there is rapid adsorption of arsenic followed by the subsequent slower adsorption. Shipley et al. [5] achieved adsorption equilibrium in almost 1 hr by performing arsenic removal experiments with magnetite nanoparticles in the acidic pH

range. Türk et al. [180] have also found that the arsenic concentration decreases from 300 to 12.2 µg/L within 15 min and equilibrium was attained in 1 hr. Zheng et al. [184] have achieved adsorption equilibrium after a long time of 25 hrs for arsenate removal by using zirconium based magnetic adsorbent. Many other researchers such as Chandra et al. [182], Shipley et al. [5] and Hai et al. [198] have also reported rapid removal of arsenic in the first step followed by subsequent slower adsorption.

Different equilibrium time have been reported in the literature for arsenic removal but have similar kinetics i.e. arsenic adsorption takes place in two steps for all the nanosystems. Initially in the first step, there is rapid removal of arsenic followed by subsequent slower adsorption in the second step. The fast removal of arsenic is attributed to the external surface adsorption so that it is easy for arsenic ions to bind with active adsorbent surface sites. As the time proceeds, the adsorbent surface sites are filled with arsenic ions and therefore the adsorption slows down.

1.6.3. Effect of adsorbent dose

It is important to know the minimum amount of adsorbent required to reduce the arsenic concentration below MCL value set by WHO i.e. 10 µg/L. Thus adsorbent dose is also an important parameter studied by various researchers in adsorption processes. They observed that with increase in adsorbent concentration, the amount of the arsenic adsorbed along with the rate of adsorption increases attaining an optimum adsorbent dose. This is due to the fact that increased adsorbent dose provides large number of surface binding sites for arsenic adsorption. After attaining an optimum dose, further increase in adsorbent dose does not cause significant change in arsenic removal efficiency due to insufficient arsenic ions present in solution with respect to available surface sites. A very small amount of magnetite nanoparticles as an adsorbent is needed to reduce the arsenic concentrations below MCL value. Shipley et al. [197] have reported that an adsorbent dose of 0.5 g/L, reduced the As(III) and As(V) concentration in water below 10 µg/L within 1 hr and 30 min, respectively.

1.6.4. Effect of initial arsenic concentration

Initial arsenic concentration is another important factor which affects the arsenic removal efficiency of iron oxide nanoparticles. Literature shows that with increase in initial arsenic concentration, arsenic removal efficiency decreases, while the adsorption capacity increases and finally the adsorbent get saturated as further addition of arsenic does not cause any

change in adsorption capacity. Khodabakhshi et al. [177] investigated the effect of initial concentrations of arsenic on its removal efficiency and observed that with increase in initial arsenic concentrations from 10 to 200 mg/L, removal efficiency of arsenic decreased from 79 % to 16 %. Thus arsenic removal is inversely proportional to initial arsenic concentration. This is attributed to the fact that for a fixed amount of adsorbent, the total available adsorption sites are limited and this leads to a decreased removal efficiency of arsenic with increase in initial arsenic concentration. The effect of initial arsenic concentration on As(III) and As(V) removal efficiency of magnetite nanoparticles was investigated by Chowdhary and yanful [181]. They reported a gradual decrease in arsenic removal efficiency with increasing initial As(III) and As(V) concentrations in the presence of the fixed adsorbent dose (20 nm magnetite particles at 0.4 g/L of solution).

1.6.5. Effect of temperature

Temperature also affects arsenic removal efficiency. It has been reported that with increase in temperature arsenic removal efficiency increases. This is because as the temperature increases the surface properties or solubility of the arsenic species changes and also their kinetic activity in solution increases which cause an increase in arsenic contact rate with the adsorbent surface. After attaining an optimum temperature, further increase in temperature causes a decrease in arsenic removal efficiency. This is due to the fact that there will be excess increase in kinetic energy with further increase in temperature which results in dissolution of the adsorbed arsenic from the surface of adsorbent. Shipley et al. [197] studied the influence of temperature variation from 20 ^{o}C to 30 ^{o}C on arsenic adsorption efficiency of magnetite nanoparticles. They found an increase in arsenate and arsenite removal efficiency with increase in temperature from 20 ^{o}C to 30 ^{o}C. The amount of arsenate and arsenite adsorbed was increased from 37.2 µg/L and 42.6 µg/L to 46.9 µg/L and 49.3 µg/L, respectively. Similar effect of temperature on arsenic removal was reported by many other researchers [182, 200-202].

1.6.6. Effect of co-existing ions on arsenic removal

The natural water contains many organic and inorganic ionic species other than arsenic which also have tendency to get adsorbs on iron oxide surface. Therefore, the arsenic adsorption efficiency is greatly affected by the presence of these ions in solution and their affinity for iron oxide surfaces [203]. Many studies have been reported in the literature on the effect of

competiting ions viz. carbonate, bicarbonate, phosphate, sulphate, chlorine, silica, organic matter etc. on the arsenic adsorption efficiency. The reported results are inconsistent stating both an effect and no effect for the same competing ion on arsenic adsorption efficiency. Phosphate is found to hinder the arsenic adsorption on iron oxide surface more in comparison to other ions. This is because phosphate and arsenic has similar structure and therefore shows similar affinity for iron oxides. Moreover, phosphate can form three different types of complexes on iron oxide surfaces i.e. protonated ($(FeO)_2(OH)PO$), nonprotonated bridging bidentate ($(FeO)_2PO_2$) and a nonprotonated monodentate ($(FeO)PO_3$) [204]. The extent of complex formation between Fe(III) and phosphates (PO_4^{3-} or HPO_4^{2-}) depends on the $[OH^-]/[PO_4^{3-}]$ or $[HPO_4^{2-}]$ ratio [205]. This indicates that phosphate tendency to enter into the coordination sheath of Fe(III) ion increases with decrease in pH, showing similar behaviour with arsenic. Also the equilibrium constants of $FePO_4$ (log K ¼ 20.8) and of $FeAsO_4$ (log K ¼ 20.1) shows similar affinities of both anions for Fe(III) cations [206]. Chowdhury and Yanful [185] used synthetic water and natural groundwater to study the influence of phosphate concentration on arsenic removal efficiency of magnetite-maghemite nanoparticles and observed a decrease in arsenic removal efficiency with increase in phosphate concentration. They observed that less than 50 % and 60 % of total arsenic was removed from synthetic water (3 mg/L PO_4^{3-} concentration and 1.2 mg/L of initial arsenic concentration) and from natural groundwater (5 mg/L PO_4^{3-} concentration and 1.13 mg/L of arsenic), respectively.

Bicarbonate also influences the arsenic adsorption on magnetite nanoparticles in a similar way as phosphate does. It has been reported that in the absence of bicarbonate ions magnetite nanoparticles remove arsenic below MCL value, but the presence of bicarbonate ions decreases the arsenic removal efficiency and increases the time of adsorption. For example, with an addition of 8.2 mM bicarbonate, As(III) and As(V) removal decreases from 51.2 μg/L and 48 μg/L to 14.4 μg/L and 25.3 μg/L, respectively [5]. In another study, it has been reported that 0.5 g/L magnetite nanoparticles remove arsenic below MCL value in about half an hr. The same amount (0.5 g/L) of magnetite nanoparticles remove As(III) and As(V) concentration below MCL value in about 1 hr and 1.5 hrs, respectively in the presence of 100 mg/L of HCO^{3-} in the solution [207].

Dhoble et al. [208] studied the influence of various cations (Ca^{2+}, Mg^{2+}, Fe^{3+}) and anions (SO_4^{2-}, PO_4^-, Cl^-, NO^{3-}) on As(III) removal efficiency by magnetic binary oxide particles. They reported that the arsenic removal efficiency decreases with increase in Ca^{2+} and Mg^{2+}

concentration, but increases with increase in Fe^{3+} concentration. They also reported that NO_3^- and SO_4^{2-} ions shows no significant effect on As(III) removal efficiency in the concentration range of 100 to 800 mg/L. The presence of Cl^- ions shows more reduction in arsenic removal efficiency at low concentration of 100 mg/L than higher Cl^- concentrations. The PO_4^{3-} ions at low concentration of 100 mg/L does not cause much interference with arsenic adsorption but when its concentration increases to 600 mg/L arsenic removal efficiency decreases and further increase in PO_4^{3-} concentration to 800 mg/L does not show much decrease in arsenic removal efficiency. Chowdhury and Yanful [185] observed no significant changes in arsenic removal efficiency of mixed magnetite-maghemite nanoparticles in the presence of elevated concentrations of SO_4^{2-} and Cl^- ions.

However, despite of having advantages, magnetite nanoparticles have some limitations, such as need of external magnetic field to separate out the magnetite nanoparticles after use. The possible way to overcome the need of external magnetic field can be the use of these materials by making their filter cartridges, but this would be quite expensive since large amount of the material would be required in cartridge making. Therefore, an immobilization of magnetite nanoparticles on an inexpensive material such as sand would be a better way to pave the method to a cost effective technology. Thus in the present work, we have synthesized an adsorbent by coating magnetite nanoparticles on sand surface via co-precipitation method. The sand is used as a substrate for magnetite to provide an economically feasible way for common man to get rid of poisonous arsenic from drinking water.

1.7. THESIS OUTLINE

Chapter 1: This chapter begins with the basic introduction of arsenic chemistry, sources, occurrence and its hazardous effects on human health. Various technologies available for arsenic removal have been explained in this chapter. In the next section, a brief description of magnetite nanoparticles, their synthesis methods and applications of magnetite nanoparticles as an adsorbent for arsenic removal have been discussed. In the last section, we have explained various factors affecting arsenic removal efficiency of magnetite nanoparticles.

Chapter 2: In this chapter, we have explained the methodology used for coating magnetite nanoparticles on sand surface for arsenic removal. The morphology, structural and elemental analysis of the synthesized adsorbent have been explained by FESEM, XRD and EDX characterization techniques. The surface area of adsorbent has also been calculated using

BET surface area analyzer. Further, the point of zero-charge of the adsorbent has also been determined. At the end of this chapter, a brief summary has been presented.

Chapter 3: This chapter starts with an introduction of various aspects associated with arsenic contamination of drinking water. In the second section of this chapter we have explained the batch adsorption experiments for As(III) removal by using magnetite nanoparticles coated sand. The effect of various experimental conditions viz. initial pH of solution, adsorbent dosage, contact time, initial As(III) concentration and effect of co-existing ions on As(III) removal efficiency have been described. The batch experiments for desorption and readsorption of As(III) by magnetite nanoparticles coated sand have also been given. In the next section a brief introduction of adsorption kinetics and adsorption isotherms theoretical models have been presented. Further the experimental As(III) batch adsorption kinetics data and isotherm data have been fitted in various theoretical models viz. pseudo-first-order, pseudo-second-order and intra-particle diffusion kinetics models; Langmuir adsorption isotherm and Freundlich isotherm models, respectively. A comparative account of maximum adsorption capacity of magnetite nanoparticles coated sand for As(III) removal with other reported low cost adsorbents have been documented. The mechanism of As(III) adsorption on adsorbent surface has also been explained. Finally, a brief summary of the chapter is given.

Chapter 4: In this chapter, we have described the potential of magnetite nanoparticles coated sand for As(V) removal by varying different parameters through batch operation mode. The desorption and readsorption experiments for As(V) has also been described to study the degradation behaviour of adsorbent. In the next section, brief description of the effect of various reaction parameters on As(V) removal efficiency have been given. Further the theoretical modelling of experimental As(V) adsorption kinetics data and adsorption isotherm data have been presented. The maximum As(V) adsorption capacity of synthesized adsorbent has also been compared with other low cost adsorbents reported in the literature. The mechanism of As(V) adsorption on magnetite nanoparticles coated sand has also been explained. In the last section, a brief summary of the chapter is given.

Chapter 5: This chapter starts with brief introduction of thermodynamics followed by batch adsorption experiments for As(III) and As(V) removal at different temperatures. In the subsequent section we have briefly explained various thermodynamic parameters associated with adsorption. The effect of temperature on As(III) and As(V) removal and theoretical modelling of isotherm data obtained at different temperatures have been described in the next

section. The various thermodynamic parameters for both As(III) and As(V) removal have also been calculated. Finally, the chapter concludes with a brief summary.

Chapter 6: This chapter deals with the column studies of As(III) and As(V) removal by magnetite nanoparticles coated sand. The influence of column bed height on As(III) and As(V) removal efficiency and breakthrough curve has been described. The theoretical modelling of breakthrough curves obtained at different bed heights have also been explained using two models i.e. Thomas model and Yoon-Nelson model. In the end, a brief summary of the chapter is presented.

Chapter 7: The last chapter includes conclusion and important findings and suggestions towards future work.

CHAPTER 2

SYNTHESIS AND CHARACTERIZATIONS OF MAGNETITE NANOPARTICLES COATED SAND

This chapter explains the synthesis of adsorbent by coating magnetite nanoparticles on the sand surface. The structural and morphological characterizations of the adsorbent (magnetite nanoparticles coated sand) are also discussed in this chapter to confirm the coating of magnetite nanoparticles on the sand surface. The surface area of sand particles before coating and after coating of magnetite nanoparticles was calculated by BET method. We have also determined the point of zero charge of magnetite nanoparticles coated sand.

2.1. MATERIALS AND METHODS

2.1.1. Materials

All the chemicals used in this study were of analytical grade and obtained from Sigma Aldrich. The chemicals were used as received without further purification. The solutions were prepared in milli-Q water. Milli-Q water was prepared by using milli-Q water purification system (Biocell Milli-Q Millipore, Elix). Iron (III) chloride hexahydrate ($FeCl_3.6H_2O$), Iron (II) chloride ($FeCl_2$) and ammonia water (NH_4OH) were used for the synthesis of Fe_3O_4 nanoparticles. The substrate sand was procured from Beas river in Mandi district, Himachal Pradesh, India. The substrate (sand) was cleaned by hydrochloric acid (HCl) and etched by aquaregia (HNO_3 : HCl) solution in 1:3 ratio, respectively before use. Potassium chloride (KCl) was used for determination of point of zero charge of the adsorbent. The pH of solutions was adjusted by using standard acid (0.1 M HNO_3) and base (0.1 M NaOH) solutions and measured with an Oakton pH meter (pH 700 Benchtop Meter).

2.1.2. Coating of magnetite nanoparticles on sand surface

Initially, sand was sieved to a geometric mean size of 0.6 to 0.9 mm and soaked in an acid solution (1.0 M HCl) for 24 hrs, which was then washed with distilled water several times and dried at 100 ^oC temperature. After cleaning, the sand was etched by using HNO_3 : HCl in a ratio 1:3 for 5 min, and then it was rinsed in a stream of water to remove the etchant solution. Thus obtained sand was dispersed in a solution containing 2:1 ratio of $FeCl_3$ and $FeCl_2$, wherein NH_4OH solution was added drop wise at vigorous magnetic stirring at 70 ^oC for 30 min under argon (Ar) gas flow. The addition of NH_4OH resulted in the co-precipitation reaction and thus the formation of magnetite (Fe_3O_4) nanoparticles inside precursor solution. Since the sand was present inside the precursor solution, the nucleation of Fe_3O_4 nanoparticles took place on the sand surface. Thus obtained mixture was aged at room temperature for 48 hrs, which was then filtered and dried in a furnace at 85 ^oC using Ar gas

environment. To ensure proper coating of Fe_3O_4 nanoparticles on the sand particles, the coated sand was washed with distilled water until a clear supernatant was obtained. After filtration, the sand was dried at 85 ^oC for 3 hrs. The Fe_3O_4 nanoparticles coated sand was stored in polyvinyl chloride (PVC) plastic bottles for further use. The Fig. 2.1 shows the schematic of magnetite nanoparticles coating on sand surface.

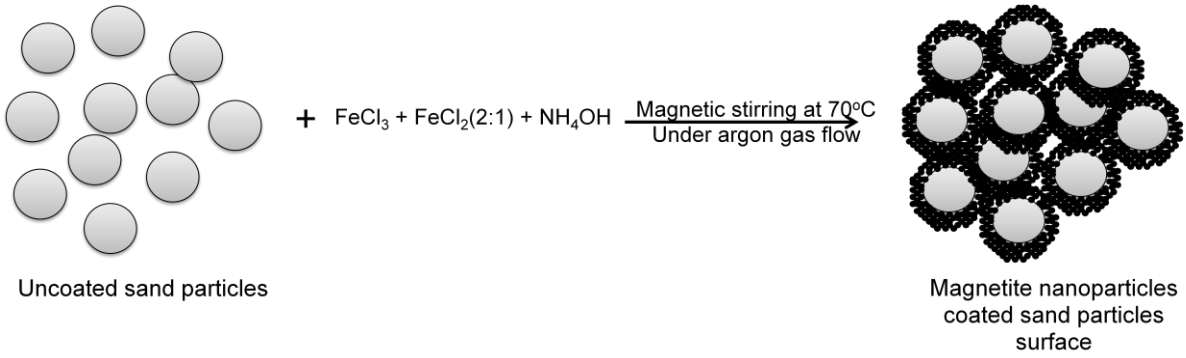

Figure 2.1: Schematic of Fe_3O_4 nanoparticles coating on sand surface.

2.1.3. Determination of point of zero charge (pH_{pzc}) of the adsorbent

We have determined the point of zero charge (pH_{pzc}) of magnetite nanoparticles coated sand (MNCS). For this 0.1 M KCl solution was prepared and 25 mL of solution was taken in different Erlenmeyer flasks. The initial pH was adjusted between 2.0 and 12.0 by using 0.1 M NaOH or 0.1 M HCl solutions. 0.2 g of magnetite nanoparticles coated sand was then added to each flask containing KCl solution of different pH. The flasks were kept in incubator shaker for 24 hrs and the final pH of the solutions was measured. The graphs were plotted between pH_{final} and $pH_{initial}$ [209]. The point of zero charge is the point where the curve $pH_{initial}$ versus pH_{final} intersects the straight line corresponding to $pH_{initial} = pH_{final}$.

2.2. CHARACTERIZATION OF THE ADSORBENT

2.2.1. Physical characterization

Fig. 2.2 (a) and 2.2 (b) shows the bare and Fe_3O_4 coated sand particles, respectively. The sand particles appear greyish white in color before coating and appear black after coating, which indicates Fe_3O_4 coating on the sand surface.

Figure 2.2: (a) Bare sand particles before coating and (b) Fe_3O_4 coated sand particles.

Fig. 2.3 (a) shows that the bare sand particles are not attracted by magnetic bead, whereas magnetite nanoparticles coated sand is attracted by the magnetic bead (Fig. 2.3 (b)). This is because the bare sand particles are non-magnetic and magnetite nanoparticles are magnetic in nature. Thus, the magnetite nanoparticles coated sand particles are attracted by magnetic bead confirming the formation of magnetic material on sand surface.

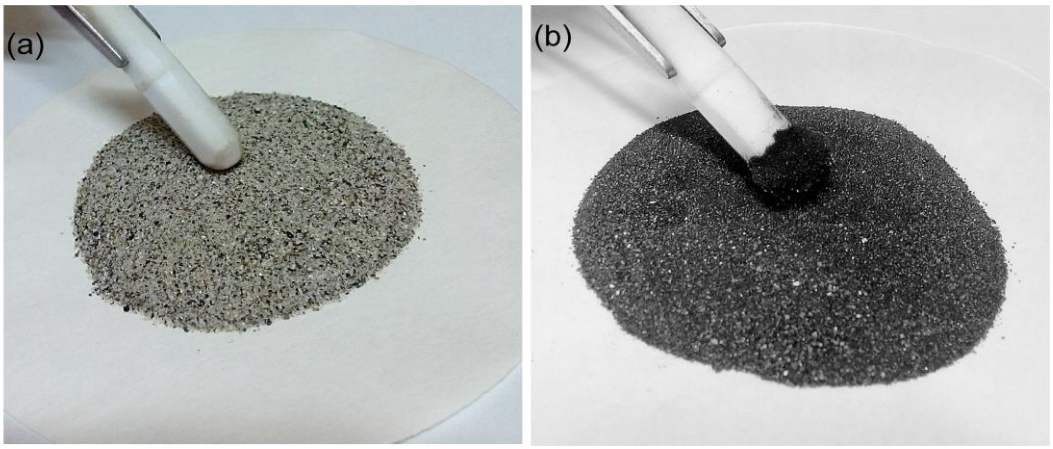

Figure 2.3: Photographs of response of (a) bare and (b) Fe_3O_4 coated sand particles to magnetic bead.

2.2.2. X-Ray Diffraction (XRD)

X-Ray Diffraction (XRD) was performed by using XRD 6000, Shimadzu analytical instrument to confirm the presence of Fe_3O_4 nanoparticles on the sand surface. The XRD data was collected using CuKα radiation of $\lambda = 1.54$ A˚, scan angle $2\theta = 10–80$ and scan rate 0.02 per second.

Fig. 2.4 shows powder XRD patterns of (a) Fe_3O_4 nanoparticles, (b) uncoated sand, and (c) Fe_3O_4 nanoparticles coated sand. In Fig. 2.4 (a), characteristic peaks at $2\theta = 30.1^o$, 35.5^o, 43.06^o, 53.04^o, 57.3^o and 62.6^o are assigned to the planes of magnetite at (220), (311), (400), (422), (511) and (440), respectively as compared with JCPDS data (PDF No. 653107). In case of the uncoated sand (Fig. 2.4 (b)), sharp and narrow peaks obtained at $2\theta = 20.83^o$, 26.68^o, 36.1^o, 39.59^o, 40.37^o, 42.57^o, 50.24^o, 60.04^o, 65.92^o and 68.13^o are assigned to the planes of quartz sand at (100), (101), (110), (012), (111), (200), (112), (211), (300) and (023), respectively as compared with JCPDS data (PDF No. 861630). The XRD pattern of coated sand (Fig. 2.4 (c)) shows characteristic peaks of pure magnetite as labelled with black dots in addition with uncoated sand peaks, indicating the formation of Fe_3O_4 nanoparticles on the sand surface.

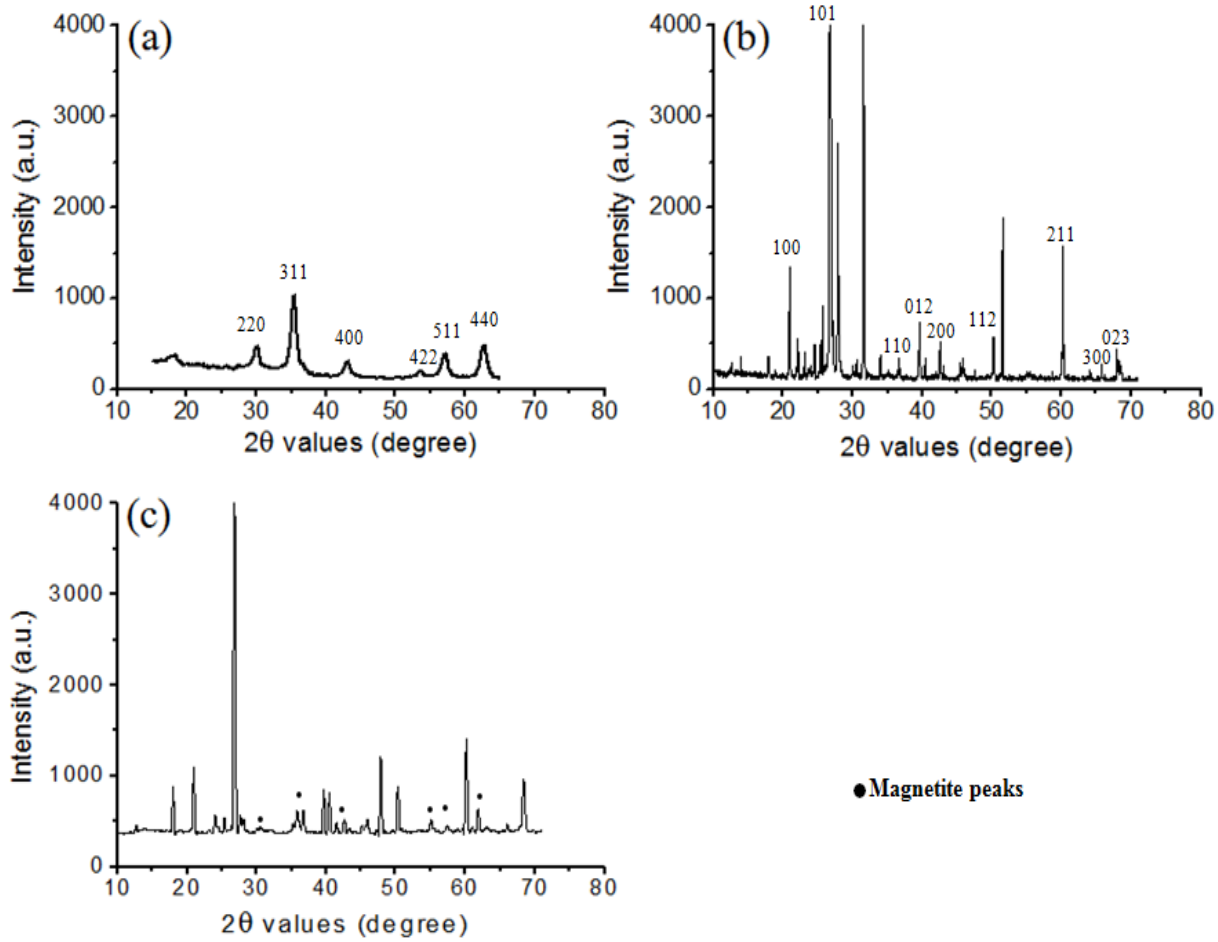

Figure 2.4: XRD pattern of (a) Fe_3O_4 nanoparticles, (b) uncoated sand and (c) Fe_3O_4 nanoparticles coated sand.

2.2.3. Field Emission Scanning Electron Microscopy (FESEM)

The morphology of Fe_3O_4 nanoparticles was examined by Field Emission Scanning Electron Microscopy (FESEM), Hitachi S-4700.

Fig. 2.5 shows FESEM images of (a) Fe_3O_4 nanoparticles, (b-c) uncoated sand, and (d-f) Fe_3O_4 nanoparticles coated sand. Some un-attached Fe_3O_4 nanoparticles were also collected from the reaction solution, which are shown by FESEM image in Fig. 2.5 (a). The bare nanoparticles have size in the range of 20-60 nm. Fig. 2.5 (b) and 2.5 (c) of bare sand particles show that the surface of sand is clear before coating and is covered with Fe_3O_4 nanoparticles of size 20-60 nm after the coating as depicted in Fig. 2.5 (d), 2.5 (e) and 2.5 (f). FESEM images in Fig. 2.5 (a) and 2.5 (d) indicate that the Fe_3O_4 nanoparticles have the same morphology both in solution as well as on the sand surface.

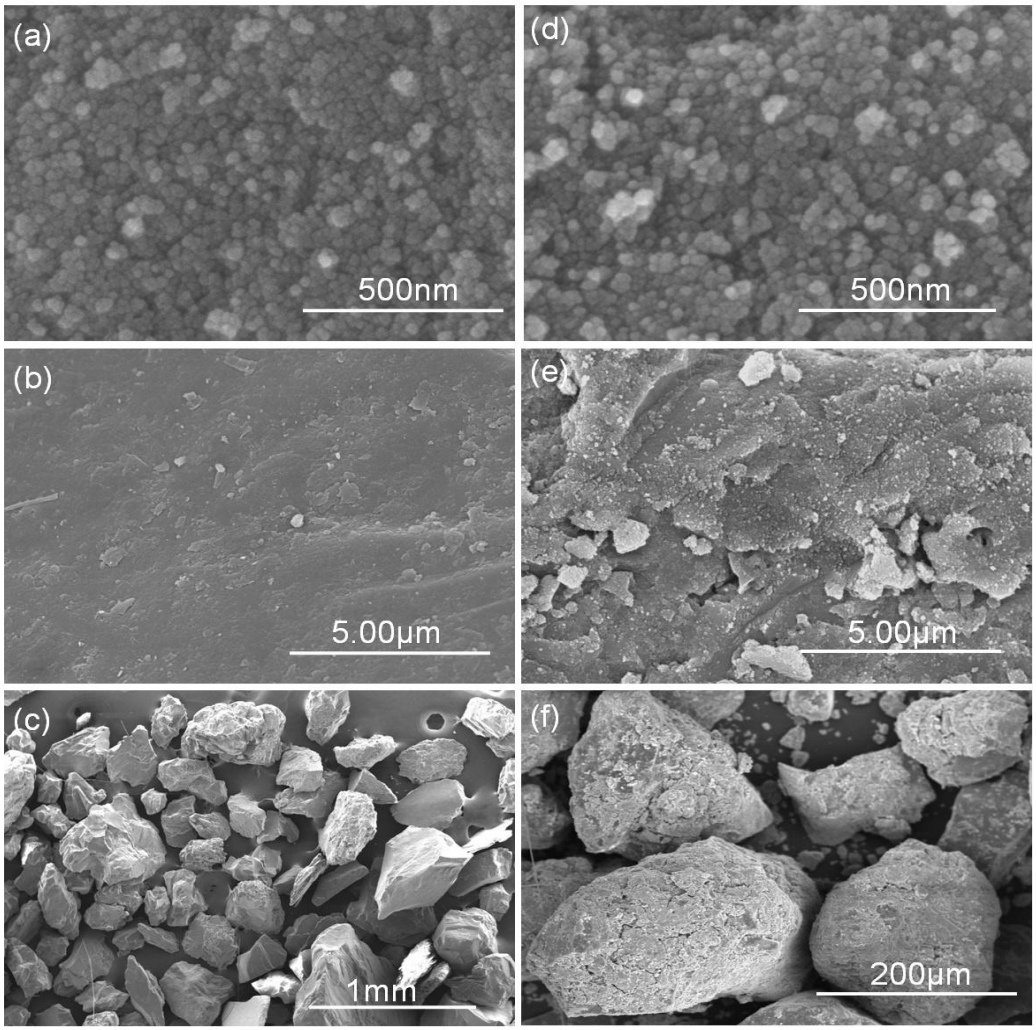

Figure 2.5: FESEM images of (a) Fe_3O_4 nanoparticles, (b-c) uncoated sand, (d-f) Fe_3O_4 nanoparticles coated on sand surface.

2.2.4. Energy Dispersive X-Ray (EDX)

The elemental analysis of uncoated sand and Fe_3O_4 nanoparticles coated sand was performed by using EDX (Oxford X-Max) attached with FESEM.

Fig. 2.6 (a) and (b) shows EDX of the uncoated sand and magnetite nanoparticles coated sand, respectively. It is clear from the Fig. 2.6 (a) that uncoated sand contains silicon and oxygen, which indicates the characteristic of quartz sand and coated sand (Fig. 2.6 (b)) contains iron also in addition with silicon and oxygen, which confirms magnetite coating on sand surface.

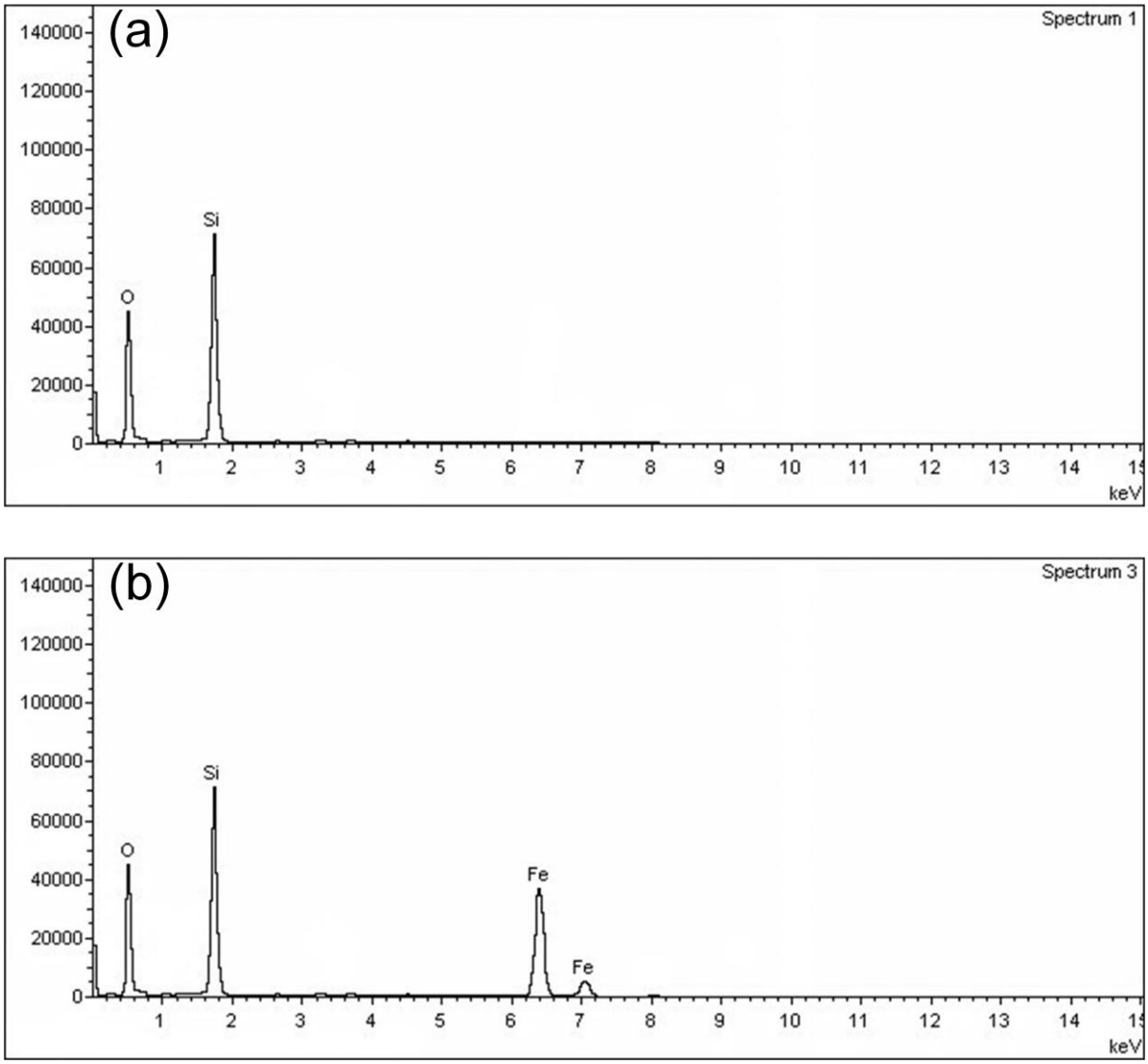

Figure 2.6: EDX spectra of (a) uncoated sand and (b) Fe_3O_4 nanoparticles coated sand.

2.2.5. Brunauer–Emmett–Teller (BET) surface area measurement

The surface area of uncoated sand and Fe_3O_4 nanoparticles coated sand was measured by BET method using Micromeritics model (ASAP-2020). The surface area of uncoated sand and Fe_3O_4 nanoparticles coated was found to be 3 m^2/g and 8 m^2/g, respectively. Thus it has been found that the surface area of coated sand was increased by 5 m^2/g than uncoated sand.

2.3. DETERMINATION OF POINT OF ZERO CHARGE OF ADSORBENT

Magnetite being an iron oxide is amphoteric in nature, i.e. it can acquire positive and negative charges when Fe-OH sites on its surface get protonated or deprotonated as shown in equation 2.1 and equation 2.2, respectively.

$$Fe\text{-}OH + H^+ \Leftrightarrow Fe\text{-}OH_2^+ \quad (2.1)$$

$$Fe\text{-}O\text{-}H \Leftrightarrow Fe\text{-}O^- + H^+ \quad (2.2)$$

The above reactions can be interpreted as the specific adsorption of H^+ and OH^- ions on the hydrated solid/water interface [210]. Thus, to predict the nature of charge on such amphoteric inorganic oxides surface at a given pH of the solution, it is required to determine their point of zero charge (pH_{pzc}).

Fig. 2.7 shows the graph of pH_{final} and $pH_{initial}$ for the determination of point of zero charge of adsorbent. The pH_{pzc} as determined from the point of intersection of $pH_{initial}$ versus pH_{final} curve with the $pH_{initial} = pH_{final}$ line is found to be nearly 7.8. This is in accordance with the point of zero charge value for magnetite determined by Namdeo and Bajpai and Tombacz et al. [210, 211]. The value of point of zero charge obtained in this study i.e. pH_{pzc} 7.8 indicates that at pH 7.8, the surface of adsorbent is neutral. Above pH 7.8 the adsorbent surface is negatively charged and below pH 7.8 the adsorbent surface is positively charged.

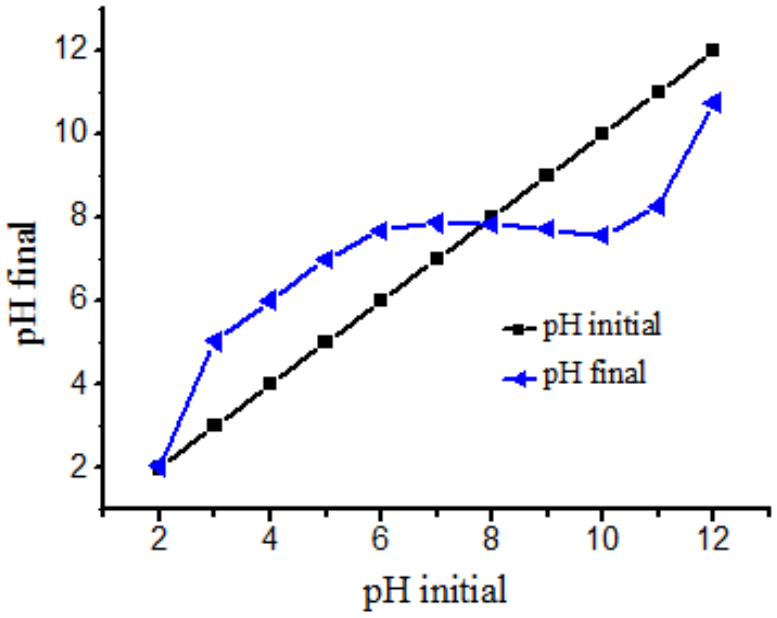

Figure 2.7: $pH_{initial}$ versus pH_{final} plot for determination of pH_{pzc} of adsorbent.

The physical and chemical properties of plain sand and magnetite nanoparticles coated sand obtained from various characterizations are given in Table 2.1.

Table 2.1: Physical and chemical properties of plain sand and magnetite nanoparticles coated sand.

S.No.	Properties	Plain sand	Magnetite nanoparticles coated sand
1.	Geometric mean size	0.6-0.9 mm	~ 0.6-0.9 mm
2.	Color	Greyish white	Black
3.	Magnetic property	Non-magnetic	Magnetic
4.	Surface area, BET (m^2/g)	3	8
5.	pH_{pzc}	-	7.8
6.	Elements present	Silicon and Oxygen	Silicon, Oxygen and Iron

2.4. SUMMARY

We have successfully coated the magnetite nanoparticles of 20-60 nm size on the sand surface. The uncoated and coated sand were characterized by using XRD, FESEM and EDX for structural, morphological and elemental analysis. The surface area of uncoated and coated sand was also calculated using BET surface area analyzer. It was found that the surface area of sand was increased by 5 m^2/g after the magnetite coating. The pH_{pzc} of adsorbent was also calculated and found to be 7.8.

CHAPTER 3

BATCH STUDIES FOR As(III) REMOVAL FROM WATER BY USING MAGNETITE NANOPARTICLES COATED SAND: ADSORPTION KINETICS AND ISOTHERMS

3.1. INTRODUCTION

Arsenic contamination of ground water and surface water is presently a worldwide concern due to its toxic and carcinogenic effects on human health. We have already discussed about chemistry, sources, occurrence and hazardous effects of arsenic on human health in chapter 1. Briefly, in aqueous environment, arsenic is predominantly found in trivalent arsenite such as $H_3AsO_3^0$, $H_2AsO_3^-$, $HAsO_3^{2-}$, AsO_3^{3-} and pentavalent arsenate such as H_3AsO_4, $H_2AsO_4^-$, $HAsO_4^{2-}$, AsO_4^{3-} states [13]. The trivalent arsenite (As(III)) is 25-60 times more toxic than pentavalent arsenate (As(V)). It is comparatively difficult to remove trivalent arsenite from water as it is non-ionic at natural water pH [32, 212]. As(III) exposure slightly higher than 0.1 mg/L in drinking water, may cause neurological damage and its concentration reaching to 0.2 mg/L creates the problem of dermatosis [213].

World Health Organization (WHO) in 1958 categorized arsenic as a toxic substance [214]. Since 1958, WHO has revised its guidelines three times for maximum acceptable concentration level of arsenic in drinking water. In the last edition in 1993, WHO reduced maximum acceptable concentration level of arsenic from 0.05 mg/L to 0.01 mg/L in drinking water with a view to further reduce its concentration in future [60]. Food and Agricultural Organization (FAO) also follows the WHO guidelines and set 0.01 mg/L as the maximum acceptable value of arsenic for irrigation water [215]. United States Environmental Protection Agency (USEPA) has also adopted the new maximum concentration limit for arsenic in drinking water on January 22, 2001 [216]. A number of countries have followed the latest guidelines of WHO, FAO and USEPA, and adopted 0.01 mg/L as their maximum acceptable arsenic value. However, still there are many countries such as China, Bangladesh, India, Nepal etc. which have kept WHO's earlier guideline value i.e. 0.05 mg/L as the maximum acceptable arsenic value [217, 218]. According to a study in 2007, over 137 million people in around 70 countries including Bangladesh, India, Taiwan, China, Chile, Vietnam, Ghana and USA are affected by arsenic poisoning of drinking water [219, 220]. To mitigate human exposure and to meet the low admissible level of arsenic in drinking water, the development of technologies at reasonable cost is a big challenge.

The countries or part of countries which are highly affected by arsenic concentration are: Victoria (Australia) where groundwater contains 1 to 300,000 μg/L arsenic and surface water contains 1 to 28,300 μg/L arsenic [221]. Ground water of northern Chile has 190 to 21,800 μg/L [222], Bangladesh has 50 to 3,200 μg/L [223, 224] and Vietnam has 1 to 3,050 μg/L concentration of arsenic [225]. North western Argentina contains 126 to 10,650 μg/L arsenic

in spring water and 52 to 1045 μg/L in river water [226]. Brazil contains 0.4 to 350 μg/L arsenic in surface water [227] and Mexico has arsenic contamination from 21 to 1,070 μg/L in wells [228-230]. Arsenic contaminated water in Canada is up to 3,000 μg/L [231], in India up to 3,880 μg/L [232-234], in Pakistan up to 906 μg/L [235], in USA up to 210 μg/L [236] and in Switzerland up to 170 μg/L [237].

In order to remove both As(III) and As(V) from water, USEPA evaluated various treatment technologies such as bioremediation, ion exchange, coagulation and filtration, reverse osmosis, electro-coagulation, adsorption etc. [121] which we have already discussed in detail in chapter 1. Most of these methods have several disadvantages such as requirement of expensive equipments, sludge production, time consuming and complexity. Among these adsorption and coagulation are believed to be the cost effective methods, however coagulation needs skilled operator and shows more effectiveness only on some specific iron and aluminium salts. However, the adsorption method due to its low cost, simplicity in design, sludge free operation, ease of operation and potential of regeneration has gained popularity. Moreover, if the adsorbent is chosen carefully and experiments are conducted in appropriate conditions then the adsorption based methods are capable of removing arsenic to a much lower level than any other method. This also shows easy separation of even small amount of toxic elements from large volume of water [238]. Many types of adsorbents such as activated alumina (AA), iron based adsorbents (IBS), chitosan based adsorbents, graphene oxide composites, magnetic nanochains etc. are commonly used for arsenic removal from water [109-118, 239-244].

Among various adsorbents iron oxide adsorbents have been widely investigated to remove arsenic from aqueous solutions due to strong affinity of iron oxides towards arsenic. The strong affinity of iron oxides to arsenic is evident from an observation in which arsenic exists on the surface of iron oxide even in natural environment [245]. Recently, the use of nanoparticles in environmental remediation processes is increased due to their small size and high surface area. Iron oxide nanoparticles, due to strong affinity to arsenic have gained growing interest in water purification [177, 193, 196]. Among different iron oxide nanoparticles, magnetite (Fe_3O_4) nanoparticles have been proved to be potential adsorbents owing to their strong adsorption capacity for arsenic removal.

In the second chapter we have discussed the synthesis of adsorbent by coating magnetite nanoparticles on sand surface by co-precipitation method. In this chapter we have described the potential of synthesized adsorbent for the removal of most toxic As(III) from drinking

water. Batch experiments were performed to analyze the influence of initial pH of the solution, adsorbent dose, initial As(III) concentration and contact time on As(III) removal efficiency. The experimental adsorption kinetics data and isotherms data was fitted in theoretical models viz. pseudo-first-order, pseudo-second order and intra-particle diffusion kinetics models; Langmuir and Freundlich adsorption isotherms models, respectively. Since in natural water other ions are also present which normally affect arsenic removal efficiency due to their competing behaviour for adsorption. Therefore, the effect of few commonly present ions such as phosphate, sulphate, bicarbonate and chlorine on As(III) removal efficiency was also investigated. Desorption and readsorption behaviour of adsorbent was also analyzed.

3.2. MATERIALS AND METHODS

3.2.1. Materials

All the chemicals used in this study were of analytical grade and purchased from Sigma Aldrich. The chemicals were used as received without further purification. All glasswares were cleaned with acid and rinsed with milli-Q water before use. The solutions were prepared in ultrapure milli-Q water. To prepare As(III) stock solution, a known amount of As(III) oxide was dissolved in milli-Q water, and 4 g/L NaOH was used to enhance its solubility. To adjust the pH of solution, standard acid and base solutions i.e. 0.1 M HNO_3 and 0.1 M NaOH were used, respectively. Disodium hydrogen phosphate anhydrous (Na_2HPO_4), sodium sulphate (Na_2SO_4), sodium bicarbonate ($NaHCO_3$) and sodium chloride (NaCl) salts were used to produce the various co-existing ions viz. PO_4^{3-}, SO_4^{2-}, HCO_3^{2-} and Cl^- in the solution.

3.2.2. Batch adsorption experiments

Batch adsorption experiments were carried out to obtain the kinetics and equilibrium data. In batch adsorption experiments the effect of various parameters viz. contact time, initial pH of aqueous solution, adsorbent dose and initial As(III) concentration on As(III) removal efficiency and adsorption capacity was investigated. All the experiments were performed at room temperature in an incubator shaker at an agitation speed of 200 rpm. To study the effect of contact time on As(III) adsorption, the contact time was varied from 30 to 420 min, using 25 g/L Fe_3O_4 coated sand adsorbent at initial As(III) concentration of 1 mg/L and pH 7.0.The effect of initial pH of the aqueous solution was studied by varying it from 2.0 to12.0 for fixed adsorbent dose, contact time 420 min, and initial As(III) concentration of 1 mg/L at room

temperature. The study of the adsorbent dose effect was accomplished, by varying it from 5 g/L to 30 g/L and keeping other parameters fixed. In order to conduct adsorption isotherm studies, concentration of As(III) was varied from 1 mg/L to 103.8 mg/L for fixed values of adsorbent dose, contact time and pH. The batch adsorption experiments were also performed to study the individual effect of prominent co-existing ions such as PO_4^{3-}, SO_4^{2-}, HCO_3^{2-} and Cl^- on the As(III) removal efficiency. The concentration of these ions was varied from 5 mg/L to 100 mg/L while other parameters were kept fixed. The above solutions after required agitation were filtered using 0.45 µm durapore filter paper, acidified with 1 % HNO_3 and finally analyzed for residual As(III) concentration using inductively coupled plasma mass spectrometer (ICP-MS).

The experiment was also performed separately for sand and magnetite nanoparticles with initial As(III) concentration of 5 mg/L and adsorbent dose (sand or magnetite) of 0.2 g/20 mL to understand the role of surface coated magnetite nanoparticles. The batch experiments were also carried out with different dosage of pure magnetite nanoparticles (real adsorbent) in order to know the amount of real adsorbent required to reduce the As(III) concentration below MCL value set by WHO i.e. 10 µg/L.

As(III) removal efficiency of Fe_3O_4 nanoparticles coated sand was calculated by using the formula:

$$\%\ \mathrm{As(III)removal} = \frac{C_o - C_e}{C_o} \times 100 \qquad (3.1)$$

and the amount of As(III) adsorbed (mg) per unit mass of adsorbent (g) i.e. q_e was determined by using the formula:

$$q_e = \frac{C_o - C_e}{M} \times V \qquad (3.2)$$

where, C_o and C_e are initial and final As(III) concentrations (mg/L), respectively, V is the volume of solution in liters and M is the mass of the adsorbent in grams.

3.2.3. Desorption and readsorption experiments

The desorption studies for As(III) were carried out using 0.1 M and 0.5 M sodium hydroxide solutions as desorbing agent. 40 mL of 10 mg/L As(III) concentration was treated with 1 g of adsorbent for 420 min of contact time. The solution was filtered and the adsorbent was washed several times with distilled water to remove any unadsorbed As(III) ions. The saturated adsorbent was then treated with 40 mL of 0.1 M and 0.5 M sodium hydroxide

solutions separately for 420 min and then filtered and washed with distilled water to remove excess of sodium hydroxide. The adsorbent was again treated with 40 mL of As(III) solution of 10 mg/L concentration to study the readsorption behaviour of adsorbent.

The As(III) desorption percentage was calculated by using equation 3.3:

$$\%\ \text{Desorption} = \frac{\text{released As(III)(mg/L)}}{\text{initially adsorbed As(III)(mg/L)}} \times 100 \qquad (3.3)$$

3.2.4. Analytical measurements

pH measurements were made with an Oakton pH meter (pH 700 Benchtop Meter) using a combined glass electrode and ATC probe. The pH meter was calibrated with buffers of pH 4.0, 7.0 and 10.0 before any measurement. The initial and residual As(III) concentrations were determined by using ICP-MS, Perkin Elmer Elan DRC 6000.

3.3. THEORETICAL INVESTIGATIONS OF EXPERIMENTAL DATA

3.3.1. Adsorption kinetics

The adsorption kinetics generally depends on the physical and/or chemical features of the adsorbent material which influence the adsorption mechanism. Therefore, it is very important to fit the experimental kinetics data in theoretical kinetic models in order to estimate the rate of adsorption and potential rate-controlling step. In the present study, we have examined the capability of most widely used kinetic models i.e. pseudo-first-order and pseudo-second-order for the better fitting of our data.

3.3.1.1. Pseudo-first-order kinetics model

The following equation 3.4 represents pseudo-first-order kinetics model [246]

$$\log(q_e - q_t) = \log q_e - \frac{k_{ads}}{2.303} t \qquad (3.4)$$

where, q_e (mg/g) and q_t (mg/g) are amount of As(III) adsorbed per unit mass of adsorbent at equilibrium and time t, respectively. The k_{ads} is pseudo-first-order rate constant, which can be obtained from slope of linear plot of $\log(q_e\text{-}q_t)$ versus time (t).

3.3.1.2. Pseudo-second-order kinetics model

The main assumptions of pseudo-second-order kinetics model are: (i) the chemical adsorption involving valence forces through sharing or exchange of electrons between adsorbent and

adsorbate is the rate limiting step and (ii) the adsorption follows the Langmuir equation i.e. there is monolayer adsorption of arsenic ions on the homogeneous adsorbent surface [247].
Equation 3.5 represents pseudo-second-order kinetics model [248]

$$\frac{t}{q_t} = \frac{1}{h} + \frac{t}{q_e} \tag{3.5}$$

and

$$h = kq_e^2 \tag{3.6}$$

where, q_e (mg/g) and q_t (mg/g) are amount of As(III) adsorbed per unit mass of adsorbent at equilibrium and time t, respectively. Here, k is the pseudo-second-order adsorption rate constant, and h is the initial adsorption rate (mg g^{-1} h^{-1}). The values of q_e (1/slope), k (slope^2/intercept) and h (1/intercept) can be calculated from the linear plot of t/q_t vs t.

3.3.1.3. Intra-particle diffusion model

It is well known that a typical adsorption of liquid adsorbate on solid adsorbent (liquid/solid adsorption process) involves either boundary layer diffusion i.e. external mass transfer or intra-particle diffusion i.e. mass transfer through pores or a combination of both. This means that the adsorption kinetics can be controlled by boundary layer diffusion or intra-particle diffusion, i.e. one of these processes can be the rate limiting step [249]. Therefore, in this study the adsorption diffusion model i.e. intra-particle diffusion model given by Weber and Morris was further applied to experimental kinetics data in order to distinguish the boundary layer diffusion or intra-particle diffusion process of adsorption.
Equation 3.7 represents intra-particle diffusion model [250]

$$q_t = k_i t^{1/2} \tag{3.7}$$

where, k_i is the intra-particle diffusion rate constant and q_t is the amount of As(III) adsorbed per unit mass of adsorbent at time '*t*'.

3.3.2. Adsorption isotherms

To design adsorption systems, adsorption isotherms also known as equilibrium data are the fundamental requirements. When the adsorption capacity of the adsorbent materials reaches to its maximum the equilibrium is attained. At equilibrium the rate of adsorption is equal to the rate of desorption. The theoretical adsorption capacity of an adsorbent material can be calculated by fitting the experimental isotherm data in theoretical adsorption isotherm

models. There are mainly two well recognized theoretical adsorption isotherm models viz. Langmuir and Freundlich models reported in the literature. The adsorption isotherm gives an idea about the interaction between adsorbate molecules (As(III) ions in this study) and adsorbent (magnetite nanoparticles coated sand in this study) in an adsorption system. These isotherms show that how the adsorbate molecules are distributed between the aqueous solution and the adsorbent surface at equilibrium. Therefore, in order to study the adsorbate-adsorbent interaction, and to compute various adsorption parameters, we have applied Freundlich and Langmuir adsorption isotherm models to fit the experimental adsorption equilibrium data of As(III) on magnetite nanoparticles coated sand.

3.3.2.1. Freundlich isotherm

Freundlich adsorption isotherm is generally based on the assumption that there is a multilayer adsorption of adsorbate molecules on the heterogeneous surface of the adsorbent. This isotherm represents an initial surface adsorption followed by a condensation effect resulting from strong adsorbate-adsorbate interaction. In many instances, the heat of adsorption decreases in magnitude with increasing extent of adsorption. This decrease in heat of adsorption is logarithmic which implies that there is exponential distribution of adsorption sites with respect to adsorption energy.

The Freundlich isotherm in linear form is represented as [251]

$$\log(q_e) = \log K_F + \frac{1}{n}\log(C_e) \qquad (3.8)$$

where, C_e is the equilibrium concentration of As(III) in the solution (mg/L), q_e is the amount of As(III) adsorbed onto the Fe_3O_4 nanoparticles coated sand at equilibrium (mg/g), K_F is the adsorption capacity indicator and n (which lies between 1 to 10) is the heterogeneity factor indicating favourable adsorption. It is reported that if the value of n lies between 2 to 10 then adsorption is considered as better adsorption and if it lies between 1 to 2 then adsorption is considered to be good.

3.3.2.2. Langmuir isotherm

Langmuir adsorption isotherm model is one of the simplest types of theoretical adsorption isotherm models. This isotherm model is based on the assumptions that (i) maximum adsorption corresponds to a saturated monolayer of adsorbate molecules on the homogeneous surface of the adsorbent. This means that Langmuir represents the equilibrium distribution of

adsorbate molecules (metal ions) between the solid and liquid phases, (ii) every adsorption site is identical and energetically equivalent, which means that thermodynamically each adsorption site can hold only one adsorbate molecule i.e. the energy of adsorption is constant and (iii) the ability of molecule to bind and adsorbed is independent of whether or not neighbouring sites are occupied. This means that there will be no interactions between adjacent adsorbate molecules on the surface and immobile adsorption sites. This also means that there is no transmigration of adsorbate molecules in the plane of adsorbent surface.

Linear form of Langmuir isotherm model can be written as [252, 253]

$$\frac{C_e}{q_e} = \frac{C_e}{q_m} + bq_m \qquad (3.9)$$

where, C_e and q_e are the As(III) concentration in the solution and As(III) amount adsorbed at equilibrium, respectively. The q_m (mg/g) is the saturated monolayer adsorption capacity, and b (L/mg) is the Langmuir constant related to the affinity between solute and adsorbent. Higher is the value of b, stronger is the affinity of metal ion adsorption.

In Langmuir adsorption isotherm, a dimensionless separation factor or equilibrium parameter, 'r' is considered as an essential feature. The value of 'r' predict the adsorption efficiency of the isotherm process i.e. whether an adsorption system is "favourable" or "unfavourable". The value of 'r' can be calculated by using the following equation [254]

$$r = \frac{1}{1 + bC_o} \qquad (3.10)$$

where, C_o is the initial concentration of As(III) and b is Langmuir constant. According to the value of 'r' shape of the isotherm can be defined as shown in Table 3.1.

Table 3.1: Type of isotherm according to value of 'r'.

Value of '*r*'	**Type of adsorption**
$0 < r < 1.0$	Favourable
$r > 1.0$	Unfavourable
$r = 1.0$	Linear
$r = 0$	Irreversible

The value $0 < r < 1.0$ represents favourable Langmuir isotherm adsorption, whereas $r = 0$ represents irreversible adsorption, $r = 1$ shows linear adsorption and $r > 1.0$ represents unfavourable adsorption.

3.3.3. Coefficient of determination or square of correlation coefficient (R^2)

When we fit the experimental data in theoretical models as explained above for adsorption kinetics and adsorption isotherms, the goodness of fit of the data is explained on the basis of R^2 value which is known as coefficient of determination or square of correlation coefficient. The brief explanation of coefficient of determination is described ahead.

The coefficient of determination denoted by R^2 and pronounced as *R* squared, is a statistical number that indicates how well data fit a theoretical or statistical model. A statistical model can be simply a straight line or a curve. The coefficient of determination R^2 is useful because it gives the proportion of the variance (fluctuation) of one quantity that is estimated from the other quantity. Further, the value of R^2 allows us to determine how certain one can be in estimating the values from a particular model or graph.

The coefficient of determination is such that $0 \leq R^2 \leq 1$ and tells the efficiency of the linear relationship between x and y. If $R^2 = 0$, then it means that the dependent quantity cannot be estimated from the independent quantity. It also indicates that the regression line does not fit the data at all which means that the data is more non-linear than the curve allows or it is random. If $R^2 = 1$, then it means that the dependent quantity can be estimated without error from the independent quantity. We can also say that the regression line fits the data well. The value of R^2 between 0 and 1 indicates the limit to which the dependent quantity is estimated [255, 256]. For example R^2 of 0.10 means that 10 percent of the variance in y is estimated from x. Moreover, the coefficient of determination defines the amount of the data that is nearest to the line of best fit. For example, if $R = 0.922$, then $R^2 = 0.850$, which means that 85 % of the total deviation in y can be explained by the sequential association between x and y (as described by the regression equation). The other 15 % of the total deviation in y leftover unexplained.

The coefficient of determination is an estimation of how well the regression line predicts the data. If the regression line passes exactly through every point on the scatter plot, it would be able to explain all of the deviation. As the line moves away from the points it becomes typical to explain the deviation.

Equation 3.11 represents the formula for calculating the coefficient of determination for a linear regression model with one independent variable [255, 256]

$$R^2 = \left\{\frac{1}{N}\frac{\sum[(x_i - \bar{x})(y_i - \bar{y})]}{(\sigma_x \times \sigma_y)}\right\}^2 \quad (3.11)$$

where, N is the number of observations used to fit the statistical model, Σ is the summation symbol, x_i is the value of ith observation of independent quantity (x), $\bar{x}$ is the mean of independent quantity (x), y_i is the value of ith observation of dependent quantity (y), $\bar{y}$ is the mean of dependent quantity (y), σ_x is the standard deviation of independent quantity (x), and σ_y is the standard deviation of dependent quantity (y).

3.4. RESULTS AND DISCUSSION

3.4.1. Effect of contact time on As(III) removal

Fig. 3.1 shows the effect of contact time on % As(III) removal efficiency and adsorption capacity (q_t = mg/g) for initial As(III) concentration of 1 mg/L. We have observed that the As(III) removal takes place in two phases i.e. fast and slower adsorption phase. Initially within 30 min of contact time rapid removal (82.84 % of As(III) was removed) of As(III) occurred and after that the arsenic removal rate decreased and took about 360 min to achieve the adsorption equilibrium as shown in Fig. 3.1. Although, the adsorption equilibrium was achieved in 360 min of contact time, but we have performed all batch adsorption experiments for prolonged contact time of 420 min to ensure complete adsorption. The observed fast adsorption of As(III) by Fe_3O_4 nanoparticles coated sand in the first phase is probably due to the external surface adsorption process. In this process, all the adsorption sites existing on the adsorbent external surface are occupied at a fast rate by adsorbing As(III) ions (in this study 30 min). The adsorption mechanism occurred in the first phase can be termed as the 'adsorption controlled by the surface process' [185]. After 30 min, when all the external adsorption sites of Fe_3O_4 are filled, the process of As(III) removal got slower because the As(III) does not find an immediate contact surface of Fe_3O_4 nanoparticles, however, the sub-layered Fe_3O_4 nanoparticles still have adsorption sites for As adsorption. Once the external adsorption surface sites are occupied, the As(III) approached to the available adsorption sites on the surface of sub-layered Fe_3O_4 nanoparticles. In this process, to reach the available adsorption sites, As(III) has to diffuse through the Fe_3O_4 nanoparticles. Due to the intra-particle diffusion of As(III), the rate of adsorption decreases and since the process is now

diffusion controlled, therefore, it can be termed as the 'adsorption controlled by diffusion' [257]. For As(III), longer is the intra-particle diffusion distance slower is the adsorption rate, as observed. At equilibrium, 99.6 % As(III) was removed for initial As(III) concentration of 1 mg/L.

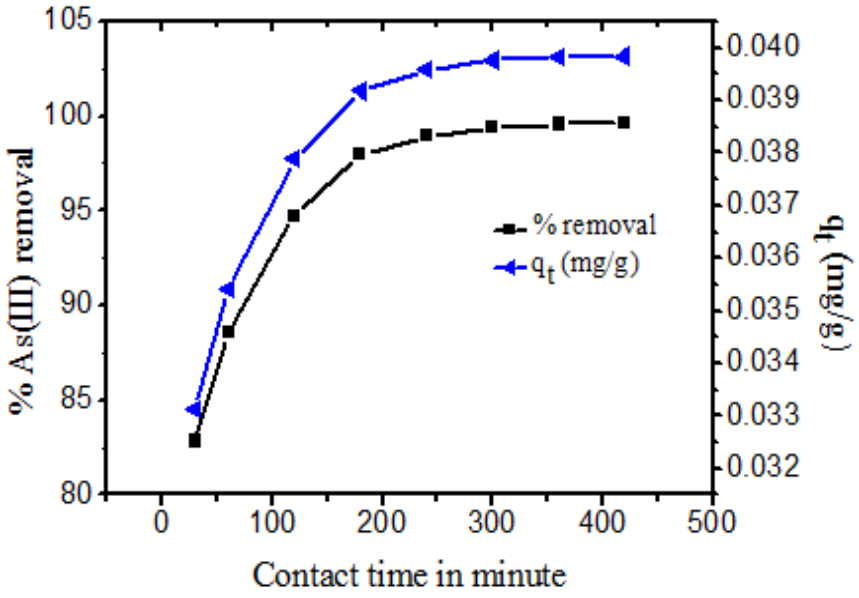

Figure 3.1: Effect of contact time on % As(III) removal efficiency and adsorption capacity (q_t = mg/g).

3.4.2. Adsorption kinetics

The plots of pseudo-first-order and pseudo-second-order kinetics model for As(III) removal are shown in Fig. 3.2 (a) and 3.2 (b), respectively. The values of various corresponding parameters; k_{ads}, k, h and coefficients of determination R^2 obtained from these plots are shown in Table 3.2. The experimental kinetics data fitted well in pseudo-second-order kinetics model with higher coefficient of determination (R^2 = 0.999) as compared to pseudo-first-order kinetics model which has comparatively lower coefficient of determination (R^2 = 0.978). Also the experimental value of q_e i.e. 0.0398 is more close to theoretical q_e value 0.040 obtained from pseudo-second-order kinetics model in comparison to 0.015 q_e value obtained from pseudo-first-order kinetics model. This also supports that data fitted well in pseudo-second-order kinetics model. These results reveal that the As(III) adsorption process is chemisorption i.e. there is some chemical bonding between adsorbent (magnetite nanoparticles coated sand) and adsorbate (As(III) ions) [257].

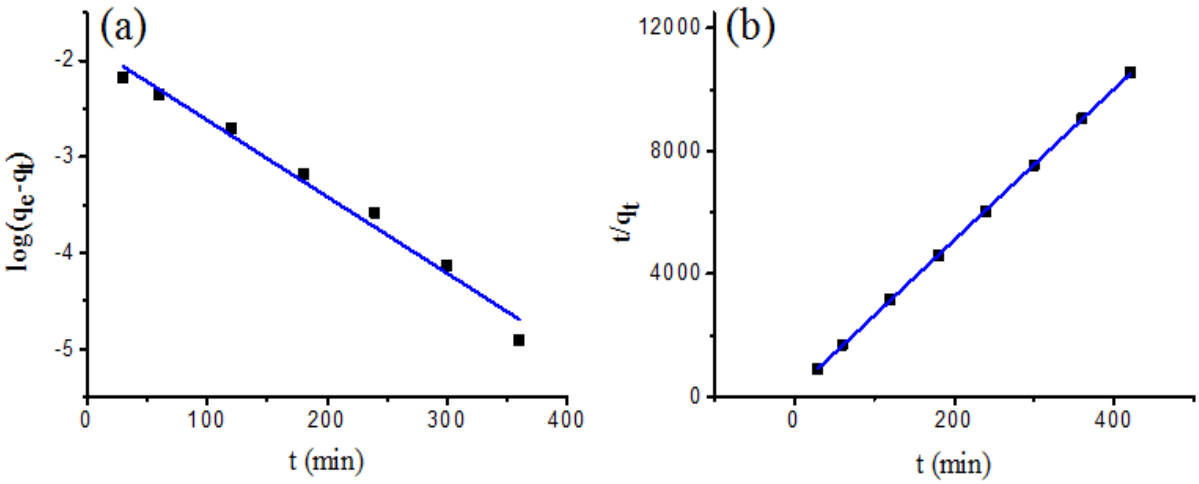

Figure 3.2: Adsorption kinetics (a) pseudo-first-order model and (b) pseudo-second-order model for As(III) removal by Fe_3O_4 nanoparticles coated sand.

Fig. 3.3 shows the plot of intra-particle diffusion model for As(III) removal by magnetite nanoparticles coated sand. The values of intra-particle diffusion rate constant obtained from slope of the plot and coefficient of determination (R^2) are given in Table 3.2. This is the assumption of intra-particle diffusion model that if the graph between amount of adsorbate adsorbed 'q_t' and square root of time '$t^{1/2}$' gives a straight line then intra-particle diffusion is the rate limiting step. Further, this model also assumed that the plot should pass through the origin for intra-particle diffusion to be the sole rate limiting step.

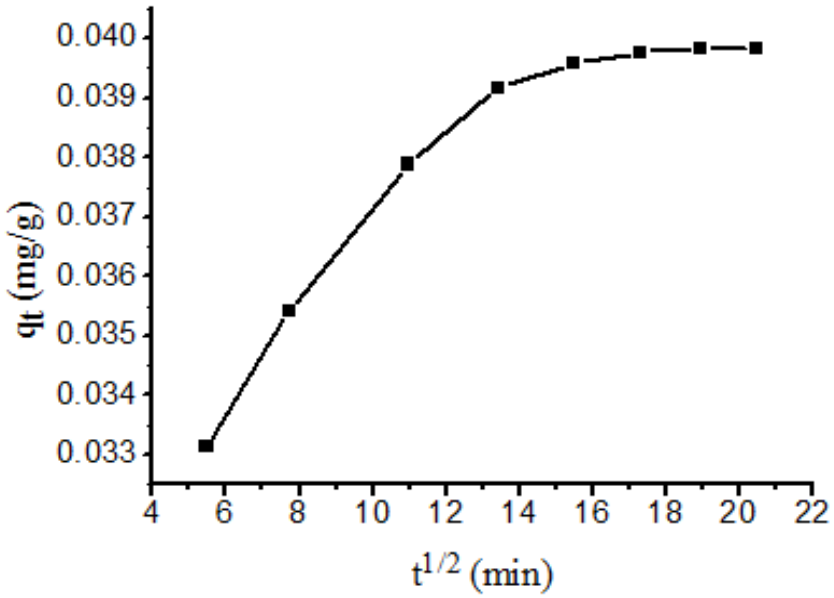

Figure 3.3: Intra-particle diffusion model for As(III) removal by Fe_3O_4 nanoparticles coated sand.

However in the present study, the plot of q_t and $t^{1/2}$ is not a straight line and also the plot is not passing through the origin (Fig. 3.3). It is clear from the Fig. 3.3 that three steps are

involved in adsorption i.e. (i) sharper portion attributing to boundary layer diffusion of solute molecules, (ii) second portion is the gradual adsorption phase where intra-particle diffusion is rate limiting step followed by, (iii) final equilibrium phase where the concentration of solute in the solution become extremely low that the intra-particle diffusion starts to slow down. These results reveal that the As(III) adsorption on magnetite nanoparticles coated sand is a complex process in which both surface adsorption and intra-particle diffusion are contributing towards the rate of adsorption [208].

Table 3.2: Pseudo-first-order and pseudo-second-order kinetic parameters and intra-particle diffusion model parameters for As(III) adsorption by Fe_3O_4 nanoparticles coated sand.

Pseudo-first-order parameters			**Pseudo-second-order parameters**				**Experi-mental q_e (mg/g)**	**Intra-particle diffusion model parameters**	
k_{ads}(min^{-1})	R^2	q_e	k (g mg^{-1} min^{-1})	h (mg g^{-1} min^{-1})	q_e(mg/g)	R^2		K_i (mg g^{-1} min$^{1/2}$)	R^2
0.0183	0.978	0.015	3.21	0.0053	0.040	0.999	0.0398	0.000432	0.824

We have also performed arsenic removal experiments separately for sand and magnetite nanoparticles with initial As(III) concentration of 5 mg/L and adsorbent dose (sand or magnetite) of 0.2 g/20 mL. With sand particles arsenic was reduced only to 4.587 mg/L from 5 mg/L initial arsenic concentration. On the other hand magnetite nanoparticles reduced arsenic concentration below 1 parts per trillion (ppt) as the amount was not detectable in the sample by ICP-MS (ICP-MS instrument lower detection limit was 1 ppt). As(III) removal efficiency of sand was found to be 8.26 % and of magnetite nanoparticles was approximately 100 % as arsenic was not detectable in the sample. Thus on the basis of results obtained we can say that sand is not able to remove arsenic. It is only magnetite nanoparticles which are responsible for arsenic removal.

3.4.3. Effect of initial solution pH on As(III) removal

The pH of water is considered an important factor in the adsorption based wastewater treatment experiments as it affects metal speciation in the water [194]. Fig. 3.4 shows the effect of water pH on the removal efficiency and adsorption capacity of As(III) by Fe_3O_4 coated sand. The effect of pH can be explained in terms of point of zero charge (pH_{pzc}) of the adsorbent (pH_{pzc} of adsorbent was nearly 7.8 as shown in Fig. 2.7 given in chapter 2) at which the surface of the adsorbent is neutral. From Fig. 3.4, it can be seen that with an increase in the pH of water from 2.0 to 8.0, As(III) removal efficiency increases from 98.92 % to 99.63 % and the adsorption capacity increases from 0.0395 to 0.0398 mg/g. This is due to the fact that below pH_{pzc} (7.8) the surface of adsorbent Fe_3O_4 is positively charged and As(III) exists in non-ionic (H_3AsO_3) state in the low pH (2.0 to 9.2) range. Therefore, when non-ionic As(III) species comes in contact with Fe_3O_4 its positively charged surface helps non-ionic As(III) to convert into anionic one, which in turn assists adsorption process [258].
With increase in pH from 8.0 to 12.0, As(III) removal efficiency decreases from 99.63 % to 62.8 % and adsorption capacity decreases from 0.0398 to 0.0251 mg/g. Above pH 9.2, As(III) dissociates and produces anionic $H_2AsO_3^-$ and $HAsO_3^{2-}$ ions and also above pH_{pzc} (7.8) the adsorbent surface become negatively charged. Therefore in this pH range, the decreasing As(III) uptake and decreasing adsorption capacity are due the following reasons: (i) the competition of excessive OH^- ions for adsorption, (ii) domination of negatively charged sites on Fe_3O_4 nanoparticles coated sand and (iii) domination of negatively charged As(III) species ($H_2AsO_3^-$). With increasing pH, there is a gradual increase in the repulsive forces between negatively charged Fe_3O_4 nanoparticles coated sand and the negatively charged As(III) ions, which results in a decreasing As(III) removal efficiency [208, 259]. We know that most of the groundwater exists in the pH range from 7.0 to 7.5, therefore, in this study we have performed other batch experiments at most natural pH '7.0'.

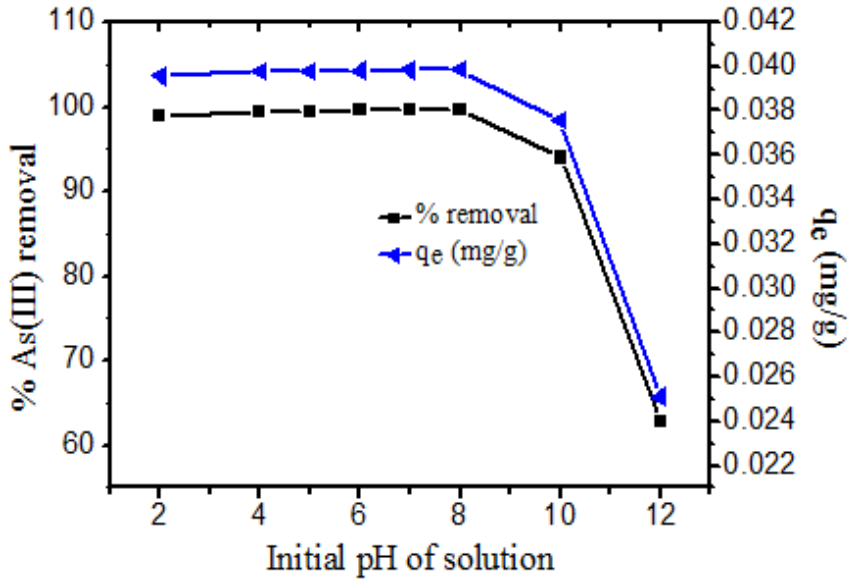

Figure 3.4: Effect of pH on % As(III) removal efficiency and adsorption capacity (q_e = mg/g).

3.4.4. Effect of adsorbent dose on As(III) removal

Fig. 3.5 shows the effect of adsorbent dose on % As(III) removal efficiency and adsorption capacity (q_e = mg/g) at fixed initial As(III) concentration of 1 mg/L. It has been observed that with an increase in adsorbent dose from 5 g/L to 30 g/L, the As(III) removal efficiency increases from 88.93 % to 99.89 %, which is obvious due to available more active sites at higher concentrations of the adsorbent [260, 261]. However, beyond 25 g/L dose, no significant change in As(III) removal efficiency was observed. On the other hand the adsorption capacity decreased from 0.178 mg/g to 0.0333 mg/g with increase in adsorbent dose. This decrease is due to the interference between binding sites at higher adsorbent dose or inadequate number of As(III) ions in the solution with respect to available binding sites [262, 263]. In this plot, the point of intersection (Fig. 3.5) is usually considered as the optimum dose that represents balance between % As(III) removal efficiency and adsorption capacity. In this study, the point of intersection is approximately at 10 g/L of adsorbent dose, but for this dose only 96.55 % As(III) removal was achieved, and 0.0344 mg/L As(III) was still there in the solution, which is higher than the MCL value set by WHO. Therefore, a dose of 25 g/L was selected for further analysis as this dose was sufficient to reduce As(III) concentration below the MCL value. However, in this study it should be noted that the dose of real adsorbent (Fe_3O_4 nanoparticles) might be much lesser than the weighted dose because it was coated on bulky sand particles, the weighted dose is actually the contribution of both

real adsorbent Fe_3O_4 nanoparticles and sand. The experiment was also performed using bare magnetite nanoparticles by varying adsorbent dose from 50 mg/L to 1 g/L to know the minimum amount of real adsorbent needed to reduce arsenic concentration below permissible limit. We have found that 200 mg/L of magnetite nanoparticles were sufficient to reduce As(III) concentration below 10 µg/L from initial As(III) concentration of 1 mg/L. The amount of real adsorbent required to reduce arsenic concentration below permissible limit is less than the commercially available adsorbent [185].

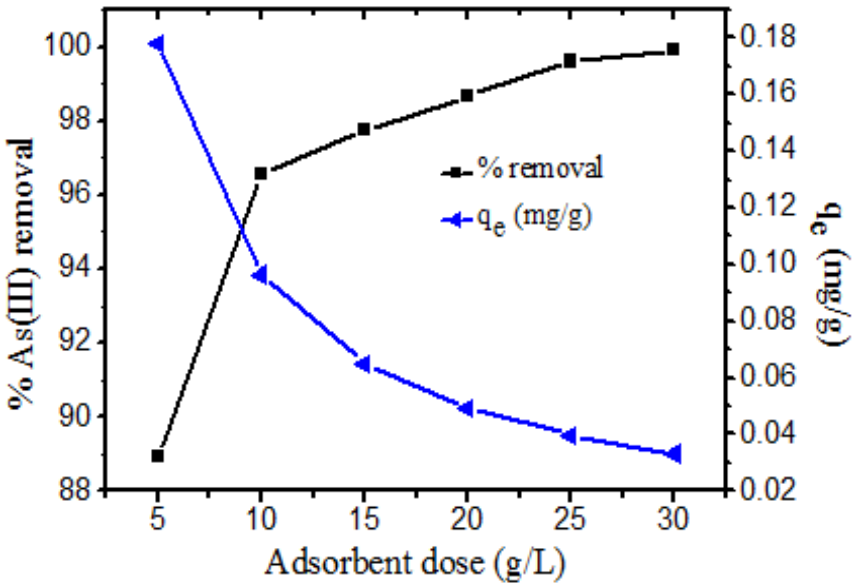

Figure 3.5: Effect of adsorbent dose on % As(III) removal efficiency and adsorption capacity (q_e = mg/g).

3.4.5. Effect of initial As(III) concentration

Fig. 3.6 shows the effect of initial As(III) concentration on the removal efficiency and adsorption capacity of Fe_3O_4 nanoparticles coated sand. It has been observed that with the increase in initial As(III) concentration the As(III) removal efficiency decreases while the adsorption capacity increases and became saturated at 80 mg/L of As(III) concentration and further addition of As(III) does not cause any significant change in adsorption capacity. This is because at lower As(III) concentration, the number of adsorbent surface active sites are sufficiently large and accommodates abundant of As(III) ions. An increase in the As(III) concentration causes a reduction in the proportion of surface active sites to As(III) ions and thus an insufficient accommodation of As(III) ions results in the decreasing % As(III) removal efficiency. Furthermore, a driving force is provided by initial As(III) concentration

to overcome all mass transfer resistances between the adsorbent and adsorption medium which results in higher adsorption capacities at higher initial As(III) concentration [262].

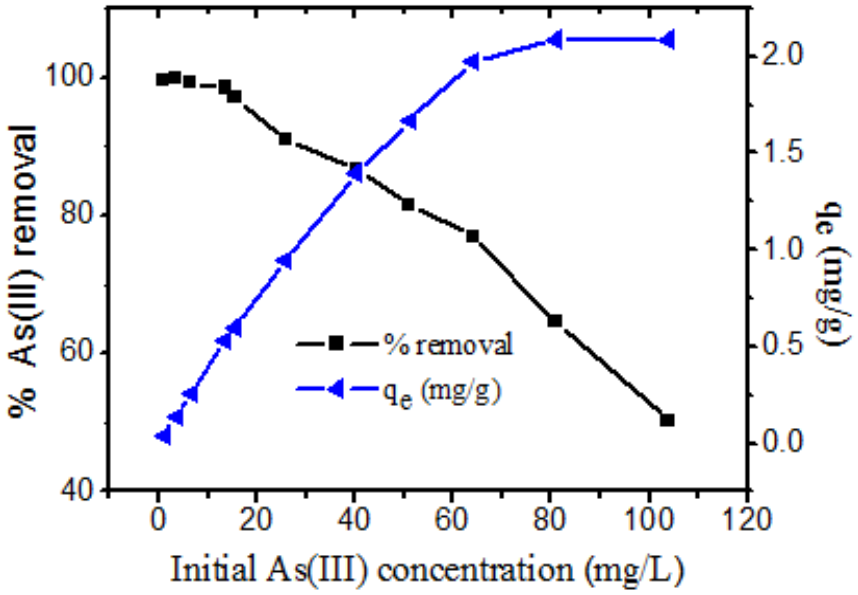

Figure 3.6: Effect of initial As(III) concentration on % As(III) removal efficiency and adsorption capacity (q_e = mg/g).

3.4.6. Adsorption isotherms

Fig. 3.7 (a) and 3.7 (b) shows the Freundlich and Langmuir adsorption isotherm plots for As(III) removal by Fe_3O_4 nanoparticles coated sand, respectively. The values corresponding to various parameters of Freundlich and Langmuir adsorption isotherms calculated from the slope and intercepts of these plots are listed in Table 3.3.

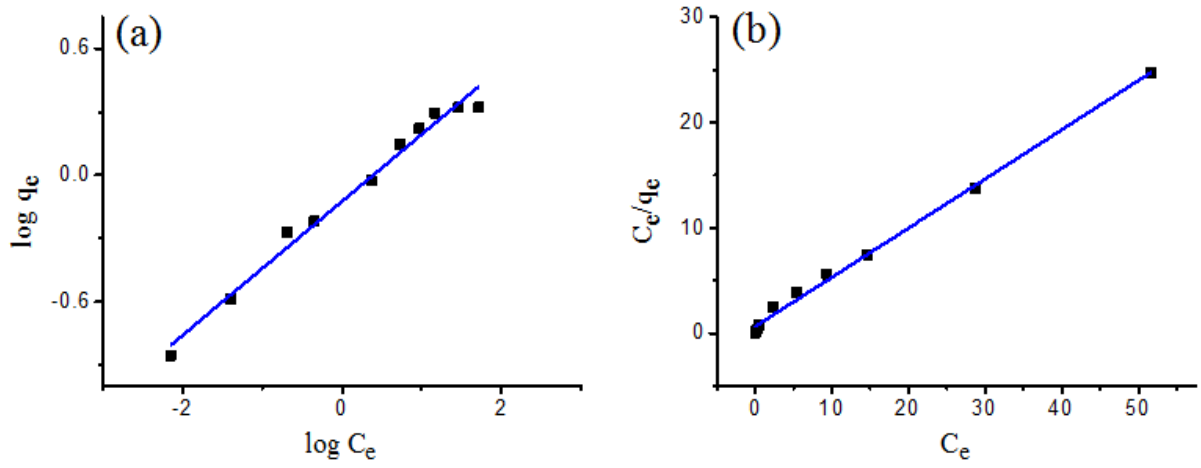

Figure 3.7: Adsorption isotherm (a) Freundlich fit and (b) Langmuir fit for As(III) adsorption by Fe_3O_4 nanoparticles coated sand.

Table 3.3: Freundlich and Langmuir adsorption isotherm parameters for As(III) adsorption by Fe_3O_4 nanoparticles coated sand.

Freundlich isotherm parameters			**Langmuir isotherm parameters**			
K_F (mg/g)	n	R^2	b (L/mg)	q_m (mg/g)	r	R^2
0.75	3.15	0.983	0.709	2.14	0.287-0.013	0.996

In this study the calculated value of n is 3.15, which lies within the limit of better adsorption i.e. $2 < n < 10$ of As(III) on Fe_3O_4 nanoparticles coated sand. The obtained higher coefficient of determination ($R^2 > 0.99$) while using Langmuir model indicates that the experimental data fitted well in Langmuir model as compared to Freundlich model where R^2 is smaller than the previous one. This interprets monolayer adsorption of As(III) on a homogeneous surface. Here, the maximum adsorption capacity (q_m) for As(III) removal is obtained 2.14 mg/g, which is comparable with other reported adsorbents. The comparison of Langmuir adsorption capacity of Fe_3O_4 nanoparticles coated sand for As(III) removal with reported low cost adsorbents is given in Table 3.4. The value of 'r' is obtained to be less than unity with a decreasing order at high As(III) concentrations, which indicates highly favourable adsorption of As(III) on Fe_3O_4 nanoparticles coated sand.

Table 3.4: Comparative account of adsorption capacities of some adsorbents for As(III) removal.

Low cost adsorbents	**Langmuir adsorption capacity q_m (mg/g)**	**References**
Iron oxide coated sand	0.029	[117]
Iron acetate coated activated alumina	0.090	[264]
China Clay and Fly ash	0.389	[265]
Iron-manganese oxide coated sand	0.55	[266]
Manganese oxide minerals	0.676	[267]
Blast furnace slag	0.70	[266]
Iron oxide impregnated activated alumina	0.734	[268]
Modified blast furnace slag	0.82	[266]
Shale sedimentary rock	0.987	[269]
TiO_2 nanoparticles	1.6	[270]
Ag-TiO_2 nanoparticles	1.71	[270]
Fe-TiO_2 nanoparticles	3.08	[270]
Fe_3O_4 nanoparticles coated sand	2.14	Present study

3.4.7. Effect of co-existing ions on As(III) removal efficiency

In contaminated ground water or surface water, arsenic is generally accompanied with many other ions. These ions may compete with arsenic ions for the adsorption sites on the surface of adsorbent (magnetite nanoparticles coated sand) and therefore interfere adsorption process. The effect of these ions on the arsenic removal efficiency of magnetite nanoparticles coated sand should be investigated before field applications of the adsorbent. Thus, in the present study we have investigated the effect of some commonly present ions viz. PO_4^{3-}, SO_4^{2-},

HCO_3^{2-} and Cl^- ions on As(III) removal efficiency. Fig. 3.8 shows the results for individual effect of various co-existing ions (PO_4^{3-}, SO_4^{2-}, HCO_3^{2-} and Cl^-) on % As(III) removal efficiency of Fe_3O_4 nanoparticles coated sand. It is observed that the presence of sulphate has a negligible effect on As(III) removal efficiency, whereas the other ions Cl^-, HCO_3^{2-}, PO_4^{3-} have an influence but still minute on As(III) removal in their concentration range of 5 mg/L to 100 mg/L.

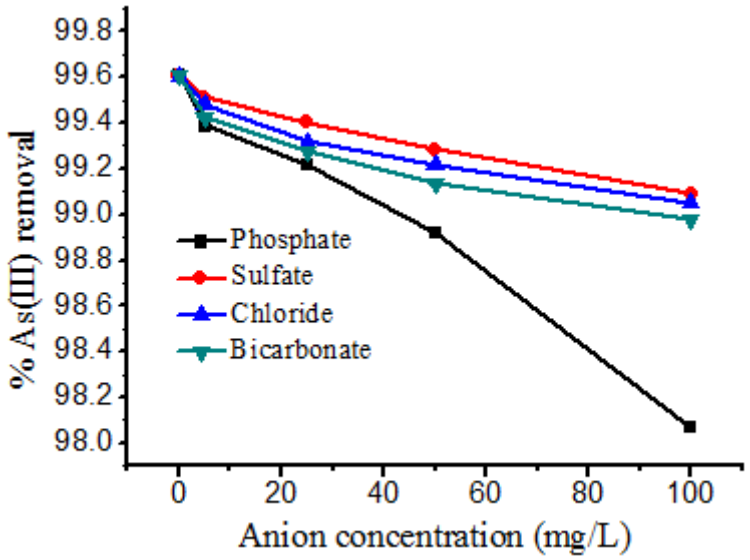

Figure 3.8: Effect of co-existing anions on As(III) removal efficiency.

The presence of these anions having little to no effect on As(III) removal efficiency may be attributed to the effect of the type of complex formed between the surface of Fe_3O_4 nanoparticles coated sand and As(III) ions [271]. It is well known that phosphate effects the arsenic removal by adsorbents. But the reported effects of phosphate on arsenic removal are not observed in the present study. The reason for little to no effect of the PO_4^{3-} ions on the arsenic adsorption may be formation of iron(III) phosphate, which could remove As(III) through oxidation followed by subsequent exchange of As(V) with PO_4^{3-} ions [272]. The results of this study show that the presence of background ions effects the As(III) removal efficiency in the order of $PO_4^{3-} > HCO_3^{2-} > Cl^- > SO_4^{2-}$, however this effect is very small.

3.4.8. Desorption and readsorption efficiency of adsorbent

The desorption data for As(III) adsorbed on magnetite nanoparticles coated sand using different concentrations of sodium hydroxide is shown in Table 3.5. It has been observed that with 0.1 M NaOH solution, 65.5 % of As(III) was desorbed from the adsorbent and with

increase in NaOH concentration to 0.5 M, 76.33 % of As(III) was desorbed. In readsorption experiment it was found that 58.33 % and 65.65 % of As(III) was readsorbed by adsorbent treated with 0.1 M and 0.5 M NaOH, respectively.

Table 3.5: Desorption data for As(III) adsorbed on magnetite nanoparticles coated sand using different concentrations of sodium hydroxide.

Concentration of As(III) (mg/L)	**Removal efficiency (%)**	**Desorption (%) with NaOH**	
		0.1 M	0.5 M
10	98.73	65.5	76.33

Fig. 3.9 demonstrates the mechanism for adsorption of As(III) species (H_3AsO_3, $H_2AsO_3^-$ and $HAsO_3^{2-}$) on Fe_3O_4 nanoparticles coated sand.

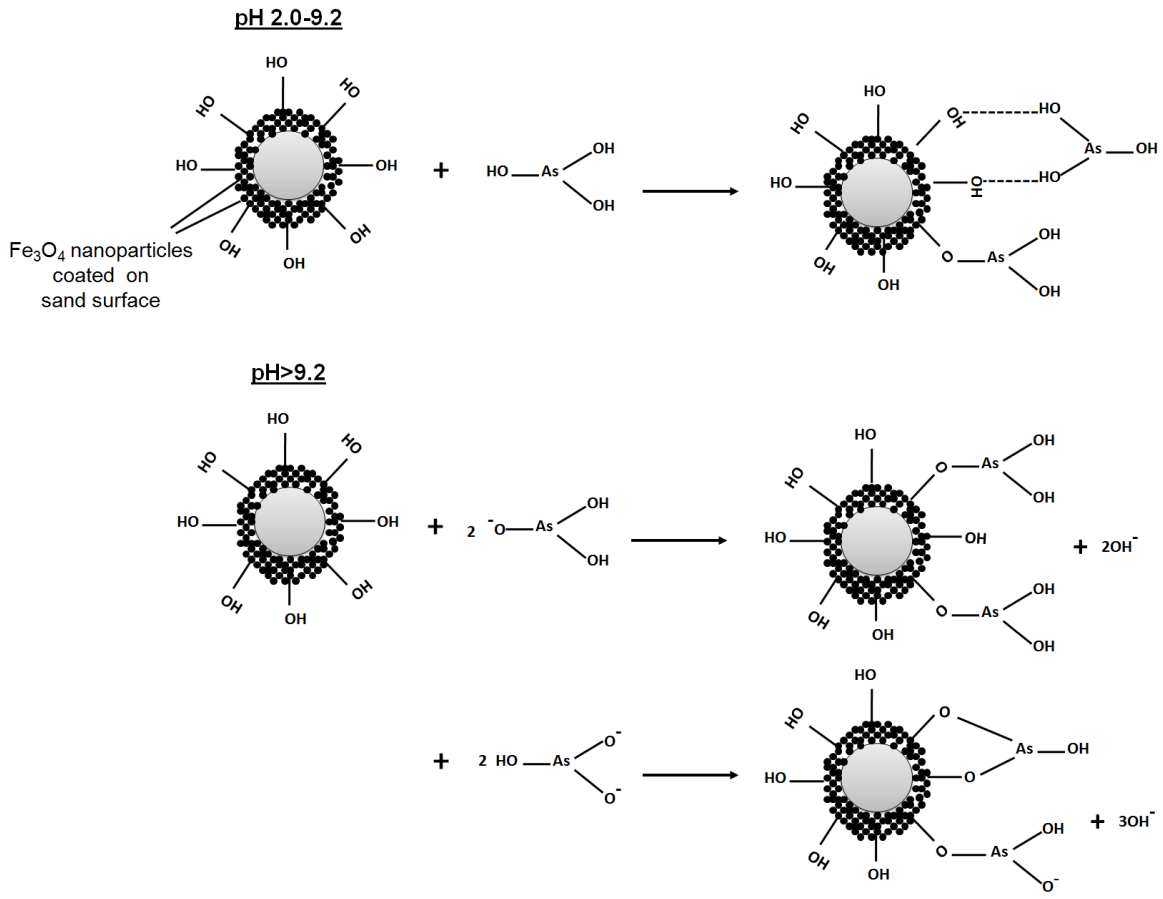

Figure 3.9: Schematic diagram for As(III) adsorption mechanism by Fe_3O_4 nanoparticles coated sand.

3.5. SUMMARY

The Fe_3O_4 nanoparticles coated sand was successfully used for As(III) removal from aqueous solution. Batch kinetics study showed that the equilibrium was reached within 360 min of contact time and the experimental kinetics data fitted well in pseudo-second order kinetics model with high coefficient of determination ($R^2 > 0.99$) as compared to pseudo-first-order kinetics model ($R^2 = 0.978$). The batch adsorption isotherm data fitted well in Langmuir adsorption isotherm with higher coefficient of determination ($R^2 > 0.99$), indicating monolayer adsorption of As(III) on homogeneous surface of adsorbent. The maximum Langmuir capacity for As(III) adsorption was found to be 2.14 mg/g. The obtained adsorbent showed a significant 99.6 % removal of As(III) in most natural conditions. Since Fe_3O_4 coated sand shows high adsorption capacity and affinity towards As(III), therefore it provides an economically feasible solution for common man to get rid of As(III) contaminated water. Also, by utilizing the Fe_3O_4 coated sand the problem of extraction of nanoparticles from treated water can be overcome by removing the adsorbent by a simple filtration process.

CHAPTER 4

BATCH STUDIES FOR As(V) REMOVAL FROM WATER BY USING MAGNETITE NANOPARTICLES COATED SAND: ADSORPTION KINETICS AND ISOTHERMS

4.1. INTRODUCTION

This chapter describes the potential of magnetite nanoparticles coated sand for As(V) removal from aqueous solution. As(III) and As(V) (predominant species of arsenic in aqueous environment) both are known to be acute toxic by Environmental Protection Agency (EPA) [273]. Thus it is required to develop a technology which can efficiently remove both As(III) and As(V) from drinking water. In previous chapter, we have described the potential of magnetite nanoparticles coated sand for As(III) removal by performing various experiments, and it is found that the synthesized adsorbent is efficient for As(III) removal. Now it is required that the synthesized adsorbent should be efficient to remove As(V) also, only then it will be a better material for arsenic removal (if it is able to remove both As(III) and As(V) efficiently).

Thus in this chapter we have discussed the use of magnetite nanoparticles coated sand for As(V) removal from water through batch operation mode. In the first section, the experimental details for performing batch adsorption experiments for As(V) removal have been discussed. The influence of various parameters such as effect of contact time, effect of pH, effect of adsorbent dose, effect of initial As(V) concentration and effect of various competing ions on As(V) removal efficiency have been discussed. The theoretical modelling of experimental adsorption kinetics and adsorption isotherms has also been discussed. Desorption and readsorption behaviour of adsorbent is discussed in the subsequent section to check the reusability of adsorbent to make it an economically feasible material. A comparative account of As(V) adsorption capacity of synthesized adsorbent with other reported adsorbents is also given. Further the mechanism of As(V) adsorption on magnetite nanoparticles coated sand is explained.

4.2. MATERIALS AND METHODS

4.2.1. Materials

All chemicals and reagents used in the experiments were of analytical grade, which were used as received. All glasswares were washed with acid and rinsed with milli-Q water. The As(V) stock solution (100 mg/L) was prepared by dissolving sodium arsenate dibasic heptahydrate ($Na_2HAsO_4.7H_2O$, Sigma Aldrich, USA product)in milli-Q water. Working solutions of As(V) were prepared freshly according to experimental requirement from the stock solution. The pH of working solutions was adjusted by standard 0.1 M HCl and 0.1 M NaOH solutions, respectively. The co-existing ions (PO_4^{3-}, SO_4^{2-}, HCO_3^{2-} and Cl^-) were

produced in the solution by dissolving disodium hydrogen phosphate anhydrous (Na_2HPO_4), sodium sulphate (Na_2SO_4), sodium bicarbonate ($CHNaO_3$) and sodium chloride (NaCl) salts.

4.2.2. Batch adsorption experiments for As(V) removal

Batch adsorption experiments were conducted for As(V) removal at room temperature (30 ± 2 ^oC) in 150 mL Erlenmeyer conical flasks by adding magnetite nanoparticles coated sand in 50 mL of aqueous As(V) solution of desired concentration. The influence of various parameters viz. contact time, initial pH of the solution, adsorbent dose and initial As(V) concentration and individual influence of co-existing ions on As(V) removal was studied in batch operation mode. All the As(V) batch adsorption experiments were performed in a temperature controlled incubator shaker at an agitation speed of 200 rpm. To study the effect of contact time, a fixed adsorbent dose (25 g/L) was added in 50 mL of aqueous As(V) solutions of desired concentration (1 mg/L) in a series of flasks. The pH of the solutions was adjusted 7.0. These flasks were agitated in incubator shaker and then the flasks were removed from incubator shaker at specific intervals of contact time i.e. 30, 60, 120, 180, 240, 300, 360 and 420 min.

The influence of initial pH of the As(V) solution on its removal efficiency was investigated by agitating the As(V) solutions of 1 mg/L concentration within a pH range of 2.0 to 12.0 and a fixed adsorbent dose of 25 g/L for 420 min of contact time. The pH of the As(V) solutions was adjusted by using 0.1 M HCl or 0.1 M NaOH solutions and was measured with an Oakton pH meter.

The effect of adsorbent dose on As(V) removal was studied by varying it from 5 g/L to 30 g/L at fixed initial As(V) concentration of 1 mg/L, pH 7.0 and contact time of 420 min. For equilibrium adsorption isotherm studies, a series of flasks containing 50 mL of As(V) solutions with varied initial concentrations ranging from 1-103.008 mg/L and fixed adsorbent dose (25 g/L) were agitated for a fixed contact time of 420 min at room temperature and pH 7.0.

Thereafter required agitation, all the above solutions were filtered through 0.45 µm durapore filter paper. The filtrate was acidified with 1% HNO_3 solution and the concentration of As(V) was quantified. The initial and residual As(V) concentrations were analyzed by using ICP-MS (Perkin Elmer Elan DRC 6000).

Since the presence of ionic species may affect the As(V) adsorption by adsorbent due to interference with As(V) uptake through competitive binding or adsorption [203]. The

individual effect of various co-existing ions viz. PO_4^{3-}, SO_4^{2-}, HCO_3^{2-} and Cl^- on As(V) removal efficiency using magnetite nanoparticles coated sand was also investigated performing the batch experiments by aforementioned method. The initial concentration of these co-existing ions was varied from 5 mg/L to 100 mg/L and the initial concentration of As(V) was kept fixed (1 mg/L). The blank As(V) solution with no co-existing ions and As(V) solutions with varied concentration of co-existing ions were agitated separately with fixed adsorbent dose of 25 g/L and pH 7.0 at an agitation speed of 200 rpm for 420 min of contact time. After required agitation the samples were filtered and analyzed for residual As(V) concentration by ICP-MS as before. The As(V) removal efficiency in presence of these co-existing ions was compared with blank samples having no co-existing ions.

In order to understand the role of surface coated magnetite nanoparticles, we have performed the batch experiments for As(V) removal with an initial As(V) concentration of 1 mg/L and adsorbent dose (sand or magnetite nanoparticles separately) of 0.2 g/20 mL. The batch experiments were also carried out with different dosage of pure magnetite nanoparticles (real adsorbent) in order to know the amount of real adsorbent required to reduce the As(V) concentration below MCL value set by WHO i.e. 10 µg/L.

The As(V) removal efficiency of magnetite nanoparticles coated sand was calculated using the formula:

$$\text{Removal efficiency (\%)} = \frac{C_o - C_e}{C_o} \times 100 \qquad (4.1)$$

and the amount of As(V) adsorbed (mg) per unit mass of adsorbent (g)was determined using the formula:

$$q_e = \frac{C_o - C_e}{M} \times V \qquad (4.2)$$

where, C_o and C_e are initial and final As(V) concentrations (mg/L), respectively, V is the volume of solution and M is the mass of adsorbent.

4.2.3. Adsorption kinetics and adsorption isotherms

The adsorption kinetics and adsorption isotherms of As(V) adsorption were also investigated in batch experiments. In order to estimate the rate at which adsorption of As(V) takes place, and to predict the rate controlling step, experimental kinetics data was fitted in pseudo-first-order and pseudo-second-order kinetics models. Equations 4.3 and 4.4 represent pseudo-first-order and pseudo-second-order kinetics models, respectively [246, 248].

$$log(q_e - q_t) = log\, q_e - \frac{k_{ads}}{2.303} t \quad (4.3)$$

$$\frac{t}{q_t} = \frac{1}{h} + \frac{t}{q_e} \quad (4.4)$$

and

$$h = kq_e^2 \quad (4.5)$$

where, q_e (mg/g) and q_t (mg/g) are amount of As(V) adsorbed per unit mass of adsorbent at equilibrium and time t, respectively. The k_{ads} and k are pseudo-first-order and pseudo-second-order adsorption rate constants, respectively, and h is initial adsorption rate (mg $g^{-1}min^{-1}$).

The As(V) adsorption data was also fitted in intra-particle diffusion model to explain the kinetics of adsorption. Equation 4.6 represents intra-particle diffusion model [250].

$$q_t = k_i\, t^{1/2} \quad (4.6)$$

where, k_i is the intra-particle diffusion rate constant and q_t is the amount of As(V) adsorbed per unit mass of adsorbent at time t.

The experimental adsorption isotherm data was fitted in theoretical Freundlich and Langmuir isotherm models. Equation 4.7 represents linear form of Freundlich isotherm model [251].

$$\log(q_e) = \log K_F + \frac{1}{n}\log(C_e) \quad (4.7)$$

where, q_e is the amount of As(V) adsorbed per unit mass of magnetite nanoparticles coated sand at equilibrium (mg/g), C_e is equilibrium concentration of As(V) in the solution (mg/L), K_F is the adsorption capacity indicator, and n ($1 < n < 10$) is adsorption intensity.

Equation 4.8 represents linear form of Langmuir isotherm model [253].

$$\frac{C_e}{q_e} = \frac{C_e}{q_m} + bq_m \quad (4.8)$$

where, q_m (mg/g) is maximum adsorption capacity, and b (L/mg) is Langmuir adsorption constant related to the affinity between the solute and adsorbent.

To predict the As(V) adsorption efficiency of the process, a dimensionless quantity 'r' is also calculated by using the formula

$$r = \frac{1}{1 + bC_o} \quad (4.9)$$

where, C_o is initial concentration of As(V) and b is Langmuir constant. The value $r < 1.0$ shows favourable adsorption, whereas $r > 1.0$ shows unfavourable adsorption.

4.2.4. Desorption and readsorption experiments

To test the reusability and degradation behaviour of magnetite nanoparticles coated sand the adsorption and desorption experiments for As(V) were performed. Desorption experiments were carried out by using 0.5 M sodium hydroxide solution as the desorbing agent. First of all, As(V) solution of 1 mg/L concentration was agitated with 1 g adsorbent for 420 min of contact time. After agitation the solution was filtered and the arsenate-loaded adsorbent was washed several times with distilled water in order to remove unadsorbed arsenate ions. The adsorbent was dried and then agitated with 40 mL of 0.5 M sodium hydroxide solution for a period of 420 min equal to adsorption time. The solution was then filtered and washed with distilled water in order to remove excess of sodium hydroxide. The adsorbent was dried and again treated with 40 mL of As(V) solution of 1 mg/L to study the readsorption behaviour of the adsorbent. The above adsorption and desorption experiments were repeated for 10 cycles. The filtrate obtained after each adsorption and desorption experiment was analyzed for As(V) concentration separately by using ICP-MS. The As(V) adsorption percentage was calculated by using equation 4.1 and As(V) desorption percentage was calculated by using equation 4.10:

$$\%\ \text{Desorption} = \frac{\text{released As(V)(mg/L)}}{\text{initially adsorbed As(V)(mg/L)}} \times 100 \qquad (4.10)$$

4.3. RESULTS AND DISCUSSION

4.3.1. Effect of contact time on As(V) removal: adsorption kinetics

Fig. 4.1 demonstrates the effect of contact time on % As(V) removal efficiency and adsorption capacity (q_t = mg/g). It is clear from Fig. 4.1, that most of the As(V) removal (87 %) occurs merely in the initial 30 min of contact time and in the next 330 min, the removal efficiency reached to 99.84 % which means that only 12.84 % of As(V) is removed in next 330 min. Thus it is concluded from these results that the uptake of As(V) species is rapid in the initial stage and gradually becomes slower with the lapse of time till equilibrium is attained. This is because initially the adsorbent has all its surface sites vacant for the adsorption and therefore the As(V) get easily adsorbed on these adsorption sites resulting in rapid As(V) uptake [185]. With the lapse of time, the available adsorbent surface active sites are occupied by As(V) and therefore the process of adsorption gets slower due to intra-

particle diffusion which is similar to the case of As(III) removal explained in previous chapter, and an equilibrium is attained at about 360 min of contact time. However, to ensure the complete adsorption all the batch experiments were performed for a contact time of 420 min. We have obtained single, smooth and continuous curve leading to equilibrium which further suggest the probability of monolayer adsorption of As(V) on the surface of magnetite nanoparticles coated sand.

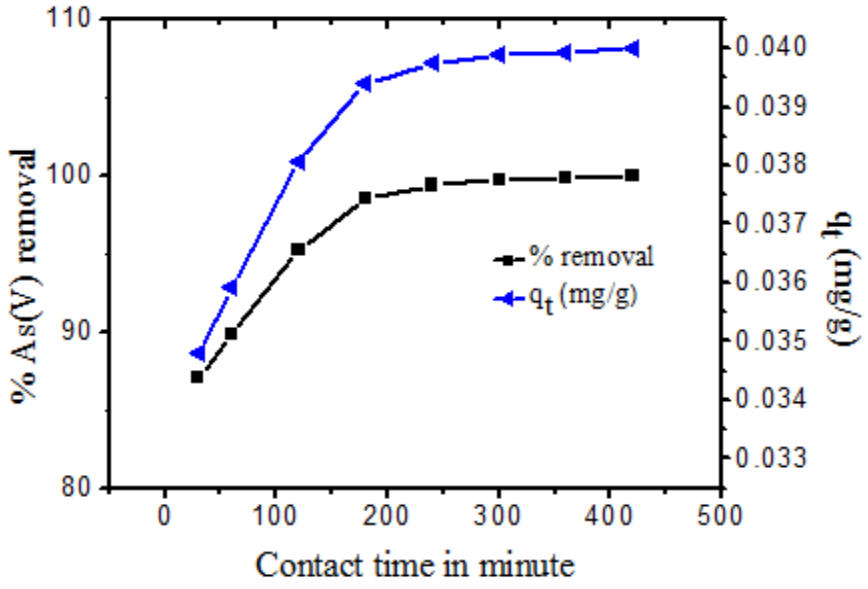

Figure 4.1: Effect of contact time on % As(V) removal efficiency and adsorption capacity (q_t = mg/g).

Experimentally observed adsorption kinetics data was fitted in pseudo-first-order and pseudo-second-order kinetics models and intra-particle diffusion model. Fig. 4.2 (a) and 4.2 (b) show linear plots of pseudo-first order and pseudo-second-order kinetics models, respectively. The corresponding parameters k_{ads}, k, h, q_e calculated from the slope and intercept of these plots and coefficient of determination R^2 obtained from these plots are given in Table 4.1. We have obtained higher values of coefficient of determination ($R^2 > 0.99$) for both pseudo-first-order and pseudo-second-order kinetics model which indicates that experimental data fitted well with both these models. But the experimental value of As(V) adsorption capacity (q_e) i.e. 0.0399 is more close to theoretical q_e value 0.0406 obtained from pseudo-second-order kinetics model in comparison to 0.008 q_e value obtained from pseudo-first-order kinetics model. This supports that the data is fitted comparatively well in pseudo-second-order kinetics model. These results reveal that As(V) adsorption process on magnetite nanoparticles

coated sand is chemisorption or we can say that chemisorption might be the rate controlling step [248, 257].

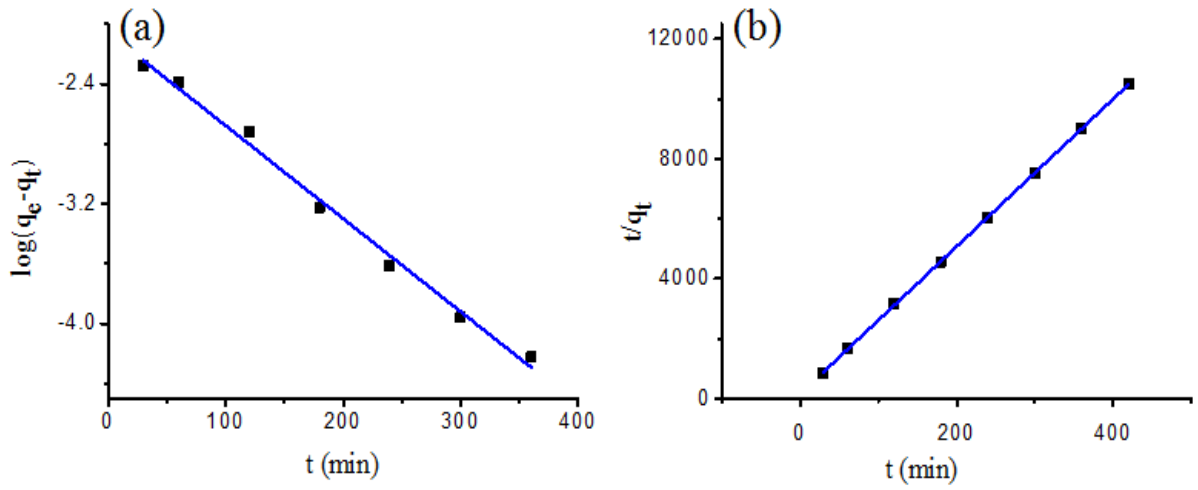

Figure 4.2: Adsorption kinetics (a) pseudo-first-order and (b) pseudo-second-order model for As(V) removal by magnetite nanoparticles coated sand.

Fig. 4.3 shows the plot of intra-particle diffusion model and values of intra-particle diffusion rate constant obtained from slope of the plot and coefficient of determination (R^2) are given in Table 4.1. The intra-particle diffusion is considered as the sole rate limiting step, if the graph between q_t and $t^{1/2}$ yields a straight line passing through the origin.

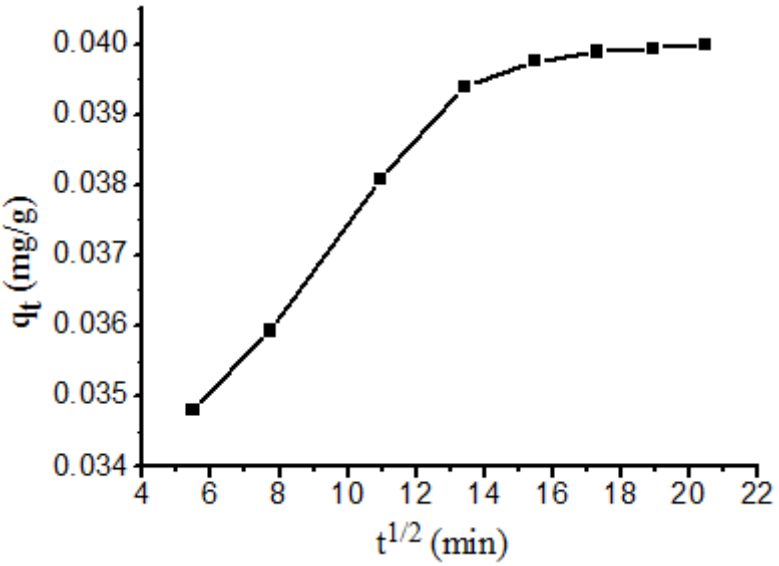

Figure 4.3: Intra-particle diffusion model for As(V) removal by Fe_3O_4 nanoparticles coated sand.

However, it can be seen from Fig. 4.3 that the graph between q_t and $t^{1/2}$ does not yields a straight line passing through the origin indicating that intra-particle diffusion is not the sole rate limiting step. Moreover, the graph shows multi-linearity, indicating that three steps are involved in As(V) adsorption process. The first, sharper portion is attributed to the external surface adsorption or boundary layer diffusion of solute molecules; the second portion of gradual adsorption is attributed to the intra-particle diffusion and the third portion is attributed to final equilibrium phase. These observations show that adsorption of As(V) on magnetite nanoparticles coated sand is a complex phenomenon which involves the contribution of both surface adsorption and intra-particle diffusion towards the rate of adsorption.

Table 4.1: Pseudo-first-order and pseudo-second-order kinetic parameters and intra-particle diffusion model parameters for As(V) removal by magnetite nanoparticles coated sand calculated from linear plots.

Pseudo-first-order parameters			**Pseudo-second-order parameters**				**Experimental adsorption capacity**	**Intra-particle diffusion model parameters**	
k_{ads} (min^{-1})	R^2	q_e (mg/g)	k (g mg^{-1} min^{-1})	h (mg g^{-1} min^{-1})	q_e (mg/g)	R^2	q_e (mg/g)	K_i (mg g^{-1} $min^{1/2}$)	R^2
0.0142	0.992	0.00874	3.754	0.00621	0.0406	0.999	0.0399	0.000356	0.858

We have also carried out As(V) removal experiments separately for sand and magnetite with initial As(V) concentration of 5 mg/L and adsorbent dose (sand or magnetite nanoparticles) of 0.2 g/20 mL. The uncoated sand particles were able to reduce As(V) only to 4.501 mg/L from initial As(V) concentration of 5 mg/L. On the other hand magnetite nanoparticles reduced As(V) concentration below 1 parts per trillion (ppt) as the amount was not detectable in the sample by ICP-MS (ICP-MS instrument lower detection limit was 1ppt). As(V) removal efficiency of sand was found to be 9.98 % and of magnetite nanoparticles was nearly

100 %. Thus the obtained results reveal that sand is not able to remove As(V). It is only magnetite nanoparticles which are responsible for As(V) removal.

4.3.2. Effect of initial solution pH on As(V) removal

Fig. 4.4 shows the effect of initial solution pH on As(V) removal efficiency by magnetite nanoparticles coated sand. It is observed that for the pH range 2.0-7.0 there is slight decrease in As(V) removal efficiency, while for the increased pH from 7.0 to 12.0, there is a drastic decrease in As(V) removal efficiency from 99.99 % to 39.33 %. It indicates that magnetite nanoparticles coated sand adsorb As(V) more efficiently in an acidic pH range than in basic pH range. The observed variation in As(V) removal efficiency at different pH values may be attributed to different affinities of magnetite nanoparticles coated sand for different As(V) species viz. AsO_4^{3-}, $HAsO_4^{2-}$, $H_2AsO_4^-$, H_3AsO_4 dominating at different pH values. It is reported that the pH range of 2.3 to 6.9 contains $H_2ASO_4^-$ as the predominant form of As(V), whose adsorption energy may be lower than that of $HAsO_4^{2-}$ and AsO_4^{3-} ion which results in comparatively more favourable adsorption of $H_2AsO_4^-$ than that of $HAsO_4^{2-}$ and AsO_4^{3-} ions [185, 274]. Except the adsorption energy, different surface charge of magnetite nanoparticles at different pH also effects As(V) removal efficiency. The surface of magnetite nanoparticles is positively charged in the pH range 2.0-7.7 and has a point of zero charge at 7.8 pH, and is negatively charged above pH 7.8. Therefore, in the acidic pH range the As(V) being negatively charged is adsorbed more efficiently on the positively charged magnetite nanoparticles coated sand due to electrostatic attraction [195]. On the other hand in the basic pH range there is repulsion between negatively charged As(V) ions and negatively charged adsorbent surface which results in drastic decrease in the As(V) removal efficiency.

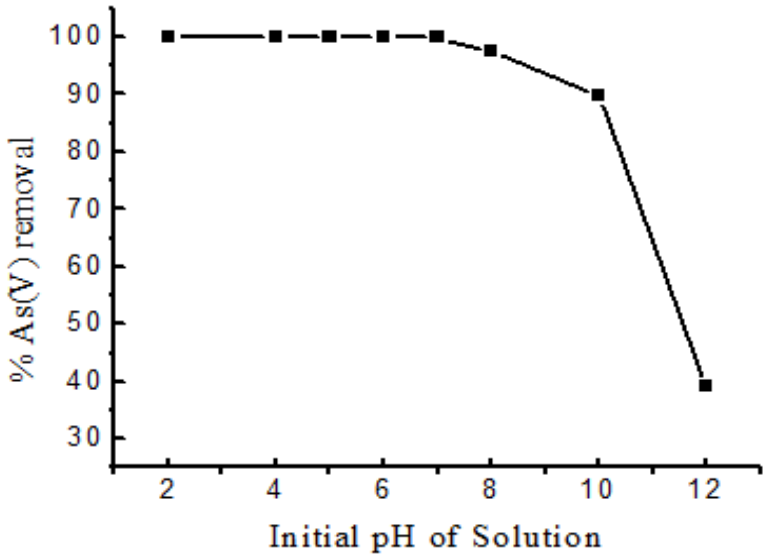

Figure 4.4: Effect of initial pH of the aqueous solution on % As(V) removal efficiency.

4.3.3. Effect of adsorbent dose on As(V) removal

The effect of adsorbent dose on both the As(V) removal efficiency and adsorption capacity (q_e = mg/g), at fixed initial As(V) concentration of 1 mg/L is shown in Fig. 4.5. From the Fig. 4.5 it can be seen that As(V) removal efficiency increases from 94.7 to 99.99 % with increase in adsorbent dose from 5 g/L to 30 g/L. However, the adsorption capacity decreases from initial value 0.189 mg/g (corresponding to 5 g/L of adsorbent dose) to 0.033 mg/g (corresponding to 30 g/L of adsorbent dose). The observed increase in the As(V) removal efficiency is due to increase in number of surface active sites with increase in adsorbent dose [260, 261]. On the other hand, the decrease in adsorption capacity is attributed to the interference between binding sites, and higher adsorbent dose or insufficiency of As(V) ions in the solution with respect to available binding sites [262, 263]. The point of intersection of the plots representing removal efficiency and adsorption capacity is generally considered as the optimum dose because it shows balance between % As(V) removal efficiency and adsorption capacity. In this study, the intersection point is obtained at the value 10 g/L of adsorbent dose. However, as observed from the experimental data the 10 g/L dose of adsorbent is not sufficient to reduce arsenic concentration to a required 10 µg/L level, therefore, here 25 g/L of adsorbent dose was selected to achieve the WHO standards. It may be noted that the dose of adsorbent includes the weight of real adsorbent (magnetite nanoparticles) and weight of sand particles, therefore in this study it is the total weight of sand and adsorbent and is obviously higher as compared with that of real adsorbent.

Therefore in order to know the minimum amount of real adsorbent required to reduce the arsenic concentration below allowable limit, the batch experiment was also performed using bare magnetite nanoparticles by varying adsorbent dose from 50 mg/L to 1 g/L. The results show that 200 mg/L of magnetite nanoparticles are sufficient to reduce As(V) concentration below 10 µg/L from initial As(V) concentration of 1 mg/L. The amount of real adsorbent i.e. magnetite nanoparticles required to reduce arsenic concentration below allowable limit is comparatively less than the commercially available adsorbent [185].

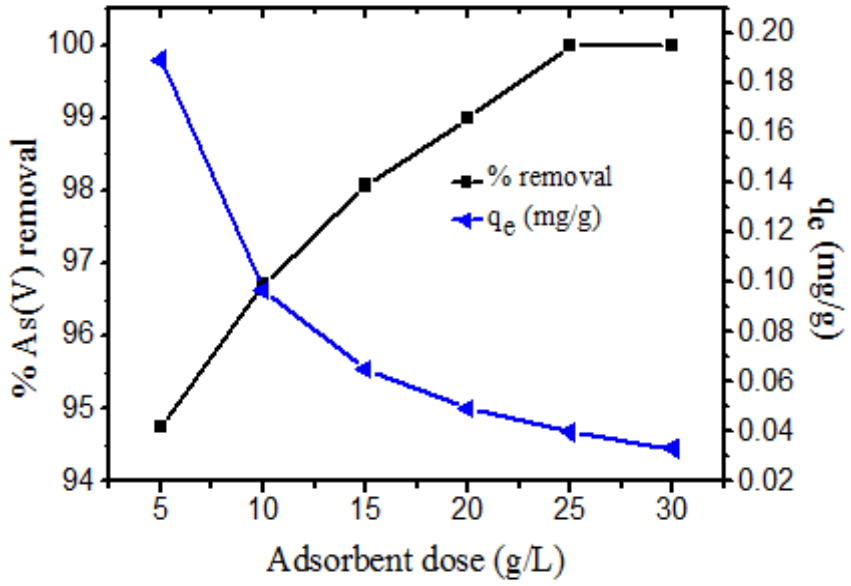

Figure 4.5: Effect of adsorbent dose on % As(V) removal efficiency and adsorption capacity (q_e = mg/g).

4.3.4. Effect of initial As(V) concentration

The effect of initial As(V) concentration on % As(V) removal efficiency and adsorption capacity of magnetite nanoparticles coated sand is shown in Fig. 4.6. It is observed that when the initial As(V) concentration increases from 1 mg/L to 103.008 mg/L, the As(V) removal efficiency decreases from 99.99 % to 51.88 %, and the adsorption capacity increases from 0.039 to 2.137 mg/g. Similar to the case of higher dose of adsorbent, here also when the initial As(V) concentration is lower it find abundant active adsorbent sites, and thus the system shows higher removal efficiency. In case when As(V) concentration is increased, the concentration of adsorbate increases, however the available active sites remains same as that in previous case, therefore, the % As(V) adsorbed amount will reduce as shown by the decreasing trend of removal efficiency of As(V) in Fig. 4.6.

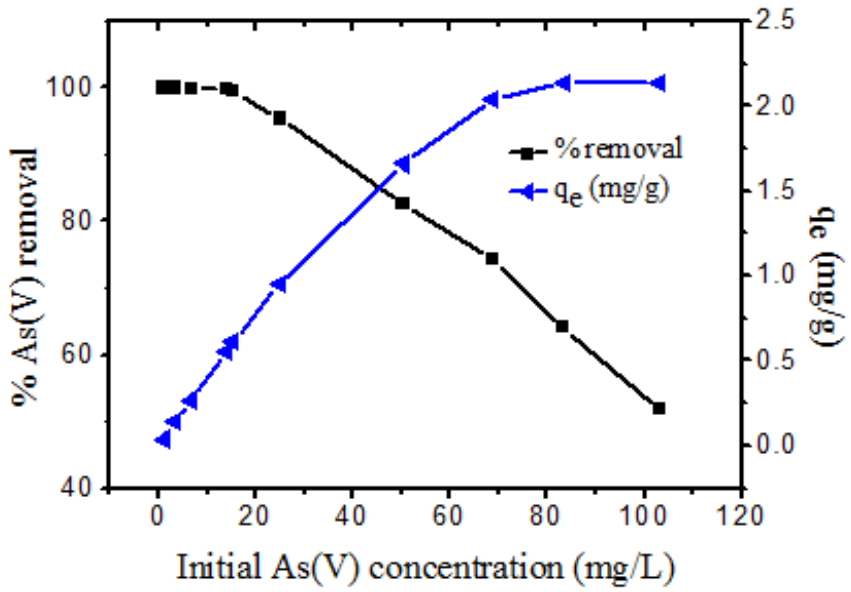

Figure 4.6: Effect of initial As(V) concentration on % As(V) removal efficiency and adsorption capacity (q_e = mg/g).

4.3.5. Adsorption isotherms

In order to describe equilibrium between adsorbed As(V) ions and As(V) ions in solution, the adsorption isotherm data was fitted in Freundlich and Langmuir isotherm models given in the equations 4.7 and 4.8. The Freundlich and Langmuir adsorption equilibrium isotherms for As(V) are shown in Fig. 4.7 (a) and (b), respectively. The values of various corresponding parameters calculated from the slope and intercept of these isotherm plots and coefficients of determination R^2 are summarized in Table 4.2. We have observed that the experimental adsorption isotherm data fitted well in Langmuir isotherm model with higher value of coefficient of determination (R^2 > 0.99) as compared to Freundlich isotherm model with lower value of coefficient of determination (R^2 = 0.95). This signifies monolayer adsorption of As(V) on homogeneous surface of the adsorbent. The value of Freundlich parameter 3.54 lying within the limit of better adsorption i.e. 2 < n < 10 indicates that As(V) exhibits better adsorption on magnetite nanoparticles coated sand. It can be seen from Table 4.2 that the maximum Langmuir adsorption capacity (q_m) for As(V) in this study is 2.15 mg/g. Further, the values of r (0.372-0.0057) are found less than unity for all As(V) concentrations ranging from 1 mg/L to 103.008 mg/L, which interpret highly favourable adsorption of As(V) on magnetite nanoparticles coated sand.

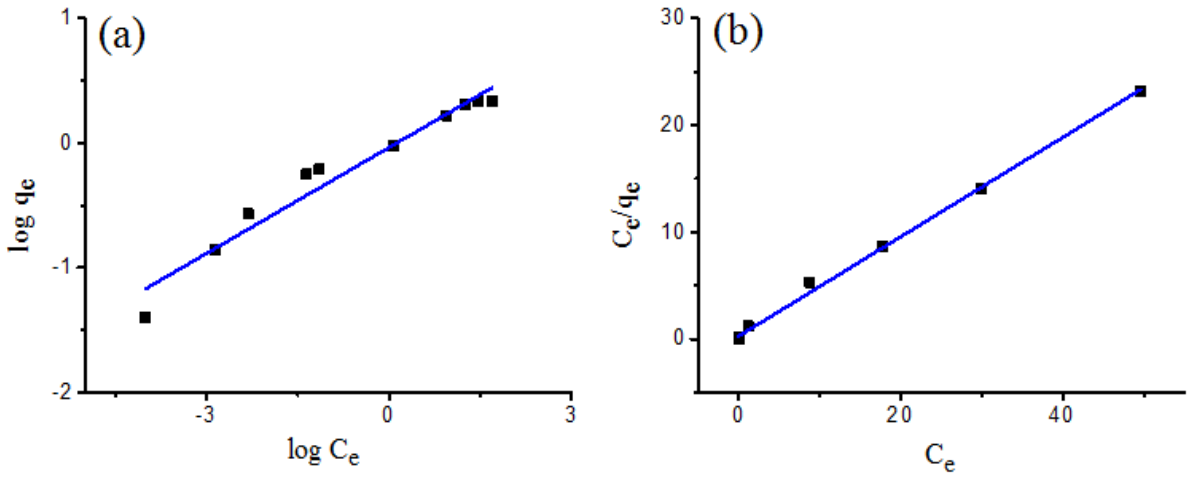

Figure 4.7: Adsorption isotherm (a) Freundlich fit and (b) Langmuir fit for As(V) adsorption by magnetite nanoparticles coated sand.

Table 4.2: Freundlich and Langmuir adsorption isotherm parameters for As(V) adsorption by magnetite nanoparticles coated sand calculated from linear plots.

Freundlich isotherm parameters			**Langmuir isotherm parameters**			
K_F (mg/g)	n	R^2	b (L/mg)	q_m (mg/g)	r	R^2
0.9203	3.54	0.951	1.686	2.15	0.372-0.0057	0.997

The adsorption capacity of magnetite nanoparticles coated sand for As(V) removal has been compared with previously reported adsorbents. The comparison is made on the basis of obtained Langmuir adsorption capacity and is listed in Table 4.3. An analytical comparison shows that the adsorption capacity of magnetite nanoparticles coated sand for As(V) is better than most of the adsorbents reported in the literature.

Table 4.3: Comparison of adsorption capacities of some adsorbents for As(V) removal.

Low cost adsorbents	**Langmuir adsorption capacity q_m (mg/g)**	**References**
Laterite soil	0.040	[275]
Sulfate modified iron-oxide coated sand	0.117	[276]
Rice polish	0.147	[259]
Magnetite nanoparticles	0.204	[180]
Natural iron ore	0.4	[277]
Iron-manganese oxide coated sand	0.77	[266]
Red mud	0.941	[278]
Bauxsol	1.081	[279]
Granular porous ferric hydroxide	1.17	[266]
Modified zeolite	1.34	[280]
Bauxsol coated sand	1.64	[281]
Activated Bauxsol coated sand	2.14	[281]
Mg-Fe-based hydrotalcite	2.642	[282]
Fe_3O_4 nanoparticles coated sand	2.15	Present study

4.3.6. Effect of co-existing ions on As(V) removal efficiency

Fig. 4.8 represents the individual effect of co-existing anions on As(V) removal efficiency by adsorbent. Here, we found that sulphate has no significant effect on As(V) removal efficiency in its concentration ranging from 5 mg/L to 100 mg/L. The presence of chloride and bicarbonate also show less influence on As(V) removal efficiency. The presence of phosphate shows comparatively highest decrease in As(V) adsorption, however this too does not affect much the removal efficiency of As(V). The decrease in the adsorption efficiency is inferred due to competition for the binding sites of the adsorbent between phosphate and As(V) since phosphate and As(V) both have similar molecular structure. The presence of co-existing ions

affects the As(V) removal efficiency by magnetite nanoparticles coated sand in the order of PO_4^{3-} > HCO_3^{2-} > Cl^- > SO_4^{2-}. However this effect is very small, therefore one can use magnetite nanoparticles coated sand as an efficient adsorbent even to purify water having co-existing anions.

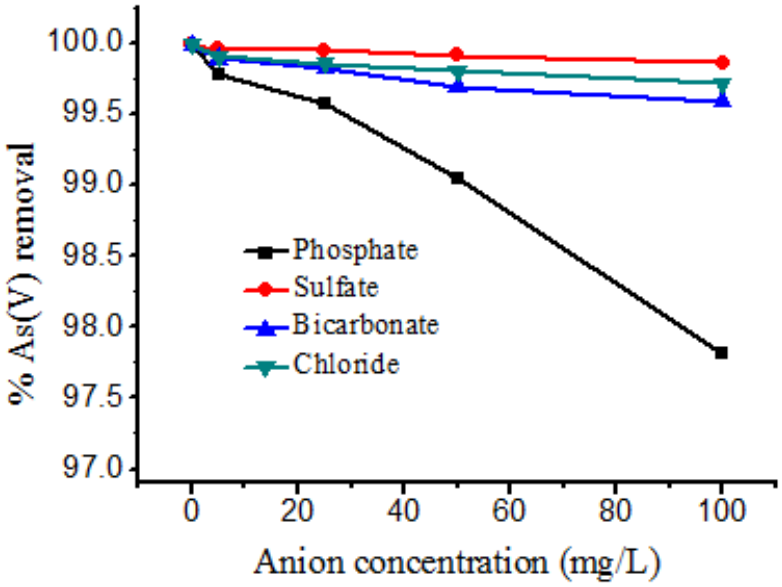

Figure 4.8: Effect of co-existing anions on As(V) removal efficiency.

4.3.7. Desorption and readsorption efficiency of adsorbent

Fig. 4.9 (a) and (b) shows the adsorption and desorption behaviour of magnetite nanoparticles coated sand, respectively. It can be seen from Fig. 4.9 (a) that in first cycle 99.99 % of As(V) is removed and with increase in number of reuse of adsorbent, its adsorption efficiency decreases. After 10 cycles of reuse of adsorbent only 20.3 % of As(V) is adsorbed due to degradation of adsorbent. Fig. 4.9 (b) shows that initially in the first cycle of desorption, 85.3 % of As(V) is desorbed with 0.5 M of NaOH solution and then desorption increases upto 4 cycles and then decreases. The As(V) desorption occurs within 75 % to 90 % in all the 10 cycles.

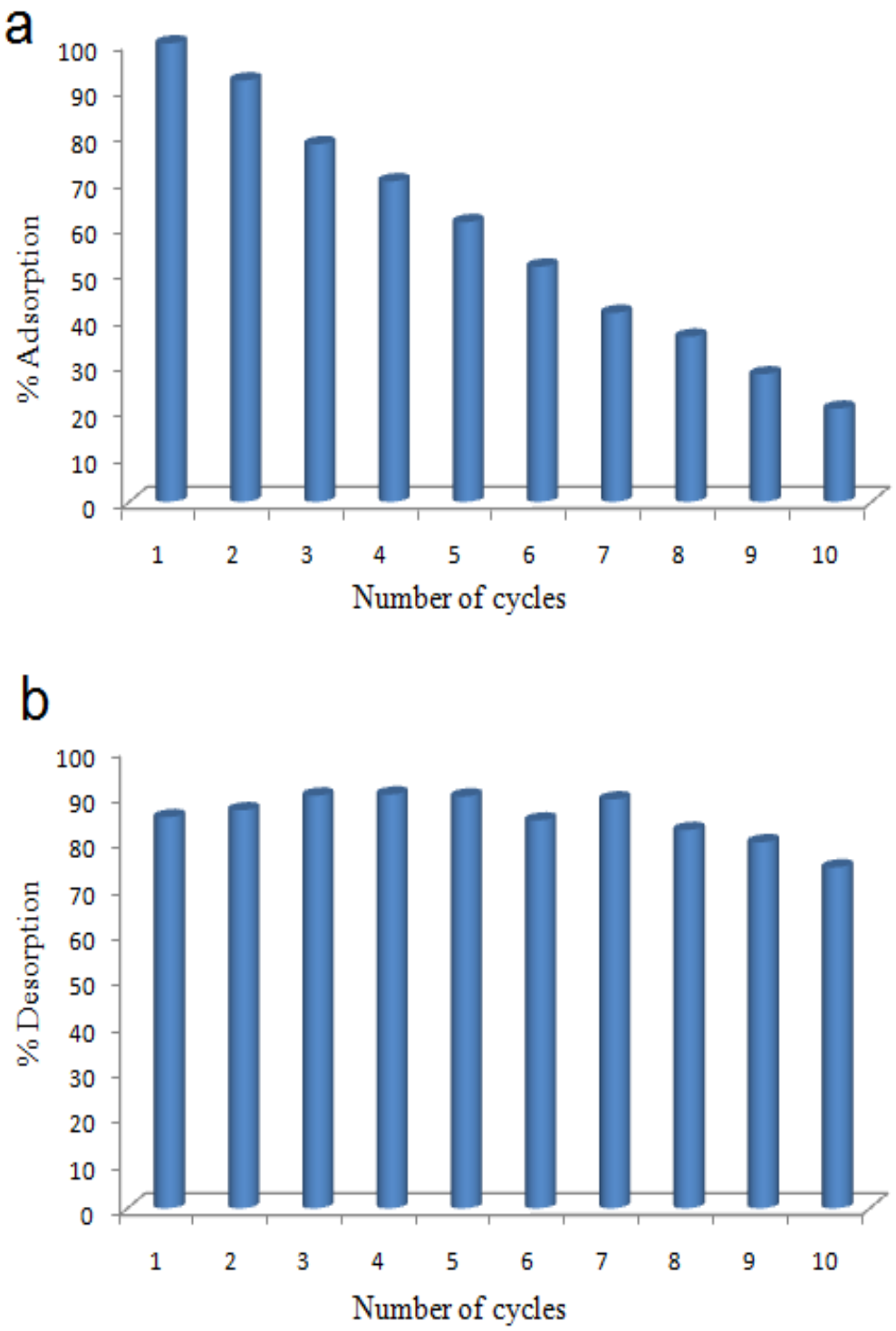

Figure 4.9: % As(V) (a) adsorption and (b) desorption behaviour of magnetite nanoparticles coated sand upto 10 cycles.

Fig. 4.10 demonstrates the mechanism for adsorption of As(V) species ($H_2AsO_4^-$ and $HAsO_4^{2-}$) on magnetite nanoparticles coated sand.

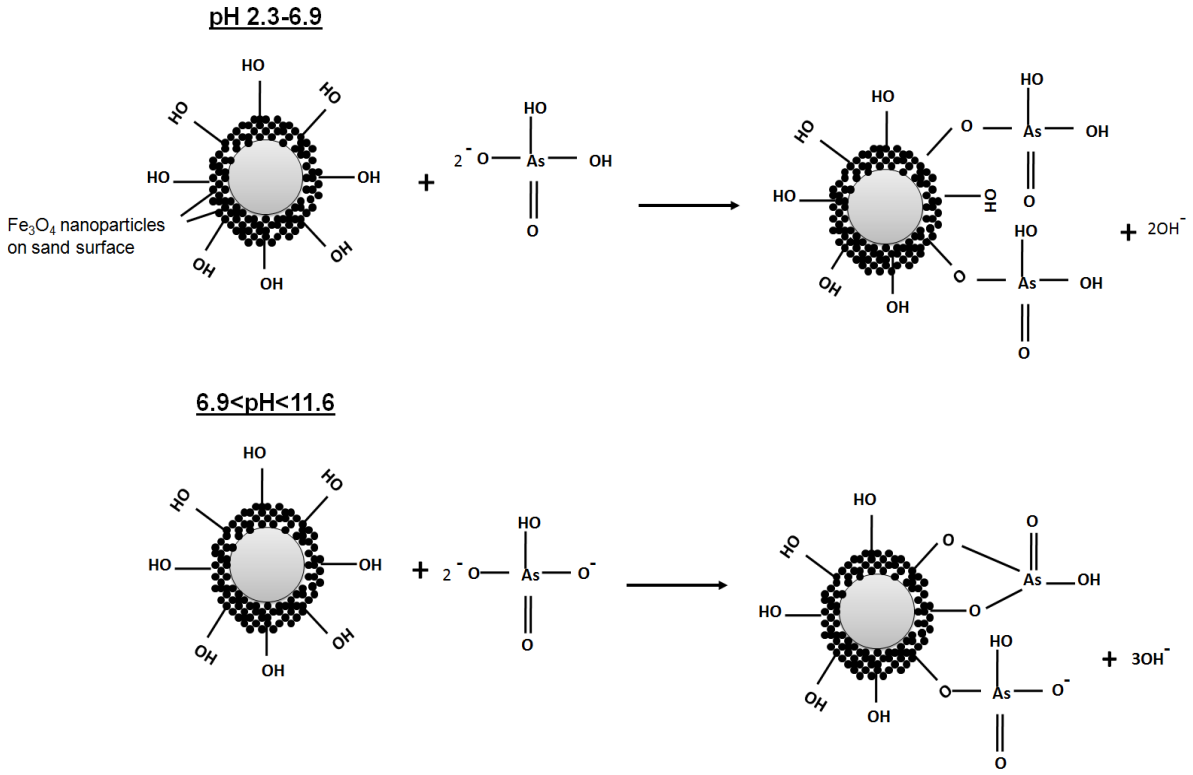

Figure 4.10: Schematic diagram for As(V) adsorption mechanism by magnetite nanoparticles coated sand.

4.4. SUMMARY

Magnetite nanoparticles coated sand was successfully utilized for As(V) removal from aqueous solution. The synthesized adsorbent was found to be a potential adsorbent for As(V) removal when compared with other reported adsorbents. The adsorption of As(V) onto magnetite nanoparticles coated sand was found to be more favourable in acidic pH rather than in basic pH conditions. The experimental adsorption kinetics data fitted well in pseudo-second-order kinetics model with higher coefficient of determination then pseudo-first-order kinetics model followed by intra-particle diffusion model. This indicates that the mechanism of As(V) adsorption by magnetite nanoparticles coated sand is complex and both surface adsorption as well as intra-particle diffusion contribute towards the rate limiting step. The experimental adsorption isotherm data fitted well in Langmuir isotherm model with higher coefficient of determination then Freundlich adsorption isotherm model indicating monolayer adsorption of As(V) on the adsorbent surface. At optimum conditions, 99.99 % of As(V)

removal was achieved by magnetite nanoparticles coated sand. The presence of co-existing ions in aqueous solution did not show any measurable effect on the As(V) removal efficiency by magnetite nanoparticles coated sand in the studied concentration range (5 mg/L to 100 mg/L) which also make it a better adsorbent. Therefore, the magnetite nanoparticles coated sand proved to be a promising and efficient adsorbent for As(V) removal from drinking water.

CHAPTER 5

EQUILIBRIUM AND THERMODYNAMIC INVESTIGATION OF As(III) AND As(V) REMOVAL BY MAGNETITE NANOPARTICLES COATED SAND

i

5.1. INTRODUCTION

Since temperature plays an important role in the adsorption processes, therefore, to fully understand the nature of adsorption, and to evaluate the feasibility of adsorption, thermodynamic study of adsorption process is required. The most imperative application of thermodynamics to adsorption process is the calculation of equilibrium between different phases of adsorbate and adsorbent [283]. In thermodynamics, equilibrium is attained when the system is in its minimum free energy state (Gibbs free energy) and is described on the basis of stoichiometric equation and thermodynamic equilibrium constant containing deeds.

There are two types of thermodynamic properties which are generally required for designing adsorption systems viz. (i) directly measurable properties including temperature and equilibrium constant, and (ii) properties which cannot be measured directly such as Gibb's free energy change, enthalpy change, entropy change, activation energy and isosteric heat of adsorption. These thermodynamic parameters are essential design variables which help in estimating the performance and understanding the mechanism of an adsorption process. These are also required for the characterization and optimization of an adsorption process [284]. Furthermore, adsorption isotherm which gives the amount of heavy metal ions (adsorbate) adsorbed on the adsorbent surface as a function of the amount at equilibrium in solutions is basis for the calculation of thermodynamic parameters. The experimentally determined data points of adsorption isotherm must be fitted in analytical equations for interpolation, extrapolation and for thermodynamic calculations [283, 285]. It should be noted that the thermodynamics applies only to equilibrium adsorption isotherms.

In this chapter we have summarized equilibrium adsorption isotherm experiments which were conducted on As(III) and As(V) removal at various temperatures along with the calculations of various thermodynamic parameters such as standard Gibbs free energy change (ΔG^o), enthalpy change *(*ΔH^o) and entropy change (ΔS^o).

5.2. EXPERIMENTAL

5.2.1. Batch adsorption isotherm experiments for As(III) and As(V) removal at different temperatures

Batch adsorption isotherm experiments were conducted to study the effect of temperature on As(III) and As(V) removal in the temperature range 25 ^oC (298 K) to 45 ^oC (318 K). As(III) or As(V) solutions of different initial concentration were taken in different flasks, respectively. The initial pH of the solutions was adjusted to 7.0 and a fixed adsorbent dose of

25 g/L was added to above solutions. These solutions were agitated at 200 rpm in an incubator shaker at different temperatures for contact time of 420 min. The solutions were then filtered using 0.45 µm durapore filter paper, acidified with 1 % HNO_3, and finally analyzed for residual As(III) or As(V) concentration using ICP-MS.

As(III) or As(V) removal efficiency and adsorption capacity were calculated by using the formula given in equations 3.1 and 3.2 as described in chapter 3.

5.3. Adsorption isotherm

Langmuir adsorption isotherm model and dimensionless factor '*r*' as described in chapter 3 and chapter 4 were employed to fit the experimental adsorption isotherm data for As(III) and As(V) removal obtained at different studied temperatures.

5.4. Thermodynamic investigation

The various thermodynamic parameters related with adsorption process i.e. standard Gibbs free energy change (ΔG^o), standard enthalpy change (ΔH^o) and standard entropy change (ΔS^o) were calculated using standard methods. The Gibbs free energy change of the adsorption process is related to the equilibrium constant as given in equation 5.1 [208, 286, 287].

$$\Delta G^o = - RTlnK_L \qquad (5.1)$$

where, ΔG^o is standard Gibbs free energy change of adsorption in kJ/mol, R is universal gas constant (8.314 J/mol K), T is temperature in Kelvin and K_L is the thermodynamic equilibrium constant given as:

$$K_L = q_{max} \times b \qquad (5.2)$$

In this equation, q_{max} is maximum Langmuir adsorption capacity and b is Langmuir isotherm constant [208, 286].

Standard Gibbs free energy change is also related to the standard enthalpy change (ΔH^o) and standard entropy change (ΔS^o) at constant temperature as given in equation 5.3.

$$\Delta G^\circ = \Delta H^\circ - T\Delta S^\circ \qquad (5.3)$$

Now using the equations 5.1 and 5.3 we have

$$lnk_L = \frac{\Delta S^\circ}{R} - \frac{\Delta H^\circ}{RT} \qquad (5.4)$$

Therefore, standard enthalpy change (ΔH^o) in kJ/mol, and standard entropy change (ΔS^o) in kJ/mol K has been calculated from the above equation 5.3 [208, 286, 287]. We can calculate the values of ΔH^o and ΔS^o from the slope and intercept of Vant Hoff's plot of lnK_L against 1/T, respectively.

The thermodynamic study in general specifies that whether the adsorption process is spontaneous or non-spontaneous and exothermic or endothermic in nature. If the standard enthalpy change (ΔH^o) for adsorption process is:

(i) Positive; the adsorption process is endothermic in nature and a given amount of heat is adsorbed by the system.

(ii) Negative; the adsorption process is exothermic in nature and a given amount of heat is evolved from the system during the metal ion binding on the adsorbent surface.

If the standard Gibbs free energy change (ΔG^o) for adsorption process is positive, then the process is non-spontaneous in nature and if it is negative, the process is called spontaneous. Further, the positive value of standard entropy change (ΔS^o) indicates an increase in the degree of randomness of the adsorbed species [288].

5.5. RESULTS AND DISCUSSION

5.5.1. Effect of temperature on As(III) and As(V) removal

Fig. 5.1 (a) and 5.1 (b) shows the effect of temperature on As(III) removal efficiency and adsorption capacity, respectively at different initial As(III) concentrations. Similarly, Fig. 5.2 (a) and 5.2 (b) shows the effect of temperature on As(V) removal efficiency and adsorption capacity, respectively at different initial As(V) concentrations. It has been observed that with increase in temperature from 25 ^oC to 45 ^oC, As(III) or As(V) removal efficiency and adsorption capacity increases for all concentrations. This increased arsenic removal efficiency and adsorption capacity of magnetite nanoparticles coated sand with increased temperature is attributed to the enlargement of pores and/or the activation of the adsorbent surface [289].

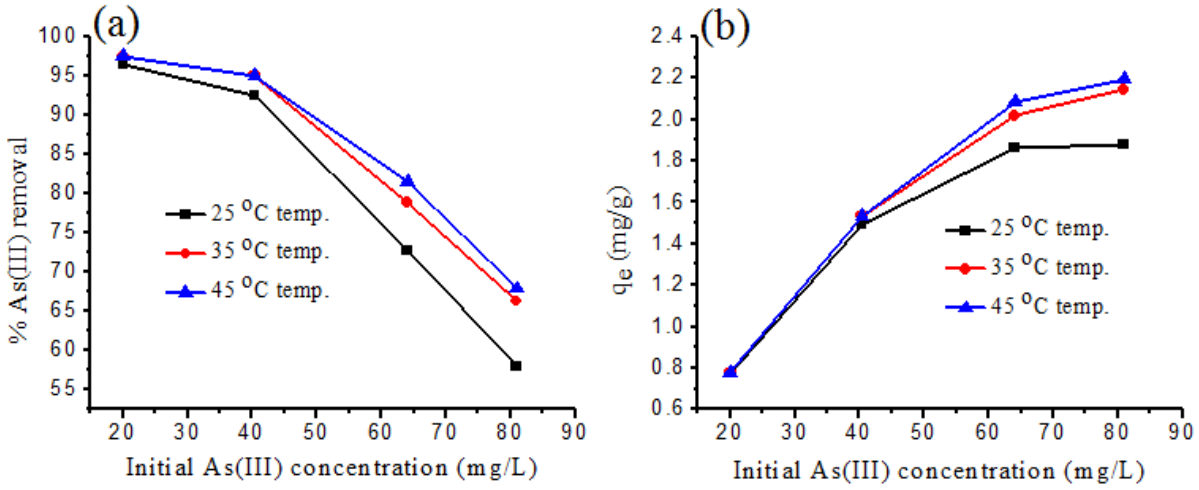

Figure 5.1: Effect of temperature on As(III) (a) removal efficiency and (b) adsorption capacity at different initial As(III) concentrations.

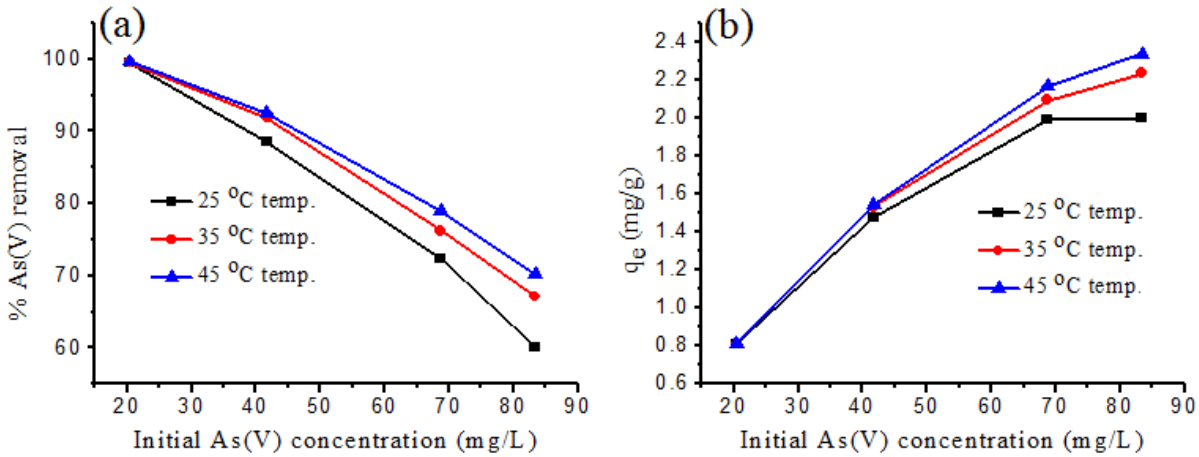

Figure 5.2: Effect of temperature on As(V) (a) removal efficiency and (b) adsorption capacity at different initial As(V) concentrations.

5.5.2. Adsorption isotherm

Fig. 5.3 (a), (b), (c) and Fig. 5.4 (a), (b), (c) shows the Langmuir adsorption isotherm fit for As(III) and As(V) removal, respectively at different temperatures. The various parameters for As(III) and As(V) removal obtained from Langmuir plots at different temperatures has been given in Table 5.1. The Langmuir isotherm constant '*b*' obtained from the intercept of Langmuir plots (Table 5.1) has been used in the thermodynamic study.

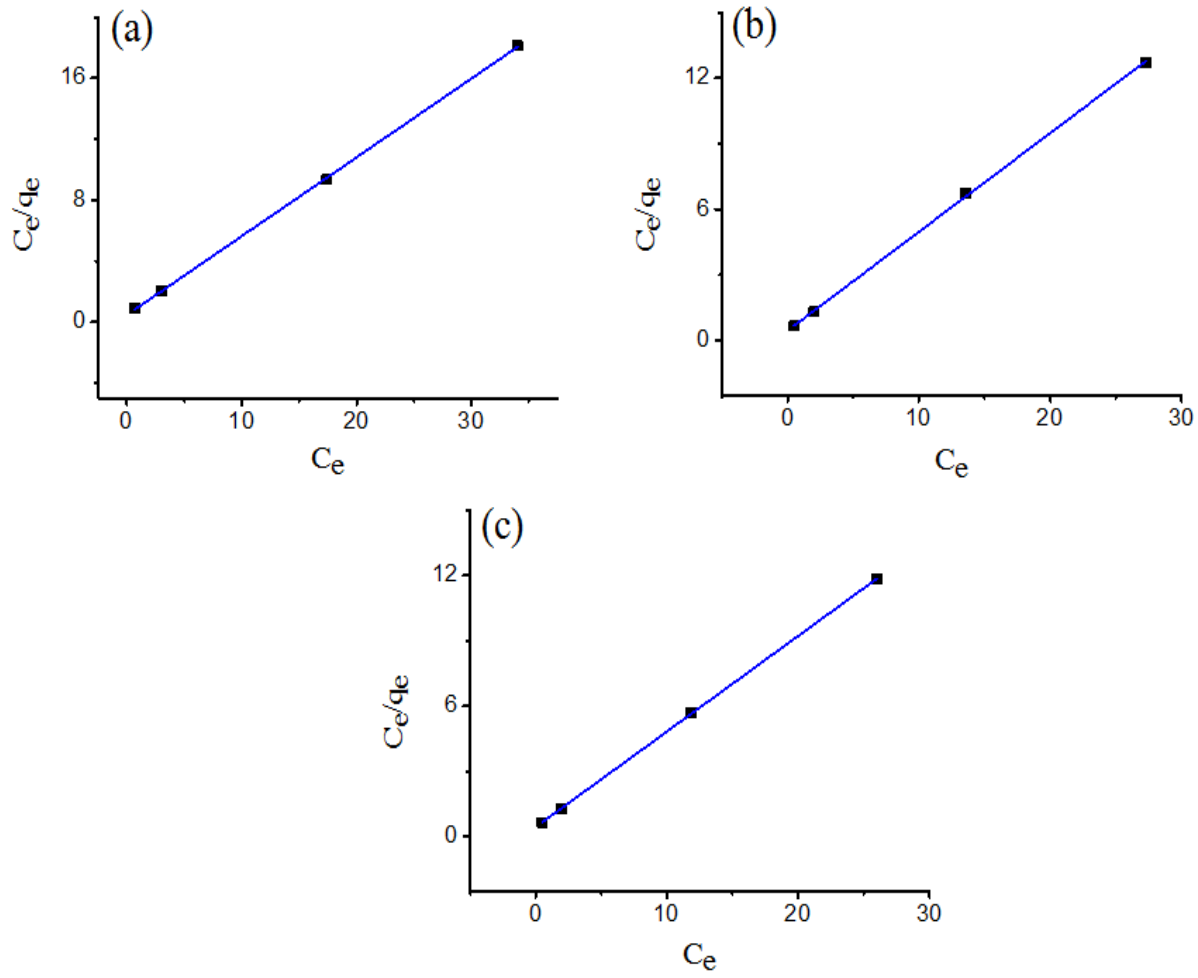

Figure 5.3: Langmuir adsorption isotherm fit for As(III) removal at (a) 25 ^{o}C (298 K) (b) 35 ^{o}C (308 K) and (c) 45 ^{o}C (318 K) temperature.

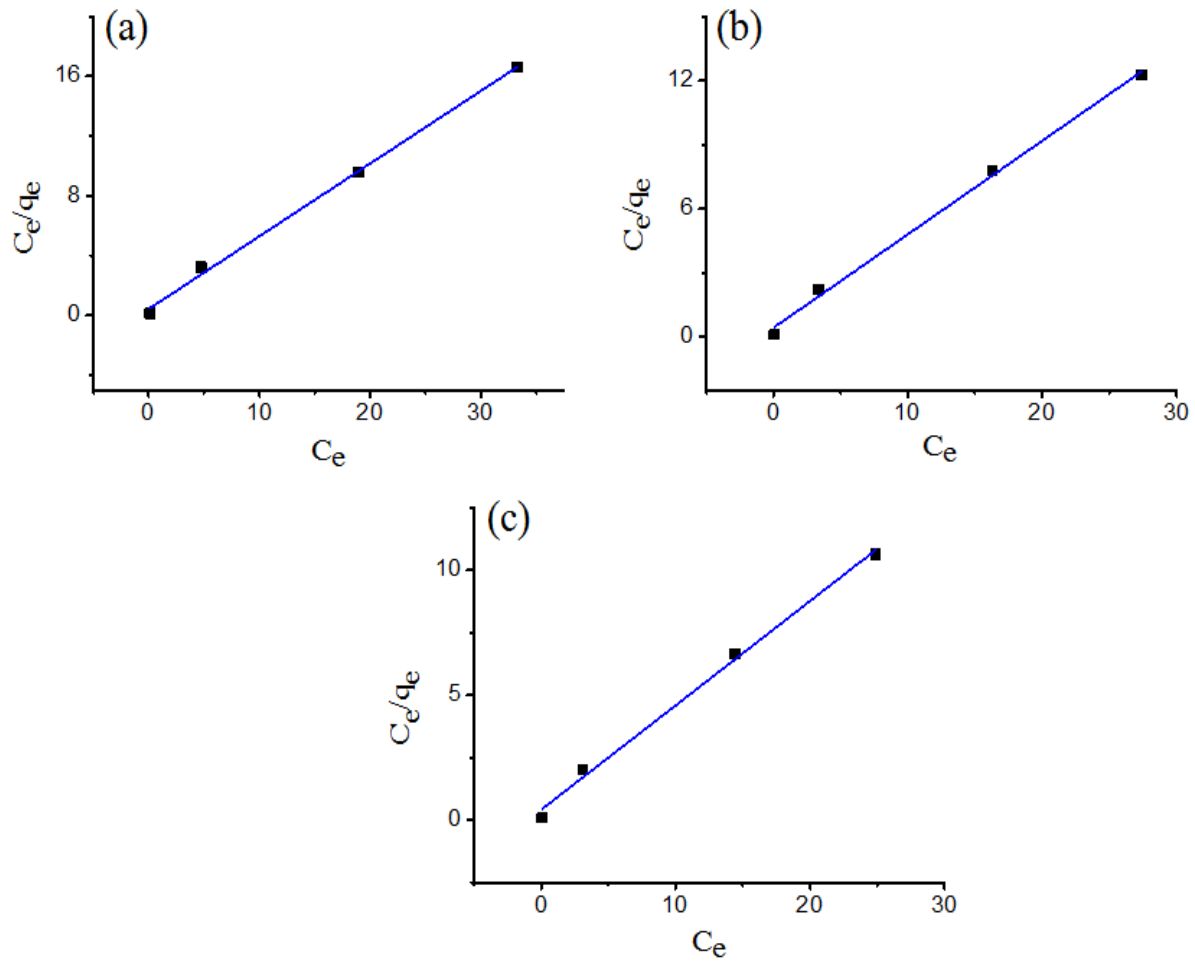

Figure 5.4: Langmuir adsorption isotherm fit for As(V) removal at (a) 25 ^{o}C (298 K) (b) 35 ^{o}C (308 K) and (c) 45 ^{o}C (318 K) temperature.

The adsorption isotherm data fitted well in Langmuir isotherm model with higher coefficient of determination, $R^2 > 0.99$ for both As(III) and As(V) at all studied temperature (Table 5.1). This has also been observed that the maximum Langmuir adsorption capacity (q_{max}) for both As(III) and As(V) has been increased with increase in the temperature from 298 K to 318 K, which shows endothermic nature of the process. Further, the values of '*r*' are found less than unity for all As(III) and As(V) concentrations at all studied temperature, which interpret highly favorable adsorption of As(III) and As(V) on magnetite nanoparticles coated sand.

Table 5.1: Langmuir adsorption isotherm parameters for As(III) and As(V) adsorption by Fe_3O_4 nanoparticles coated sand at different temperatures.

Arsenic species	**Temp. in K**	**Langmuir isotherm parameters**				**Experimental q_m (mg/g)**
		***b* (L/mg)**	**q_m (mg/g)**	***r***	**R^2**	
As(III)	298	1.10299	1.9336	0.0434-0.0111	0.9997	1.877
	308	1.01556	2.211	0.0469-0.01202	0.9995	2.146
	318	1.01329	2.277	0.04702-0.01205	0.9999	2.198
As(V)	298	1.12109	2.056	0.04202-0.01059	0.996	2.002
	308	1.04747	2.283	0.04484-0.01133	0.995	2.236
	318	1.02442	2.393	0.0458-0.01158	0.993	2.338

5.5.3. Thermodynamic studies

The values of standard Gibbs free energy change(ΔG^o) for the adsorption process were calculated by using K_L values obtained from the Langmuir model at different temperatures and thermodynamic parameters associated with adsorption, i.e. standard free energy change (ΔG^o), standard enthalpy change (ΔH^o), standard entropy change (ΔS^o) are given in Table 5.2. The values of enthalpy change (ΔH^o) and entropy change (ΔS^o) for As(III) and As(V) were calculated from the slope and intercept of the plot of $\ln K_L$ versus $1/T$ (Fig. 5.5 (a) and 5.5 (b)). The ΔG^o values for both As(III) and As(V) are found to be negative for all studied temperature conditions, indicating the spontaneous nature of adsorption [287]. It has also been found that the ΔG^o value for As(III) and As(V) decreases from -1876.485 J/mol to -2210.421 J/mol and -2069.080 J/mol to -2371.174 J/mol, respectively with the increase in temperature from 298 K to 318 K. This decrease in ΔG^o with the increase in temperature indicates that the spontaneity degree of the adsorption process for both As(III) and As(V) has been increased with increase in temperature. The values of enthalpy change (ΔH^o) and

entropy change (ΔS^o) comes out to be positive for both As(III) and As(V) (Table 5.2). The positive values of ΔH^o indicate the endothermic nature of the adsorption process. This result is also supported by the increase in As(III) and As(V) adsorption capacity of magnetite nanoparticles coated sand with an increase in the temperature (Table 5.1). The positive values of ΔS^o suggests an increase in the degree of randomness at solid-liquid interface during the adsorption of As(III) and As(V) on magnetite nanoparticles coated sand [290].

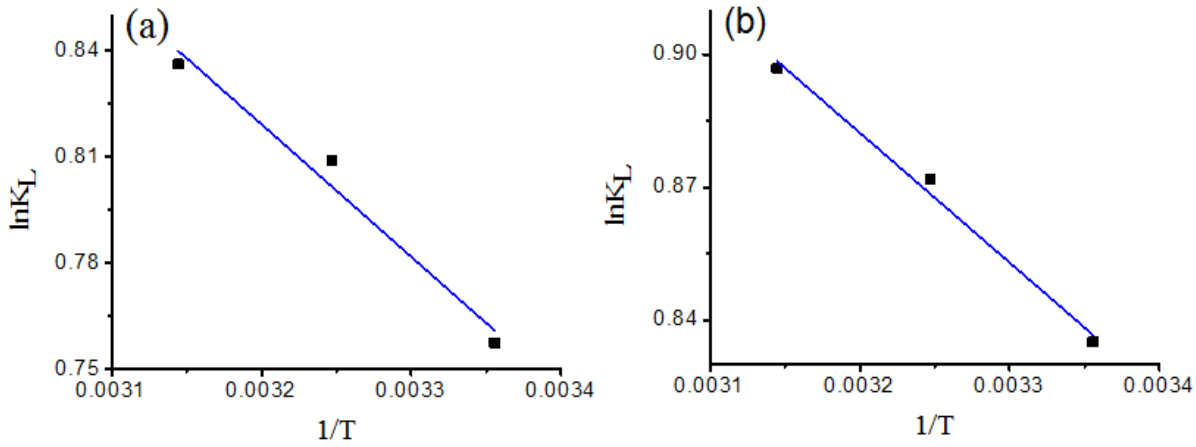

Figure 5.5: Plot of lnK_L vs 1/T for determination of thermodynamic parameters for (a) As(III) and (b) As(V) removal.

Table 5.2: Thermodynamic parameters obtained from ln$K_L$vs 1/T plot for As(III) and As(V) removal.

Arsenic species	**Thermodynamics parameters**					**$K_L(b \times q_{max})$ (L/g) At different temperature**		
	ΔH^o (kJ/mol)	**ΔS^o (J/mol)**	**ΔG^o (J/mol) At different temperature**					
			298 K	308 K	318 K	298 K	308 K	318 K
As(III)	3.108	16.757	-1876.485	-2071.318	-2210.421	2.1327	2.2454	2.30726
As(V)	2.436	15.132	-2069.080	-2232.631	-2371.174	2.3051	2.3914	2.4519

5.6. SUMMARY

We have observed that with increase in temperature from 25 ^{o}C to 45 ^{o}C, As(III) adsorption capacity of magnetite nanoparticles coated sand increased from 1.877 mg/g to 2.192 mg/g and As(V) adsorption capacity increased from 2.002 mg/g to 2.338 mg/g. This indicates that the arsenic adsorption process on magnetite nanoparticles coated sand is more favorable at higher temperature. Further, As(III) and As(V) adsorption isotherm data fitted well in Langmuir isotherm model with higher coefficients of determination ($R^2 > 0.99$) at all studied temperatures. The values of K_L were obtained from Langmuir isotherm models and were used to calculate various thermodynamic parameters associated with adsorption, i.e. standard Gibbs free energy change (ΔG^o), standard enthalpy change (ΔH^o) and standard entropy change (ΔS^o). The values of ΔG^o comes out to be negative and ΔH^o comes out to be positive for both As(III) and As(V), which indicates that the adsorption process is spontaneous and endothermic in nature, respectively. The value of ΔS^o comes out to be positive, which revealed an increase in degree of randomness at the solid-liquid interface during the adsorption of both As(III) and As(V).

CHAPTER 6

COLUMN STUDIES FOR THE ADSORPTION OF As(III) AND As(V): EFFECT OF COLUMN BED HEIGHT

6.1. INTRODUCTION

There are two types of adsorption studies viz. batch mode and continuous flow mode or column studies reported in the literature for arsenic removal from aqueous solution. Mostly the researchers prefer batch mode to conduct adsorption studies because a small amount of material is required and it is less time consuming method. Batch operations are very easy to operate on the laboratory scale but these are not convenient for the field applications. The batch operations are useful only for the treatment of small quantities of wastewater. Batch equilibrium experiment shows the adsorption capacity of the adsorbent, which provide fundamental information about the effectiveness of adsorbate–adsorbent system [291]. However in most of the treatment systems such as column operations, contact time is not sufficiently long for the attainment of equilibrium and therefore the data obtained from batch adsorption mode is generally not applicable to these systems. In other words the adsorption capacity data obtained from batch studies may not provide accurate scale-up information regarding the column operation systems [292]. So, it is very important to check the practical applicability of the adsorbent in the continuous flow mode. The continuous flow system is an effective process for the treatment of large-scale wastewater volumes and cyclic adsorption/desorption. The experimental breakthrough curve can be predicted from column adsorption studies which further help in the determination of column bed operation life span and regeneration time [293]. In addition basic engineering data can be easily obtained from the continuous flow systems. In fact from industrial point of view, the removal of pollutants including dyes, heavy metal ions etc. using continuous flow systems is found to be very useful and reliable. However, few studies have been reported in the literature on removal of arsenic and other pollutants in continuous flow mode [212, 291, 294-296]. Thus there is an urgent need of extensive research in this field.

In previous chapters, we have described the effect of various parameters on As(III) and As(V) removal through batch operation mode. In this chapter, we have documented the column bed adsorption experiments for both As(III) and As(V) removal from drinking water by using magnetite nanoparticles coated sand. The effect of column bed height (*h*) on the breakthrough curves was studied and the obtained breakthrough curves were analyzed using kinetics models viz. Thomas model and Yoon–Nelson model.

6.2. EXPERIMENTAL

6.2.1. Column adsorption experiments

A column study was conducted by using an ordinary 100 mL burette made of borosilicate glass with an internal diameter of 2 cm and height 55 cm. The effect of bed height on breakthrough curve was studied by varying the bed height from 5 cm to 10 cm. The bottoms of the columns were plugged in with glass wool just to make a support for the magnetite nanoparticles coated sand to prevent its floating from the outlet. The columns were packed with the desired amount of magnetite nanoparticles coated sand to the required height. The column was then operated in such a manner that a calculated amount of As(III) solution of required concentration was constantly added to it through a graduated cylinder and allowing it to flow along gravity in down flow mode with a constant rate. The rate of flow was checked by measuring the amount of As(III) solution in mL flowing per minute at regular intervals of time. Once the column started, the samples were collected at different time intervals using reagent bottles. This process was continued until the column gets exhausted and the amount of arsenic in different samples was then analyzed for residual arsenic concentrations.

Similar columns were also run for As(V) removal by varying the bed height (5 cm and 10 cm). All the columns were run at room temperature at neutral pH 7.0. Fig. 6.1 represents schematic of experimental setup for column studies of arsenic removal.

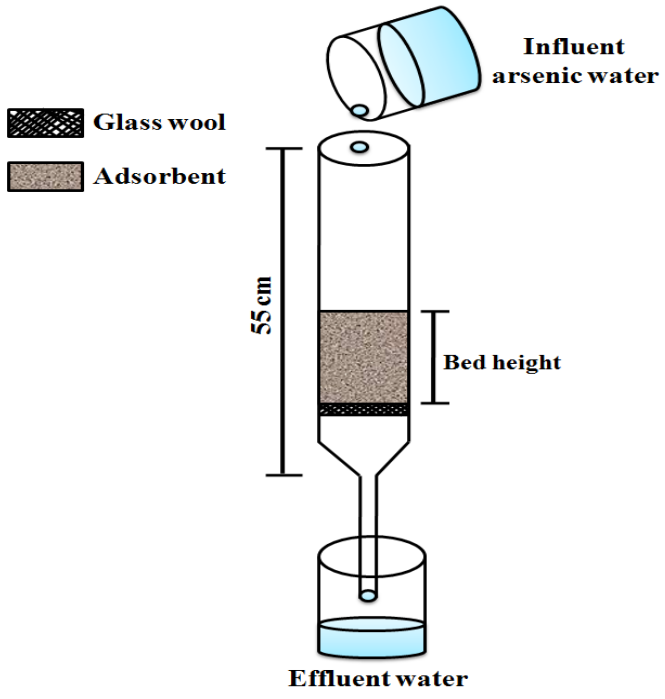

Figure 6.1: Schematic of experimental setup for column studies of arsenic removal.

6.3. ANALYSIS OF COLUMN DATA

6.3.1. Mathematical analysis

Breakthrough curves were obtained from the data generated by column experiments. Dynamic response of the adsorption column was determined by the breakthrough time and shape of the breakthrough curve. It is important to calculate the various parameters associated with column studies. Therefore, the mathematical analysis of the parameters associated with column breakthrough curve was done as described ahead [212, 293, 297, 298].

The effluent volume was calculated by using equation 6.1

$$V_{eff} = Qt_{total} \quad (6.1)$$

where, V_{eff} is the effluent volume collected in mL, Q is the volumetric flow rate in mL/min and t_{total} is the total flow time in min.

The maximum column bed capacity q_{total} in mg for a given inlet arsenic concentration and flow rate was calculated by using equation 6.2

$$q_{total} = \frac{QA_c}{1000} = \frac{Q}{1000}\int_{t=0}^{t=t_{total}} c_{ads}\, dt \quad (6.2)$$

where, q_{total} is the maximum bed capacity in mg and C_{ads} is the adsorbed arsenic concentration in mg/L. The plot of adsorbed arsenic concentration (C_{ads}, mgL^{-1}) versus time (t, min) gives area under the breakthrough curve (A_c).

The maximum adsorption capacity i.e. $q_{o,exp}$ at the exhaustion time was calculated by using equation 6.3

$$q_{o,exp} = \frac{q_{total}}{m} \quad (6.3)$$

where, m is the amount of the magnetite nanoparticles coated sand in grams packed in column.

Total amount of arsenic sent to column (M_{total}) was obtained from equation 6.4

$$M_{total} = \frac{C_o Q t_{total}}{1000} \quad (6.4)$$

where, M_{total} is the total amount of arsenic sent to the column in mg, C_o is the initial arsenic concentration in mg/L.

The total arsenic removal percentage is equal to the ratio of maximum column bed capacity (q_{total}) and total amount of arsenic sent to the column (M_{total}) as shown in equation 6.5

$$Total\ arsenic\ removal(\%) = \frac{q_{total}}{M_{total}} \times 100 \quad (6.5)$$

The time required for the arsenic contaminated water to fill the empty column is defined as empty bed residence time (*EBRT*), which is given by equation 6.6

$$EBRT = \frac{Bed\ volume}{volumetric\ flow\ rate\ of\ the\ liquid} \qquad (6.6)$$

The various parameters as described above viz. effluent volume (V_{eff}), total amount of arsenic adsorbed (q_{total}), total amount of arsenic sent to the column (M_{total}), total percentage removal of arsenic, empty bed resistance time (EBRT) were calculated for As(III) and As(V) removal using magnetite nanoparticles coated sand in fixed-bed adsorption column for different bed heights and are listed in Table 6.1.

6.3.2. Modelling of breakthrough curves

The dynamic behaviour of the column was predicted and analysed with two models i.e. (i) Thomas model and (ii) Yoon-Nelson model.

6.3.2.1. Thomas model

Thomas elaborated a model for adsorption processes in which external and internal diffusion constraints are not present. It demonstrates that the rate driving force obeys the second order reversible reaction kinetics and the Langmuir isotherm. The expression provided by Thomas compute the maximum solid phase concentration of solute on the adsorbent and the adsorption rate constant for an adsorption column [299]. The linearized form of the model is given as

$$ln\left[\left(\frac{C_0}{C_t}\right) - 1\right] = \left(\frac{K_{Th} q_0 m}{Q}\right) - \left(\frac{K_{Th} q_0 V_{eff}}{Q}\right) \qquad (6.7)$$

where, K_{Th} is the Thomas rate constant (mL min^{-1} mg^{-1}), q_o is the arsenic adsorbed per gram of the adsorbent (mg g^{-1}) and m is the amount of adsorbent packed in the column (g). The kinetic coefficient K_{Th} and the adsorption capacity of the column q_o can be determined from plot of $\ln((C_o/C_t) - 1)$ against t ($=V_{eff}/Q$) as per equation 6.7 at a given flow rate.

6.3.2.2. The Yoon-Nelson model

Yoon-Nelson model is very simple and straightforward model, which doesn't demand any information related to the property of adsorbate, adsorbent type, and the physical property of the adsorption bed. The Yoon and Nelson model is principally based on the belief that the rate of decrease in the probability of adsorption for each adsorbate molecule is proportional to

the probability of adsorbate adsorption and the probability of adsorbate breakthrough on the adsorbent [300]. The linearized form of Yoon and Nelson model for a single component system is expressed as

$$ln\frac{C_t}{C_o - C_t} = K_{YN}t - \tau K_{YN} \quad (6.8)$$

where, K_{YN} is the rate constant (min^{-1}) and τ is the time required for 50 % adsorbate breakthrough (min).

The values of parameters K_{YN} and τ for the adsorbate can be calculated from the plot of $\ln(C_t/(C_o - C_t))$ versus sampling time (t) according to eq. 6.8.

6.4. RESULTS AND DISCUSSION

6.4.1. Adsorption column behaviour: effect of bed height

We have studied the effect of bed height on column adsorption of As(III) and As(V) using magnetite nanoparticles coated sand. To study the effect of bed height on breakthrough curve, two columns of bed height 5 cm and two columns of bed height 10 cm of magnetite nanoparticles coated sand were taken, keeping the influent As(III) or As(V) concentration at 1mg/L and flow rate of 5 mL/min. The breakthrough curves for As(III) removal at two different bed heights of 5 cm and 10 cm are shown in Figs. 6.2 (a) and 6.2 (b) and for As(V) removal, the breakthrough curves are shown in Figs. 6.3 (a) and 6.3 (b), respectively. It has been observed that all the arsenic ions were adsorbed initially, resulting in zero arsenic concentration in the effluent. The arsenic concentration in the effluent gradually rose as the adsorption continued. Initially when arsenic-bearing water is introduced in the down flow mode from the top of the clean bed of magnetite nanoparticles coated sand, most of the arsenic removal occurs in a narrow band at the top of the column, referred to as adsorption zone. As column runs continuously, the adsorption zone progresses downward through the bed as the upper part of the column bed become saturated with arsenic. Eventually, the adsorption zone reaches the bottom of the column, and the arsenic concentration starts rising in the effluent [270]. By plotting the arsenic concentration (in mg/L) in the effluent i.e. C_t/C_o against time (in min) we obtained breakthrough curves as shown in Fig. 6.2 (a), (b) and Fig. 6.3 (a), (b). In breakthrough curve the point at which the arsenic concentration reaches its maximum acceptable value i.e. 0.01 mg/L or 10 µg/L is referred to as the breakthrough point and the time at which the breakthrough point is obtained is called breakthrough time. The column was considered to be exhausted when As(III) or As(V) concentration in the effluent

reaches 50 % of the influent As(III) or As(V) concentration. The breakthrough time 't_b' (corresponding to C_t/C_o = 0.01) and exhaustion time 't_e' (corresponding to C_t/C_o = 0.5) obtained for As(III) and As(V) at different bed heights are shown in Table 6.1.

We have found that with the increase in bed height from 5 cm to 10 cm the breakthrough time for As(III) increases from 360 to 1020 min and for As(V) increases from 420 to 1020 min. Similarly, the exhaustion time also increases from 1260 to 3360 min for As(III) and from 1800 to 3540 min for As(V), with increasing bed height. Further, the As(III) spiked water's volume corresponding to 5 cm and 10 cm bed height treated at the breakthrough time was 1800 mL and 5100 mL, and at the exhaustion time it was 6300 mL and 16800 mL, respectively. While the As(V) spiked water's volume corresponding to 5 cm and 10 cm bed height, treated at the breakthrough time was 2100 mL and 5100 mL, and at exhaustion time was 9000 mL and 17700 mL, respectively.

From Table 6.1, it is clear that the bed capacity, % removal of As(III) or As(V), breakthrough time (corresponding to an effluent concentration = 0.01 C_o) and exhaustion time (corresponding to an effluent concentration = 0.5 C_o) increased with an increase in bed height. The increase in the adsorption with bed height is due to large contact time and more adsorbent doses in larger beds, which provide large adsorption sites for the adsorption of As(III) and As(V), respectively. The increase in breakthrough time with increasing bed height suggests that breakthrough time is the determining quantity of the process [270, 212].

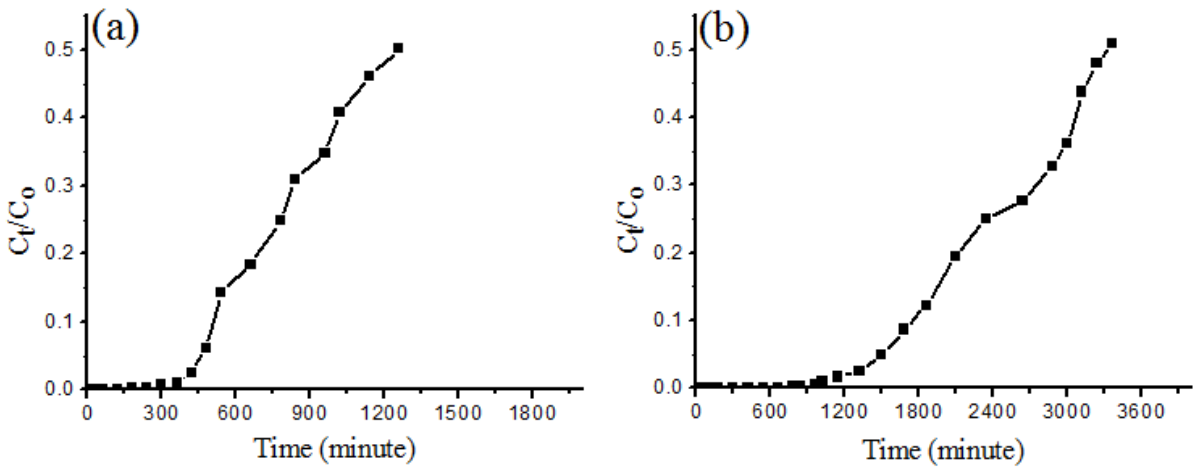

Figure 6.2: Effect of bed height (a) 5 cm and (b) 10 cm on breakthrough curve for As(III) adsorption on magnetite nanoparticles coated sand.

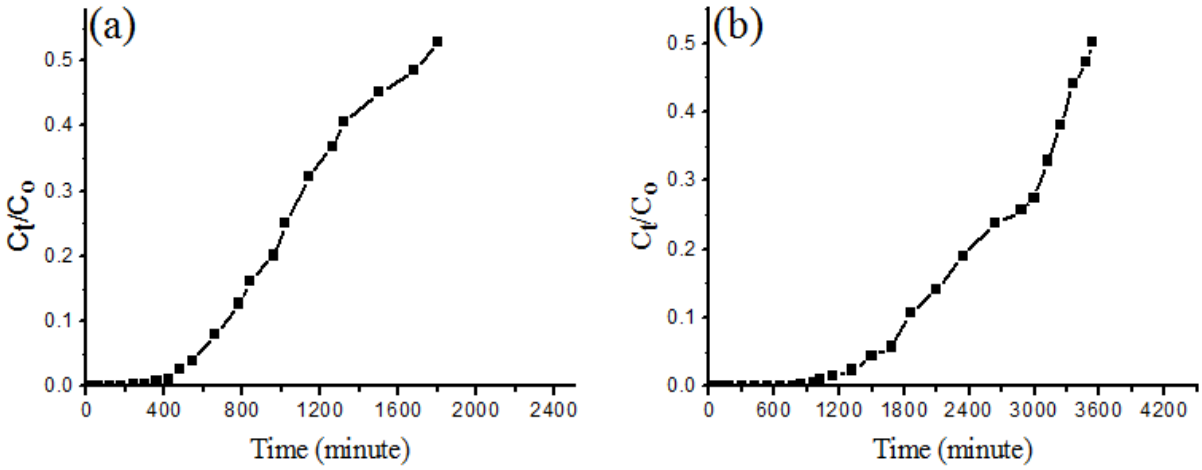

Figure 6.3: Effect of bed height (a) 5 cm and (b) 10 cm on breakthrough curve for As(V) adsorption on magnetite nanoparticles coated sand.

Fig. 6.4 (a), (b) and Fig. 6.5 (a), (b) shows the plot of C_{ads} ($C_{ads} = C_o - C_t$ in mg/L) versus time in min. for As(III) and As(V) removal at different bed heights of 5 cm and 10 cm, respectively. The area under the breakthrough curve (A_c) was calculated from these plots and used in equation 6.2 to calculate the q_{total} for As(III) and As(V) at different bed heights.

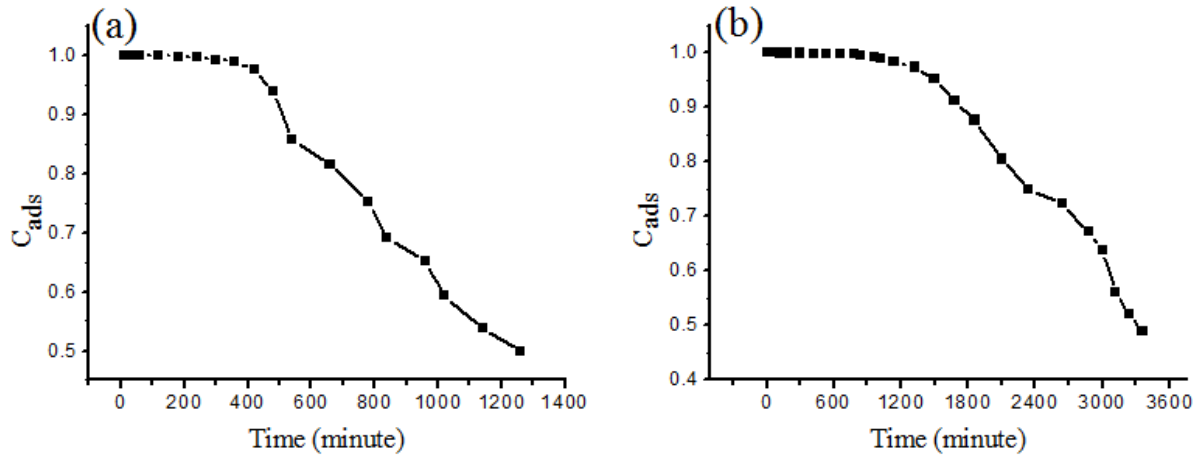

Figure 6.4: C_{ads} vs effluent time plot for As(III) adsorption at different bed heights (a) 5 cm and (b) 10 cm.

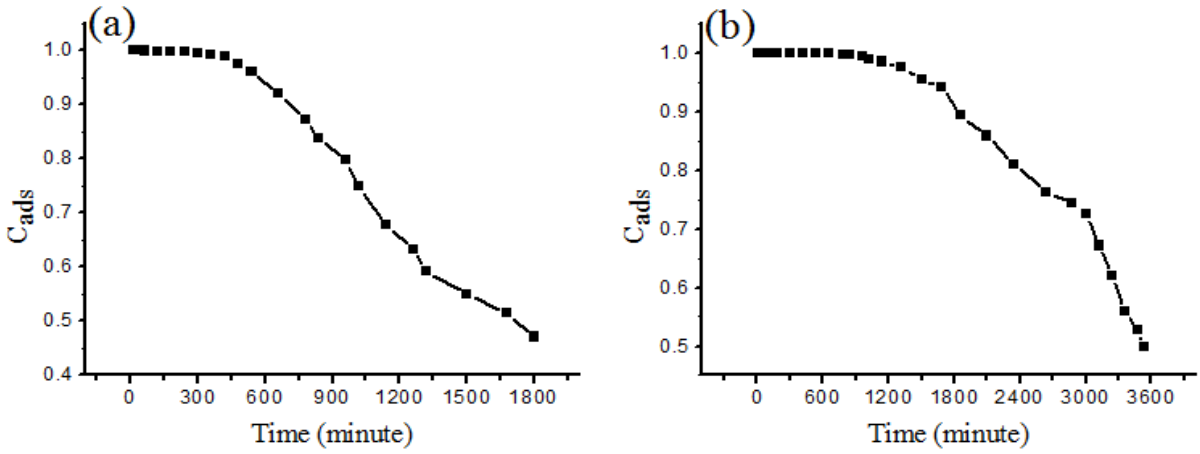

Figure 6.5: C_{ads} vs effluent time plot for As(V) adsorption at different bed heights (a) 5 cm and (b) 10 cm.

Table 6.1: Fixed bed adsorption column data and parameters obtained for As(III) and As(V) removal by using magnetite nanoparticles coated sand at different bed heights.

Arsenic species	***h*** **(cm)**	***C_o*** **(mg/ L)**	***Q*** **(mL / min)**	**EBRT (min)**	***t_b*** **(min)**	***t_{total}*** **or *t_e*** **(min)**	***v_{eff}*** **(mL)**	***M_{total}*** **(mg)**	***q_{total}*** **(mg)**	**% removal**
As(III)	5	1.0	5	2	360	1260	6300	6.3	5.023	79.73
As(III)	10	1.0	5	4	1020	3360	16800	16.8	15.28	90.96
As(V)	5	1.0	5	2	420	1800	9000	9	7.005	77.83
As(V)	10	1.0	5	4	1020	3540	17700	17.7	15.66	88.99

6.4.2. Application of Thomas model

The experimental column data was fitted with Thomas model to investigate the breakthrough behaviour of As(III) or As(V) adsorption onto magnetite nanoparticles coated sand. The Thomas kinetic coefficient K_{Th} was determined by applying Thomas model to the data in the concentration (C_t) range of 0.01 mg $L^{-1} < C_t < 0.5\ C_o$ with respect to the bed height. Fig. 6.6 (a), (b) and Fig. 6.7 (a), (b) shows the plots of Thomas kinetics model for adsorption of As(III) and As(V) on magnetite nanoparticles coated sand at different bed heights. The slope and intercepts obtained from the linear regression performed on each set of transformed data provides the different coefficients.

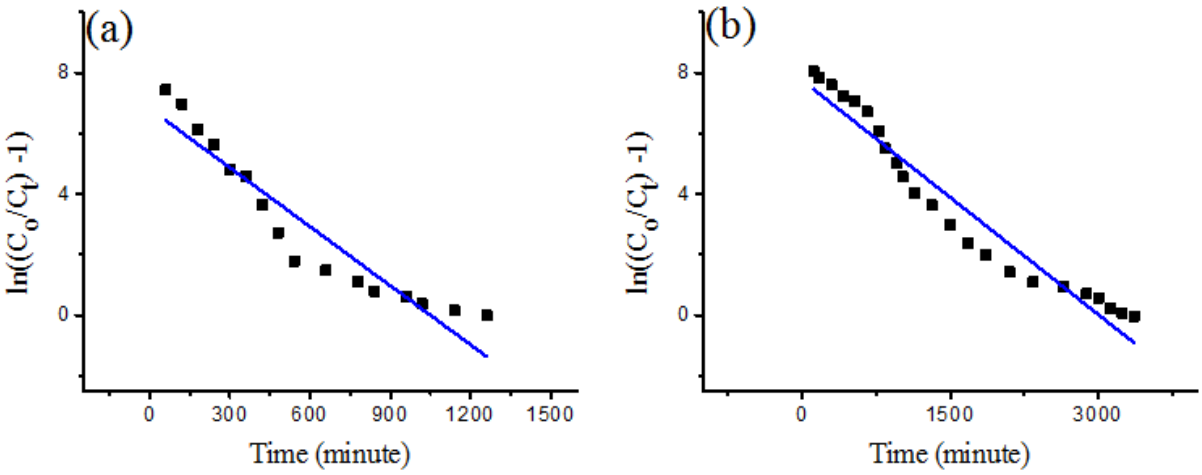

Figure 6.6: Thomas kinetic plot for adsorption of As(III) on magnetite nanoparticles coated sand: (a) 5 cm bed height, (b) 10 cm bed height.

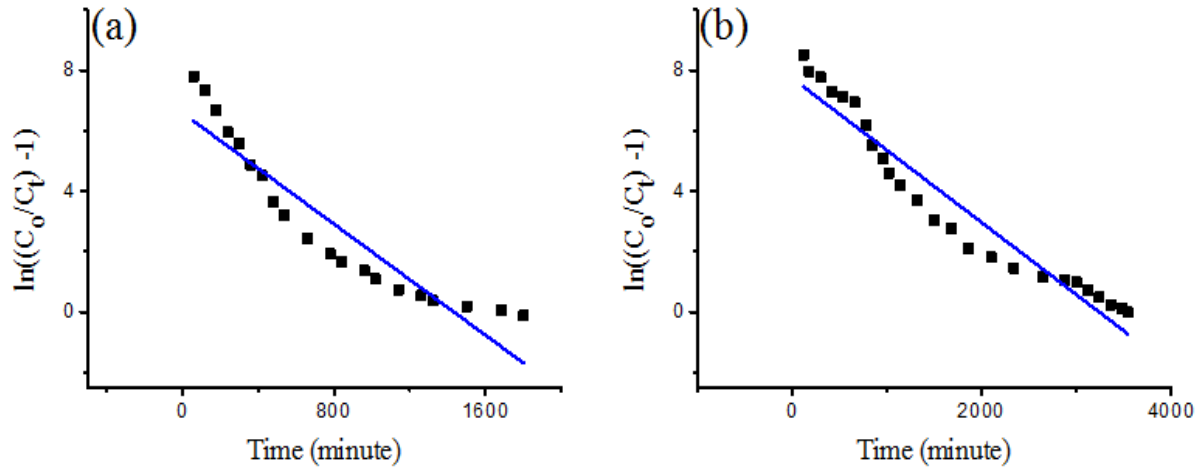

Figure 6.7: Thomas kinetic plot for adsorption of As(V) on magnetite nanoparticles coated sand: (a) 5 cm bed height, (b) 10 cm bed height.

The value of coefficient of determination R^2 for the above plots is found to be in the range of 0.87 to 0.94 indicating good fits of the experimental data in Thomas model as shown in Table 6.2. The values of K_{Th} and q_o obtained from the slope and intercepts of the above plots (Fig. 6.6 (a), (b) and Fig. 6.7 (a), (b)) for As(III) and As(V) at different bed heights are also given in the Table 6.2. The obtained results show that the bed capacity $q_{o,cal}$ increases with increase in bed height from 5 cm to 10 cm for both As(III) and As(V) and the K_{Th} decreases. Further, the experimental and calculated q_o values are very close to each other which also support that the experimental data fits well in Thomas model.

Table 6.2: Thomas model parameters obtained from the linear plots of Thomas model for As(III) and As(V) adsorption onto magnetite nanoparticles coated sand at different bed heights.

Arsenic species	***h* (cm)**	**C_o (mg L^{-1})**	***Q* (mL min^{-1})**	**K_{Th} (mL mg^{-1} min^{-1})**	**$q_{o,cal}$ (mg g^{-1})**	**$q_{o,exp}$ (mg g^{-1})**	**R^2**
As(III)	5	1.0	5	6.48	0.400	0.382	0.8936
As(III)	10	1.0	5	2.58	0.557	0.566	0.9406
As(V)	5	1.0	5	4.6	0.545	0.533	0.8716
As(V)	10	1.0	5	2.39	0.600	0.580	0.9339

6.4.3. Application of Yoon-Nelson Model

The breakthrough behaviour of As(III) and As(V) adsorption on magnetite nanoparticles coated sand was also investigated by applying another theoretical model developed by Yoon-Nelson. This model introduces the parameter τ, which shows treatment time taken C_t (effluent arsenic concentration) to be half of the initial concentration (C_o/2). Fig. 6.8 and Fig. 6.9 show the plots of Yoon-Nelson kinetics model for adsorption of As(III) and As(V) on magnetite nanoparticles coated sand, respectively at different bed heights. The slope and intercepts of the linear plots of $\ln(C_t/(C_o-C_t))$ versus time t with respect to bed height for both As(III) and As(V) (Fig. 6.8 and Fig. 6.9) provide the values of the model parameters K_{YN} (rate constant) and τ as presented in Table 6.3. With the increase in bed height from 5 cm to 10 cm, the value of K_{YN} (rate constant) decreases from 0.00648 to 0.00258 for As(III) and from 0.0046 to 0.00239 for As(V). The value of τ increases with the increase in bed height for both As(III) and As(V). The values of coefficient of determination R^2 ranging from 0.87 to 0.94 (Table 6.3) indicate that the experimental data fitted well with this model.

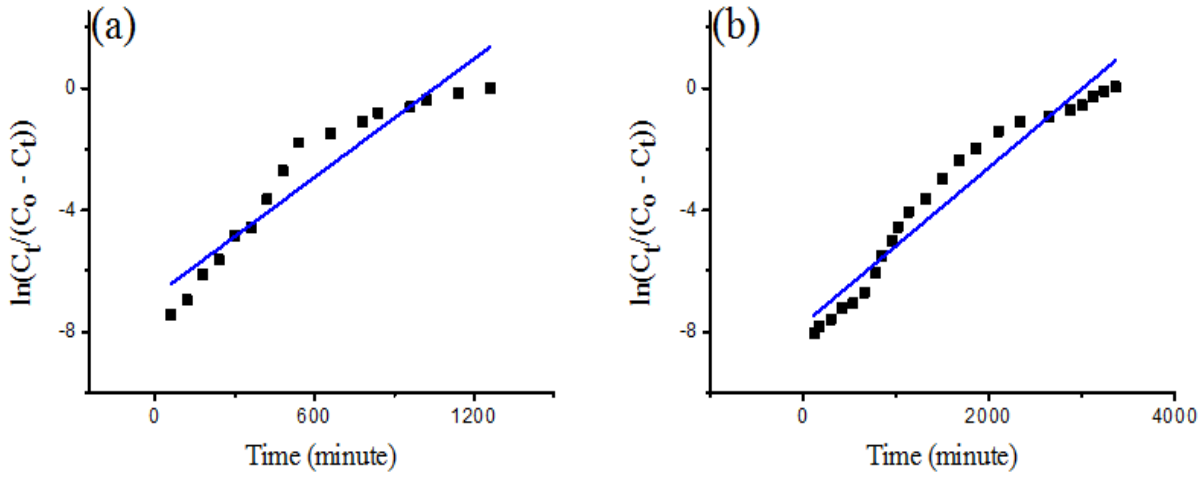

Figure 6.8: Yoon-Nelson kinetic plot for adsorption of As(III) on magnetite nanoparticles coated sand: (a) 5 cm bed height, (b) 10 cm bed height.

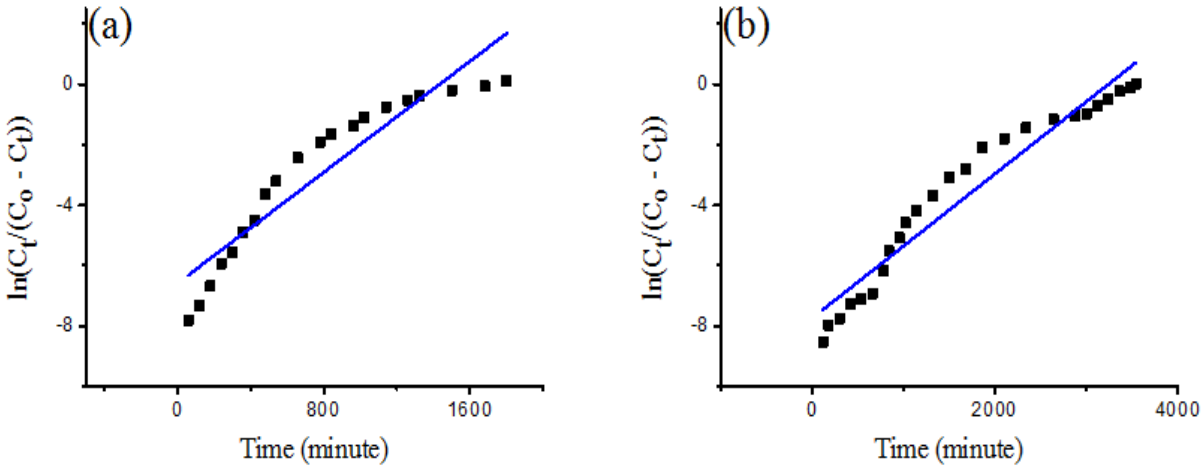

Figure 6.9: Yoon-Nelson kinetic plot for adsorption of As(V) on magnetite nanoparticles coated sand: (a) 5 cm bed height, (b)10 cm bed height.

Table 6.3: Yoon-Nelson model parameters obtained from linear plots of Yoon-Nelson model for As(III) and As(V) adsorption onto magnetite nanoparticles coated sand at different bed heights.

Arsenic species	***h*** **(cm)**	C_o **(mg** L^{-1}**)**	***Q*** **(mL** min^{-1}**)**	K_{YN} **(l** min^{-1}**)**	**τ (min)**	R^2
As(III)	5	1.0	5	0.00648	1050.88	0.8936
As(III)	10	1.0	5	0.00258	3007.69	0.9406
As(V)	5	1.0	5	0.0046	1433.23	0.8716
As(V)	10	1.0	5	0.00239	3239.24	0.9339

6.5. SUMMARY

Experimental and theoretical investigations were carried out on adsorption of As(III) and As(V) from aqueous solution onto magnetite nanoparticles coated sand by using column operation mode at different bed heights of 5 cm and 10 cm. From the column studies it has been observed that magnetite nanoparticles coated sand is an effective adsorbent for the removal of As(III) and As(V) from the aqueous environment. The adsorption is strongly dependent on the bed height. The breakthrough time and exhaustion time of the column increases with the increase in bed height. The bed capacity q_o also increases with increase in bed height for both As(III) and As(V). The experimental data fitted well in theoretical kinetics models viz. Thomas and Yoon-Nelson model with coefficients of determination ranging from 0.87 to 0.94. Thus the Thomas and Yoon-Nelson models provides a very good description of the breakthrough curves obtained at different bed heights for both As(III) and As(V) removal and proposed for use in the column design.

CHAPTER 7

SUMMARY AND FUTURE SUGGESTIONS

i

7.1. SUMMARY AND IMPORTANT FINDINGS

A low cost adsorbent has been synthesized by coating magnetite nanoparticles on the sand surface via co-precipitation method under continuous argon gas flow. The use of sand being an inexpensive material as a substrate for magnetite nanoparticles would pave the method to a cost effective technology. The synthesized adsorbent was characterized by FESEM, XRD and EDX for morphological, structural and elemental analysis of the adsorbent and to confirm the coating of magnetite nanoparticles on the sand surface. The surface area of adsorbent was also measured using BET surface area analyzer. FESEM study showed that the surface of sand was clear before coating and after coating the surface was covered with magnetite nanoparticles indicating the formation of magnetite nanoparticles on the sand surface. The FESEM study also showed that the magnetite nanoparticles have almost same morphology and size (20-60 nm) in the solution and on the surface of sand. The formation of magnetite nanoparticles on sand surface was also confirmed by the presence of magnetite peaks (well matched with JCPDS file PDF NO. 653107) in addition to uncoated sand peaks in XRD spectra of adsorbent. EDX analysis showed the presence of iron in coated sand along with Si and O elements, which also confirms the incorporation of magnetite nanoparticles on sand surface. BET surface area analysis showed that magnetite nanoparticles coating increased the surface area of sand by 5 m^2/g. The point of zero charge of adsorbent was also determined and found to be 7.8. This indicates that at pH 7.8, the adsorbent surface has neutral charge, below this pH the adsorbent surface is positively charged and above pH 7.8 the adsorbent surface acquires negative charge.

The potential of synthesized adsorbent was investigated for As(III) and As(V) removal by both batch operation mode and column operation mode. The batch studies were performed for both As(III) and As(V) removal by varying the different parameters viz. contact time, initial pH of the aqueous solution, adsorbent dose and initial As(III) or As(V) concentrations. The batch studies showed that equilibrium was achieved within 360 minutes of contact time for both As(III) and As(V) removal. The pH studies showed that maximum As(III) removal occur at pH-8.0 and maximum As(V) removal occur at pH-2.0, indicating acidic conditions are more favourable for As(V) removal. Further, we have found that 25 g/L of magnetite nanoparticles coated sand was sufficient to reduce the arsenic concentrations below 10 µg/L i.e. maximum contaminant level set by WHO. At optimum conditions, 99.96 % of As(III) and 99.99 % of As(V) removal was achieved by magnetite nanoparticles coated sand at initial As(III) or As(V) concentrations of 1 mg/L, respectively. Theoretical investigation of the

experimental kinetics data and isotherm data was also carried out to know the mechanism of adsorption. The batch kinetics data was fitted in pseudo-first-order and pseudo-second-order kinetics model. It has been observed that the experimental data fitted well in pseudo-second-order kinetics model with higher coefficients of determination ($R^2 > 0.99$) for both As(III) and As(V) removal as compared to pseudo-first-order kinetics model with lower coefficients of determination. The intra-particle diffusion model was also used to test the adsorption data. We have found that the plot of intra-particle diffusion model for both As(III) and As(V) removal did not yield a straight line passing through the origin, which indicates that intra-particle diffusion is not the sole rate limiting step. These observations reveals that arsenic adsorption on magnetite nanoparticles coated sand is a complex phenomenon which involves the contribution of both surface adsorption and intra-particle diffusion towards the rate of adsorption. Further, the adsorption isotherm data was fitted in Langmuir and Freundlich adsorption isotherms. The results showed that the data fitted well in Langmuir adsorption isotherm with higher coefficients of determination for both As(III) and As(V) as compared to Freundlich isotherm model indicating monolayer adsorption of arsenic ions on the homogeneous surface of the adsorbent. The Langmuir adsorption capacity for As(III) and As(V) removal was found to be 2.14 mg/g and 2.15 mg/g which is comparatively more than some adsorbents reported in the literature. The individual effect of various co-existing ions viz. PO_4^{3-}, SO_4^{2-}, HCO_3^{2-} and Cl^- on As(III) and As(V) removal efficiency was also investigated by performing the batch adsorption experiments in presence of these ions separately. The results showed that these ions affects the As(III) or As(V) removal efficiency of magnetite nanoparticles coated sand in the order of $PO_4^{3-} > HCO_3^{2-} > Cl^- > SO_4^{2-}$. However this effect was very small, probably due to strong complex formed between arsenic and magnetite. The batch desorption and readsorption studies were also performed for As(III) and As(V) by using sodium hydroxide solution as the desorbing agent. These studies showed that the arsenic removal efficiency of adsorbent decreases with repeated cycles due to the degradation of adsorbent.

We have also performed the batch adsorption experiments separately for As(III) and As(V) removal using pure magnetite nanoparticles and uncoated sand to know the role of magnetite nanoparticles i.e. real adsorbent. The experiments were also performed with different dosage of magnetite nanoparticles in order to know the amount of real adsorbent required to reduce the arsenic concentrations below 10 µg/L. The results showed that As(III) or As(V) removal was negligible in presence of uncoated sand, while pure magnetite nanoparticles reduce the

arsenic concentrations below 10 µg/L. It was also observed that 200 mg/L of magnetite nanoparticles i.e. real adsorbent were sufficient to reduce As(III) or As(V) concentrations below 10 µg/L.

As an important factor, the effect of temperature was also studied on As(III) and As(V) removal by performing batch adsorption experiments at different temperatures. The thermodynamic parameters associated with adsorption viz. ΔG^o, ΔS^o and ΔH^o were also calculated in order to completely understand the nature of adsorption. The results showed that As(III) or As(V) adsorption capacity of adsorbent increases with increase in temperature. The obtained negative values of ΔG^o at all studied temperature conditions indicate that adsorption process is spontaneous in nature. Further, decrease in negative values of ΔG^o with increase in temperature suggests that the spontaneity of the adsorption process increases with increase in temperature. The positive values of ΔH^o and ΔS^o for both As(III) and As(V) indicate that the adsorption process is endothermic in nature and there is increase in degree of randomness or free active sites at the solid-liquid interface during the adsorption of arsenic on adsorbent surface, respectively.

The column studies were also performed for the practical applications of the adsorbent. The experiments were performed at different bed heights of 5 cm and 10 cm at a constant flow rate of 5 mL/min in down flow mode. The results showed that the breakthrough time and exhaustion time increases with increase in bed height for both As(III) and As(V) removal. The experimental results of column study were fitted in two widely used theoretical models i.e. Thomas model and Yoon-Nelson model. These models provide good fit to the column breakthrough curve data with coefficients of determination ranging between 0.8716 and 0.9406.

Both batch adsorption experiments and column adsorption experiments are equally important. At one side the batch experiments give information about the equilibrium time, optimum adsorbent dose, and best suited pH to obtain the maximum arsenic removal. This study also indicates the nature of adsorption, whether it is physical or chemical, monolayer or multilayer, endothermic or exothermic, spontaneous or non-spontaneous in nature. On the other side, the data obtained from the column studies gives an idea about the amount of adsorbent required in making filter cartridge to treat a particular amount of arsenic contaminated water. The breakthrough time and exhaustion time obtained from column studies also gives a clear picture about the time at which the filter cartridge should be regenerated or replaced.

This thesis report the use of magnetite nanoparticles coated sand for arsenic removal from aqueous solution. The magnetite nanoparticles coated sand shows high adsorption capacity for As(III) and As(V) removal both in batch operation mode and column operation mode. Therefore by utilizing the filtration properties of sand and adsorption properties of magnetite nanoparticles, the synthesized adsorbent provides an economically feasible solution for a common man to get rid of poisonous arsenic from drinking water.

7.2. FUTURE SUGGESTIONS

- In future, the attempts could be made to increase the adsorption capacity of the adsorbent so as to increase the breakthrough time and exhaustion time of the column. This can be achieved by decreasing the size of the magnetite nanoparticles coated on the sand surface by varying the reaction parameters for coating.
- The column could be regenerated by using sodium hydroxide or some other desorbing agent and could be reused. This will increase the scope of the material.
- The disposal of waste generated is a big issue as arsenic is poisonous and therefore disposal of arsenic saturated adsorbent is of great concern. Thus in future possible measures to deal with the waste disposal management can be studied.
- In this thesis, we have reported the use of synthesized adsorbent for arsenic removal from synthetic water. The real life applications of the adsorbent i.e. field trials could also be performed. This could be done by treating the arsenic contaminated water samples collected from natural water sources of arsenic contaminated area.
- The adsorbent could also be synthesized on some other inexpensive substrates viz. glass wool, glass beads, cement, natural rock etc. and their potential could be checked for arsenic removal.
- In this thesis, we have used synthesized magnetite nanoparticles coated sand for arsenic removal from aqueous solution. In future, affinity of the adsorbent could also be checked for some other heavy metal ions i.e. chromium, nickel, lead etc.

REFERENCES

[1] Harth O., "*Water balance; transport of fluids and solutes*", In: Schmidt R.F., Thews G., editors, "Human physiology", Springer-Verlag Berlin Heidelberg, New York, pp. 643-657, 1983.

[2] Shiklomanov I., "*World fresh water resources*", In: Gleick P.H., editor, Water in crisis: A guide to the world's fresh water resources, Oxford University press, New York, pp. 13-24, 1993.

[3] An B., Steinwinder T.R., Zhao D., "*Selective removal of asenate from drinking water using a polymeric ligand exchanger*", Water Research, vol. 39(20), pp. 4993-5004, November 2005.

[4] National Research Council (NRC), "*Arsenic in drinking water: 2001 update*", National Academy Press, Washington DC, pp. 1-226, 2001.

[5] Shipley H.J., Yean S., Kan A.T., Tomson M.B., "*A sorption kinetics model for arsenic adsorption to magnetite nanoparticles*", Environmental Science and Pollution Research, vol. 17(5), pp. 1053-1062, June 2010.

[6] Mohan D., Pittman Jr. C.U., "*Arsenic removal from water/wastewater using adsorbents - a critical review*", Journal of Hazardous Materials", vol. 142(1-2), pp. 1-53, April 2007.

[7] Carabantes A.G., de Fernicola N.A.G.G., "*Arsénico en el agua de bebida: un problema de salud pública*", Revista brasileira de ciências farmacêuticas, vol. 39(4), pp. 365-372, December 2003.

[8] Driehaus W., Seith R., Jekel M., "*Oxidation of arsenate (III) with manganese dioxides in water treatment*", Water Research, vol. 29(1), pp. 297-305, January 1995.

[9] Jain C.K., Ali I., "*Arsenic: occurrence, toxicity and speciation techniques*", Water Research, vol. 34(17), pp. 4304-4312, December 2000.

[10] Smedley P.L., Nicolli H.B., Macdonald D.M.J., Barros A.J., Tullio J.O., "*Hydrogeochemistry of arsenic and other inorganic constituents in groundwaters from La Pampa, Argentina*", Applied Geochemistry, vol. 17(3), pp. 259–284, March 2002.

[11] Ferguson J.F., Gavis J., "*A review of the arsenic cycle in natural waters*", Water Research, vol. 6(11), pp. 1259–1274, November 1972.

[12] World Health Organization (WHO), "*Guidelines for drinking-water quality*", 3rd edition incorporating the first and second addenda, Vol. 1, Recommendations, WHO Press, Geneva, Switzerland, pp. 306, 2008.

[13] Smedley P.L., Kinniburgh D.G., "*A review of the source, behavior and distribution of arsenic in natural waters*", Applied Geochemistry, vol. 17(5), pp. 517-568, May 2002.

[14] Greenwood N.N., Earnshaw A., "*Chemistry of the elements*", 2nd edition, Elsevier, pp. 1-1600, 2012.

[15] Bednar A.J., Garbarino J.R., Ranville J.F., Wildeman T.R., "*Presence of organoarsenicals used in cotton production in agricultural water and soil of the southern United States*", Journal of Agricultural and Food Chemistry, vol. 50(25), pp. 7340–7344, November 2002.

[16] Xu Z., Jing C., Li F., Meng X., "*Mechanisms of photocatalytical degradation of monomethylarsonic and dimethylarsinic acids using nanocrystalline titanium dioxide*", Environmental Science & Technology, vol. 42(7), pp. 2349–2354, February 2008.

[17] Min S.Y., Kim B.K., Park S.J., Chang Y.Y., Yang J.K., "*Removal efficiency of arsenic by adsorbents having different type of metal oxides*", Environmental Engineering Research, vol. 14(2), pp. 134-139, June 2009.

[18] Wang S., Mulligan C.N., "*Occurrence of arsenic contamination in Canada: sources, behavior and distribution*", Science of The Total Environment, vol. 366(2-3), pp. 701–721, August 2006.

[19] Bard A.J., Parsons R., Jordan J., "*Standard potentials in aqueous solutions*", Marcel Dekker, New York, pp. 1-848, 1985.

[20] Mondal P., Majumder C.B., Mohanty B., "*Laboratory based approaches for arsenic remediation from contaminated water: recent developments*", Journal of Hazardous Materials, vol. 137(1), pp. 464–479, September 2006.

[21] Bissen M., Frimmel F.H., "*Arsenic: a review. Part I: Occurrence, toxicity, speciation, mobility*", Acta Hydrochimica et Hydrobiologica, vol. 31(1), pp. 9–18, July 2003.

[22] Onishi H., "*Arsenic"*, In: Wedepohl K.H., editor, Handbook of geochemistry, Vol. II, Springer-Verlag Berlin Heidelberg, New York, 1969.

[23] O'Day P.A., "*Chemistry and mineralogy of arsenic*", Elements, vol. 2, pp. 77-83, April 2006.

[24] Matschullat J., "*Arsenic in the geosphere – a review*", Science of The Total Environment, vol. 249(1-3), pp. 297–312, April 2000.

[25] Fatoki O.S., Akinsoji O.S., Ximba B.J., Olujimi O., Ayanda O.S., "*Arsenic contamination: Africa the missing gap*", Asian Journal of Chemistry, vol. 25(16), pp. 9263-9268, September 2013.

[26] Report, Bureau of reclamation, Technical Service Center, Water Treatment Engineering and Research Group, Denver, 2001.

[27] Polizzotto M.L., Harvey C.F., Li G., Badruzzman B., Ali A., Newville M., Sutton S., Fendorf S., "*Solid-phases and desorption processes of arsenic within Bangladesh sediments*", Chemical Geology, vol. 228(1-3), pp. 97–111, April 2006.

[28] Jackson B.P., Miller W.P., "*Soluble arsenic and selenium species in fly ash/organic waste-amended soils using ion chromatography-Inductively Coupled Plasma Mass Spectrometry*", Environmental Science & Technology, vol. 33(2), pp. 270-275, December 1998.

[29] Ruiz-Chanco M.J., Lopez-Sanchez J.F., Rubio R., "*Analytical speciation as a tool to assess arsenic behavior in soils polluted by mining*", Analytical and Bioanalytical Chemistry, vol. 387(2), pp. 627-635, January 2007.

[30] Mandal B.K., Suzuki K.T., "*Arsenic round the world: a review*", Talanta, vol. 58(1), pp. 201–235, August 2002.

[31] Leist M., Casey R.J., Caridi D., "*The management of arsenic wastes: problems and prospects*", Journal of Hazardous Materials, vol. 76(1), pp. 125–138, August 2000.

[32] Korte N.E., Fernando Q., "*A review of arsenic(III) in groundwater*", Critical Reviews in Environmental Control, vol. 21(1), pp. 1–39, 1991.

[33] Chen S.L., Yeh S.J., Yang M.H., Lin T.H., "*Trace element concentration and arsenic speciation in the well water of Taiwan area with endemic Blackfoot disease*", Biological Trace Elements Research, vol. 48(3), pp. 263–274, June 1995.

[34] McNeill L.S., Edwards M., "*Predicting arsenate removal during metal hydroxide precipitation*", Journal of American Water Works Association, vol. 89(1), pp. 75–86, January 1997.

[35] Nriagu J., Bhattacharya P., Mukherjee A., Bundschuh J., Zevenhoven R., Loeppert R., "*Arsenic in soil and groundwater: an overview*", In: Bhattacharya P., Mukherjee A.B., Bundschuh J., Zevenhoven R., Loeppert R.H., editors, Arsenic in soil and groundwater environment-biogeochemical interactions, health effects and remediation, Elsevier, Amsterdam, pp. 3–60, 2007.

[36] Das D., Samanta G., Mandal B.K., Chowdhury T.R., Chanda C.R., Chowdhury P.P., Basu G.K., Chakraborti D., "*Arsenic in groundwater in six districts of west Bengal, India*", Environmental Geochemistry and Health, vol. 18(1), pp. 5-15, March 1996.

[37] Bhattacharya P., Chatterjee D., Jacks G., "*Occurrence of arsenic-contaminated groundwater in alluvial aquifers from Delta Plains, Eastern India: options for safe drinking water supply*", International Journal of Water Resources Development, vol. 13(1), pp. 79–92, 1997.

[38] Nickson R., McArthur J., Burgess W., Ahmed K.M., Ravenscopft P., Rahman M., "*Arsenic poisoning of Bangladesh groundwater*", Nature, vol. 395, pp. 338, September 1998.

[39] Roy M., Nilsson L., Pal P., "*Development of groundwater resources in a region with high population density: a study of environmental sustainability*", Journal of Environmental Sciences, vol. 5(4), pp. 251–267, November 2008.

[40] Choong T.S.Y., Chuah T., Robiah Y., Koay F.G., Azni I., "*Arsenic toxicity, health hazards and removal techniques from water: an overview*", Desalination, vol. 217(1-3), pp. 139–166, November 2007.

[41] Mondal P., Bhowmick S., Chatterjee D., Figoli A., Van der Bruggen B., "*Remediation of inorganic arsenic in groundwater for safe water supply: A critical assessment of technological solutions*", Chemosphere, vol. 92(2), pp. 157–170, June 2013.

[42] Francesconi K.A., Kuehnelt D., "*Arsenic compounds in the Environment*", In: Frankenberger W.T., editor, Environmental chemistry of arsenic, New York, Marcel Dekker, Inc., pp. 51-94, 2002.

[43] Mitra S.R., Mazumder D.N.G., Basu A., Block G., Haque R., Samanta S., Ghosh N., Smith M.M.H., von Ehrenstein O.S., Smith A.H., "*Nutritional factors and susceptibility to arsenic-caused skin lesions in West Bengal, India*", Environmental Health Perspectives, vol. 112(10), pp. 1104-1109, July 2004.

[44] Hadi A., Parveen R., "*Arsenicosis in Bangladesh: prevalence and socioeconomic correlates*", Public Health, vol. 118(8), pp. 559-564, December 2004.

[45] Vahter M., Concha G., Nermell B., Nilsson R., Dulout F., Natarajan A.T., "*A unique metabolism of inorganic arsenic in native Andean women*", European Journal of Pharmacology: Environmental Toxicology and Pharmacology, vol. 293(4), pp. 455-462, December 1995.

[46] Steinmaus C., Yuan Y., Bates M.N., Smith A.H., "*Case-control study of bladder cancer and drinking water arsenic in the western United States*", American Journal of Epidemiology, vol. 158(12), pp. 1193-1201, December 2003.

[47] Rossman T.G., Uddin A.N., Burns F.J., Bosland M.C., "*Arsenite is a cocarcinogen with solar ultraviolet radiation for mouse skin: an animal model for arsenic carcinogenesis*", Toxicology and Applied Pharmacology, vol. 176(1), pp. 64-71, October 2001.

[48] Munoz O., Diaz O.P., Leyton I., Nunez N., Devesa V., Suner M.A., Velez D., Montoro R., "*Vegetables collected in the cultivated Andean area of Northern Chile: total and inorganic arsenic contents in raw vegetables*", Journal of Agricultural and Food Chemistry, vol. 50(3), pp. 642-647, December 2001.

[49] Wang J.P., Qi L., Moore M.R., Ng J.C., "*A review of animal models for the study of arsenic carcinogenesis*", Toxicology Letters, vol. 133(1), pp. 17-31, July 2002.

[50] IARC (International Agency for Research on Cancer), In: "*IARC Monographs on the evaluation of carcinogenic risk to humans: overall evaluations of carcinogenicity: an updating of IARC monographs*", 1-42(7), Lyon, France, International Agency for Research on Cancer, pp. 100-206, 1987.

[51] National Research Council (NRC), "*Arsenic in drinking water*", National Academy Press, Washington, D.C., 1999.

[52] Saha J.C., Dikshit A.K., Bandyopadhyay M., Saha K.C., "*A review of arsenic poisoning and its effects on human health*", Critical Reviews in Environmental Science and Technology, vol. 29(3), pp. 281-313, June 2010.

[53] Ng J.C., "*Environmental contamination of arsenic and its toxicological impact on humans*", Environmental Chemistry, vol. 2(3), pp. 146–60, 2005.

[54] Harvard University. "*The arsenic project website*", Internet. April 20, 2001, Available: http://phys4.harvard.edu/~wilson/arsenic_project_introduction.html.

[55] Yoshida T., Yamanchi H., Jun G.F., "*Chronic health effect in people exposed to arsenic via the drinking water: dose–response relationship in review*", Toxicology and Applied Pharmacology, vol. 198(3), pp. 243–252, August 2004.

[56] Wieneke J.K., Yager J.W., Varkonyi A., Hultner M., Lutze L.H., "*Study of arsenic mutagenesis using the plasmid shuttle vector pZ189 propagated in DNA repair proficient human cells*", Mutatation Research/Reviews in Mutation Research, Vol. 386(3), pp. 335–344, June 1997.

[57] Helledy T., Nilsson R., Jenssen D., "*Arsenic(III) and heavy metal ions induce intrachromosomal homologous recombination in the hprt gene of V79 Chinese hamster ovary cells*", Environmental and Molecular Mutagenesis, vol. 35(2), pp. 114–122, March 2000.

[58] Hei T.K., Filipic M., "*Role of oxidative damage in the genotoxicity of arsenic*", Free Radical Biology and Medicine, vol. 37(5), pp. 574–581, September 2004.

[59] Cuzick J., Sasieni P., Evans S., "*Ingested arsenic, keratoses, and bladder cancer*", American Journal of Epidemiology, vol. 136(4), pp. 417-421, August 1992.

[60] World Health Organization (WHO), "*Guidelines for drinking water quality recommendations*", 2nd edition, WHO Press, Geneva, Switzerland, 1993.

[61] Garelic H., Dybowska A., Valsami-Jones E., Priest N.D., "*Remediation technologies for arsenic contaminated drinking waters*", Journal of Soils and Sediments, vol. 5(3), pp. 182-190, August 2005.

[62] Masscheleyn P.H., Delaune R.D., Patrick Jr. W.H., "*Effect of redox potential and pH on arsenic speciation and solubility in a contaminated soil*", Environmental Science &Technology, vol. 25(8), pp. 1414–1419, August 1991.

[63] Johnston R., Heijnen H., "*Safe water technology for arsenic removal*", In: Ahmed M.F., Ali M.A., Adeel Z., editors, Technologies for arsenic removal from drinking water, pp. 1–22, 2001.

[64] Robins R.G., Nishimura T., Singh P., "*Removal of arsenic from drinking water by precipitation, adsorption or cementation*", In Proceedings of BUET-UNU Workshop, 2001.

[65] Twidwell L.G., McCloskey J., Miranda P., Gale M., "*Technologies and potential technologies for removing arsenic from process and mine wastewater*", In Proceedings of REWAS 99, San Sebastian, Spain, September 1999.

[66] Rott U., Friedle M., "*Eco-friendly and cost-efficient removal of arsenic, iron and manganese by means of subterranean ground-water treatment*", Water Supply, vol. 18(1/2), pp. 632-636, 2000.

[67] Kim M.J., Nriagu J., "*Oxidation of arsenite in groundwater using ozone and oxygen*", Science of The Total Environment, vol. 247(1), pp. 71–79, February 2000.

[68] Frank P., Clifford D., "*Arsenic(III) oxidation and removal from drinking water*", U.S. Environmental Protection Agency, EPA-600-52-86/021, pp. 2–86, 1986.

[69] Pettine M., Campanella L., Millero F.J., "*Arsenite oxidation by H_2O_2 in aqueous solutions*", Geochimica et Cosmochimica Acta, vol. 63(18), pp. 2727–2735, September 1999.

[70] Emett M.T., Khoe G.H., "*Photochemical oxidation of arsenic by oxygen and iron in acidic solutions*", Water Research, vol. 35(3), pp. 649–656, February 2001.

[71] Bissen M., Frimmel F.H., "*Arsenic - a review. Part II: oxidation of arsenic and its removal in water treatment*", Acta Hydrochimica et Hydrobiologica, vol. 31(2), pp. 97–107, September 2003.

[72] Lee Y., Um I.K., Yoon J., "*Arsenic(III) oxidation by iron(VI) (ferrate) and subsequent removal of arsenic(V) by iron(III) coagulation*", Environmental Science & Technology, vol. 37(24), pp. 5750–5756, November 2003.

[73] Ghurye G., Clifford D., Tripp A., "*Iron coagulation and direct microfiltration to remove arsenic from groundwater*", Journal of American Water Works Association, vol. 96(4), pp. 143–152, April 2004.

[74] Vasudevan S., Mohan S., Sozhan G., Raghavendran N.S., Murugan C.V., "*Studies of oxidation of As(III) to As(V) by in-situ-generated hypochlorite*", Industrial & Engineering Chemistry Research, vol. 45(22), pp. 7729–7732, September 2006.

[75] Dodd M.C., Vu N.D., Ammann A., Le V.C., Kissner R., Pham H.V., Cao T.H., Berg M., von Gunten U., "*Kinetics and mechanistic aspects of As(III) oxidation by aqueous chlorine, chloramines, and ozone: relevance to drinking water treatment*", Environmental Science & Technology, vol. 40(10), pp. 3285–3292, April 2006.

[76] Sharma V.K., Dutta P.K., Ray A.K., "*Review of kinetics of chemical and photocatalytical oxidation of arsenic(III) as influenced by pH*", Journal of Environmental Science and Health, Part. A: Toxic/Hazardous Substances and Environmental Engineering, vol. 42(7), pp. 997–1004, June 2007.

[77] Borho M., Wilderer P., "*Optimized removal of arsenate(III) by adaptation of oxidation and precipitation processes to the filtration step*", Water Science and Technology, vol. 34(9), pp. 25-31, February 1999.

[78] De Luca S.J., Idle C.N., Chao A.C., "*Quality improvement of biosolids by ferrate(VI) oxidation of offensive odour compounds*", Water Science & Technology, vol. 33(3), pp. 119-130, December 1996.

[79] Sharma V.K., Smith J.O., Millero F.J., "*Ferrate(VI) oxidation of hydrogen sulfide*", Environmental Science & Technology, vol. 31(9), pp. 2486-2491, August 1997.

[80] Sharma V.K., Rivera W., Smith J.O., O'Brien B., "*Ferrate(VI) oxidation of aqueous cyanide*", Environmental Science & Technology, vol. 32(17), pp. 2608-2613, July 1998.

[81] Sylvester P., Rutherford Jr L.A., Gonzalez-Martin A., Kim J., Rapko B.M., Lumetta G.J., "*Ferrate treatment for removing chromium from high-level radioactive tank waste*", Environmental Science & Technology, vol. 35(1), pp. 216-221, November 2000.

[82] Vogels C.M., Johnson M.D., "*Arsenic remediation in drinking waters using ferrate and ferrous ions*", Report, New Mexico Water Resources Research Institute, New Mexico State University, Las Cruces, NM, pp. 1-21, June 1998.

[83] Gihring T.M., Druschel G.K., McCleskey R.B., Hamers R.J., Banfield J.F., "*Rapid arsenite oxidation by thermos aquaticus and thermos thermophilus: field and laboratory investigations*", Environmental Science & Technology, vol. 35(19), pp. 3857-3862, October 2001.

[84] Zaw M., Emett M.T., "*Arsenic removal from water using advanced oxidation processes*", Toxicology Letters, vol. 133(1), pp. 113–118, July 2002.

[85] Sorlini S., Gialdini F., "*Conventional oxidation treatments for the removal of arsenic with chlorine dioxide*, hypochlorite, potassium permanganate and monochloramine", Water Research, vol. 44(19), pp. 5653-5659, November 2010.

[86] Criscuoli A., Majumdar S., Figoli A., Sahoo G.C., Bafaro P., Bandyopadhyay S., Drioli E., "*As(III) oxidation by MnO_2 coated PEEK-WC nanostructured capsules"*, Journal of Hazardous Materials, vol. 211-212, pp. 281–287, April 2012.

[87] Ghurye G., Clifford D., "*As(III) oxidation using chemical and solid-phase oxidants*", Journal of American Water Works Association, vol. 96(1), pp. 84–96, January 2004.

[88] Liu G., Zhang X., Talley J.W., Neal C.R., Wang H., "*Effect of NOM on arsenic adsorption by TiO_2 in simulated As(III)-contaminated raw waters*", Water Research, vol. 42(8-9), pp. 2309–2319, April 2008.

[89] Dutta P.K., Ray A.K., Sharma V.K., Millero F.J., "*Adsorption of arsenate and arsenite on titanium dioxide suspensions*", Journal of Colloid and Interface Science, vol. 278(2), pp. 270–275, October 2004.

[90] Kocar B.D., Inskeep W.P., "*Photochemical oxidation of As(III) in ferrioxalate solutions*", Environmental Science & Technology, vol. 37(8), pp. 1581–1588, April 2003.

[91] Neppolian B., Celik E., Choi H., "*Photochemical oxidation of arsenic(III) to arsenic(V) using peroxydisulphate ions as an oxidizing agent*", Environmental Science & Technology, vol. 42(16) pp. 6179–6184, August 2008.

[92] Dutta P.K., Pehkonen S.O., Sharma V.K., Ray A.K., "*Photocatalytic oxidation of arsenic(III): evidence of hydroxyl radicals*", Environmental Science & Technology, vol. 39(6), pp. 1827-1834, March 2005.

[93] Yoon S.H., Lee J.H., "*Oxidation mechanism of As(III) in the UV/TiO_2 system: evidence for a direct hole oxidation mechanism*", Environmental Science & Technology, vol. 39(24), pp. 9695–9701, December 2005.

[94] García M.G., d'Hiriart J., Giullitti J., Lin H., Custo G., del Hidalgo M.V., Litter M.I., Blesa M.A., "*Solar light induced removal of arsenic from contaminated groundwater: the interplay of solar energy and chemical variables*", Solar Energy, vol. 77(5), pp. 601–613, November 2004.

[95] Yang H., Lin W.Y., Rajeshwar K., "*Homogeneous and heterogeneous photocatalytic reactions involving As(III) and As(V) species in aqueous media*", Journal of Photochemistry and Photobiology A: Chemistry, vol. 123(1-3), pp. 137–143, May 1999.

[96] Bissen M., Vieillard-Baron M.M., Schindelin A.J., Frimmel F.H., "*TiO_2-catalyzed photooxidation of arsenite to arsenate in aqueous samples*", Chemosphere, vol. 44(4), pp. 751–757, August 2001.

[97] Khan M.M.T., Yamamoto K., Ahmed M.F., "*A low cost technique of arsenic removal from drinking water by coagulation using ferric chloride salt and alum*", Water Science and Technology: Water Supply, vol. 2(2), pp. 281-288, April 2002.

[98] Edwards M., "*Chemistry of arsenic removal during coagulation and Fe-Mn oxidation*", Journal of American Water Works Association, vol. 86(9), pp. 64-78, September 1994.

[99] Baskan M.B., Pala A., "*A statistical experiment design approach for arsenic removal by coagulation process using aluminum sulphate*", Desalination, vol. 254(1-3), pp. 42–48, May 2010.

[100] Laky D., Licsko I., "*Arsenic removal by ferric-chloride coagulation-effect of phosphate, bicarbonate and silicate*", Water Science & Technology, vol. 64(5), pp. 1046–1055, September 2011.

[101] Shen Y.S., "*Study of arsenic removal from drinking water*", Journal of American Water Works Association, vol. 65(8), pp. 543-548, August 1973.

[102] Rios G.B., Almeraya F., Herrera M.T.A., "*Electrode passivation in the electro-coagulation process*", Portugaliae Electrochimica Acta, vol. 23(1), pp. 17–34, 2005.

[103] Kumar P.R., Chaudhari S., Khilar K., Mahajan S.P., "*Removal of arsenic from water by electrocoagulation*", Chemosphere, vol. 55(9), pp. 1245-1252, June 2004.

[104] Lakshmanan D., Clifford D.A., Samanta G., "*Ferrous and ferric ion generation during iron electrocoagulation*", Environmental Science & Technology, vol. 43(10), pp. 3853-3859, May 2009.

[105] Balasubramanian N., Madhavan K., "*Arsenic removal from industrial effluent through electrocoagulation*", Chemical Engineering & Technology, vol. 24(5), pp. 519-521, May 2001.

[106] Hansen H.K., Nunez P., Grandon R., "*Electrocoagulation as a remediation tool for wastewaters containing arsenic*", Minerals Engineering, vol. 19(5), pp. 521-524, April 2006.

[107] Masel R.I., "*Principles of adsorption and reaction on solid surfaces*", John Wiley and sons, 1996.

[108] Crittenden B., Thomas W.J., "*Adsorption technology and design*", 1st edition, Butterworth- Heinemann, 1998.

[109] Sun X., Doner, H.E., "*Adsorption and oxidation of arsenite on goethite*", Soil Science, vol. 163(4), pp. 278–287, April 1998.

[110] Wang C., Luo H., Zhang Z., Wu Y., Zhang J., Chen S., "*Removal of As(III) and As(V) from aqueous solutions using nanoscale zero valent iron-reduced graphite oxide modified composites*", Journal of Hazardous materials, vol. 268(15), pp. 124 –131, March 2014.

[111] JessenS., Larsen F., Koch C.B., Avin E., "*Sorption and desorption of arsenic to ferrihydrite in a sand filter*", Environmental Science & Technology, vol. 39(20), pp. 8045–8051, September 2005.

[112] Lakshmipathiraj P., Narasimhan B.R.V., Prabhakar S., Bhaskar R.G., "*Adsorption studies of arsenic on Mn-substituted iron oxyhydroxide*", Journal of Colloid and Interface Science, vol. 304(2), pp. 317–322, December 2006.

[113] Banerjee K., Amy G. L., Prevost M., Nour S., Jekel M., Gallagher P.M., Blumenschein C.D., "*Kinetic and thermodynamic aspects of adsorption of arsenic*

onto granular ferric hydroxide (GFH)", Water Research, vol. 42(13), pp. 3371–3378, July 2008.

[114] Zhang Y.M., Yang M., Huang X., "*Arsenic(V) removal with a Ce(IV)-doped iron oxide adsorbent*", Chemosphere, vol. 51(9), pp. 945–952, June 2003.

[115] Guo H.M., Stuben D., Berner Z., "*Adsorption of arsenic (III) and arsenic (V) from groundwater using natural siderite as the adsorbent*", Journal of Colloid and Interface Science, vol. 315(1), pp. 47–53, November 2007.

[116] Kundu S. Gupta A.A., "*Sorption kinetics of As(V) with iron-oxide coated cement-a new adsorbent and its application in the removal of arsenic from real life groundwater samples*", Journal of Environmental Science and Health. Part A, Toxic/Hazardous Substances & Environmental Engineering, vol. 40(12), pp. 2227-2246, February 2007.

[117] Gupta V.K., Saini V.K., Jain N., "*Adsorption of As(III) from aqueous solutions by iron oxide coated sand*", Journal of Colloid and Interface Science, vol. 288(1), pp. 55-60, August 2005.

[118] Sinha S., Amy G., Yoon Y., Her N., "*Arsenic removal from water using various adsorbents: magnetic ion exchange resins, hydrous ion oxide particles, granular ferric hydroxide, activated alumina, sulfur modified iron, and iron oxide-coated microsand*", Environmental Engineering Research, vol. 16(3), pp. 165-173, September 2011.

[119] Kim J., Benjamin M.M., "*Modeling a novel ion exchange process for arsenic and nitrate removal*", Water Research, vol. 38(8), pp. 2053-2062, April 2004.

[120] Nenov D.V., Kamenski D., "*Ion exchange resins of increased selectivity towards arsenic*", Environmental Protection Engineering, vol. 12(3), pp. 79-87, 1986.

[121] United States Environmental Protection Agency (USEPA), "*Technologies and costs for removal of arsenic from drinking Water*", U.S. EPA, EPA 815-R-00-028, Prepared by Malcolm Pirnie, Inc. under contract 68C60039 for EPA ORD, Washington, DC, December 2000.

[122] United States Environmental Protection Agency (USEPA), "*Regulations on the disposal of arsenic residuals from drinking water treatment plants*", Office of Research and Development, U.S. EPA, EPA 600-R-00- 025. May 2000.

[123] ShihM.C., "*An overview of arsenic removal by pressure-driven membrane processes*", Desalination, vol. 172(1), pp. 85-97, February 2005.

[124] Han B., Runnels T., Zimbron J., Wickramasinghe R., "*Arsenic removal from drinking water by flocculation and microfiltration*", Desalination, vol. 145(1-3), pp. 293– 298, September 2002.

[125] Gecol H., Ergican E., Fuchs A., "*Molecular level separation of arsenic(V) from water using cationic surfactant micelles and ultrafiltration membrane*", Journal of Membrane Science, vol. 241(1), pp. 105–119, September 2004.

[126] Iqbal J., Kim H.J., Yang J.S., Baek K., Yang J.W., "*Removal of arsenic from groundwater by micellar-enhanced ultrafiltration (MEUF)*", Chemosphere, vol. 66(5), pp. 970–976, January 2007.

[127] Figoli A., Cassano A., Criscuoli A., Mozumder M.S.I., Uddin M.T., Islam M.A., Drioli E., "*Influence of operating parameters on the arsenic removal by nanofiltration*", Water Research, vol. 44(1), pp. 97–104, January 2010.

[128] Waypa J.J., Elimelech M., Hering J.G., "*Arsenic removal by RO and NF membranes*", Journal of American Water Works Association, vol. 89 (10) pp. 102–114, October 1997.

[129] Schneiter R.W., Middlebrooks E.J., "*Arsenic and fluoride removal from groundwater by reverse osmosis*", Environmental International, vol. 9(4), pp. 289-291, June 2003.

[130] Velizarov S., Crespo J., Reis M., "*Removal of inorganic anions from drinking water supplies by membrane bio/processes*", Reviews in Environmental Science and Biotechnology, vol. 3(4), pp. 361–380, December 2004.

[131] Fox K.R., "*Field experience with point-of-use treatment systems for arsenic removal*", Journal of American Water Works Association, vol. 81(2), pp. 94–101, February 1989.

[132] Geucke T., Deowan S., Hoinkis J., Pätzold C., "*Performance of a small-scale RO desalinator for arsenic removal*", Desalination, vol. 239(1-3), pp. 198–206, April 2009.

[133] Visoottiviseth P., Francesconi K., Sridokchan W., "*The potential of Thai indigenous plant species for the phytoremediation of arsenic contaminated land*", Environmental Pollution, vol. 118(3), pp. 453–461, August 2002.

[134] Ma L.Q., Komar K.M., Tu C., Zhang W., Cai Y., Kennelley E.D., "*A fern that hyperaccumulates arsenic*", Nature, vol. 409(6820), pp. 579, February 2001.

[135] Mouchet P., "*From conventional to biological removal of iron and manganese in France*", Journal of Water Works Association, vol. 84(4), pp. 158–167, April 1992.

[136] Leblanc M., Achard B., Othman D.B., Luck J.M., Bertrand-Sarfati J., Personne J.C., "*Accumulation of arsenic from acidic mine waters by ferruginous bacterial accretions (stromatolites)*", Applied Geochemistry, vol. 11(4), pp. 541–554, July 1996.

[137] Fukushi K., Sasaki M., Sato T., Yanase N., Amano H.,Ikeda H., "*A natural attenuation of arsenic in drainage from an abandoned arsenic mine dump*", Applied Geochemistry, vol. 18(8), pp. 1267–1278, August 2003.

[138] Katsoyiannis I.A., Zouboulis A.I.,Jekel M., "*Kinetics of bacterial As(III) oxidation and subsequent As(V) removal by sorption onto biogenic manganese oxides during groundwater treatment*", Industrial & Engineering Chemistry Research, vol. 43(2), pp. 486–493, January 2004.

[139] Parknikar K.M., "*Potential application of microbiological processes for the removal of arsenic from groundwater*", A paper presented in the International Conference on Arsenic Pollution of Groundwater in Bangladesh: Causes, Effects and Remedies, Dhaka, Bangladesh, February 1998.

[140] Iberhan L.,Wisniewski M., "*Removal of arsenic(III) and arsenic(V) from sulfuric acid solution by liquid-liquid extraction*", Journal of Chemical Technology and Biotechnology, vol. 78(6), pp. 659-665, June 2003.

[141] De Lourdes Ballinas M., de San Miguel E.R., Munoz M., de Gyves J., "*Arsenic(V) extraction from sulfuric acid media using DBBP-D_2EHPA organic mixtures*", Industrial & Engineering Chemistry Research, vol. 42(3), pp. 574-581, February 2003.

[142] Cathum S.J., Brown C.E., Obenauf A., Punt M., "*Speciation of arsenic using chelation solvent extraction and high performance liquid chromatography*", Clean-Soil, Air, Water, vol. 35(1), pp. 71-80, February 2007.

[143] Marr R., Bart H.J., Wachter R., "*Method of removing arsenic from a copper electrolyte*", US patent, 1985.

[144] Cundy A.B., Hopkinson L., Whiteby R.L.D., "*Use of iron-based technologies in contaminated land and groundwater remediation: a review*", Science of The Total Environment, vol. 400(1-3), pp. 42-51, August 2008.

[145] United States Environmental Protection Agency (USEPA), "*Permeable reactive barrier technologies for contaminant remediation*", EPA 600/R-98/125. Washington, DC 20460: U.S. EPA, 94 pp. 604, 1998.

[146] Bartzas G., Komnitsas K., "*Solid phase studies and geochemical modeling of low-cost permeable reactive barriers*", Journal of Hazardous Materials, vol. 183(1-3), pp. 301-308, November 2010.

[147] Lo I.M.C., Surampalli R.Y., Lai K.C.K., "*Zero-valent iron reactive materials for hazardous waste and inorganics removal*", Reston, Vieginia: American Society of Civil Engineers (ASCE), pp. 1-360, 2007.

[148] Kirchmer C., De Esparza M.L.C., "*Remoción de Arsénico en aguas con alto contenido de Magnesio*", CEPIS. Lima, Peru, 1978.

[149] Viraraghavan T., Subramanian S., Swaminathan V., "*Drinking water without arsenic: a review of treatment technologies*", Environmental systems reviews, Environmental Systems Information Center, Bangkok, Thailand, vol. 37, 1994.

[150] De Esparza M.L.C., "*Removal of arsenic from drinking water and soil bioremediation*", International Congress Mexico City, 20-24 June 2006.

[151] Peng F.F., Di P., "*Removal of arsenic from aqueous solution by adsorbing colloid flotation*", Industrial & Engineering Chemistry Research, vol. 33(4), pp. 922-928, April 1994.

[152] Huang S.D., Tzuoo J.J., Gau H.S., Fann C.F., "*Effect of Al(III) as an activator for adsorbing colloid flotation*", Separation Science and Technology, vol. 19(13-15), pp. 1061-1072, December 2006.

[153] Zhao Y.C., Zouboulis A.L., Matis K.A., "*Removal of molybdate and arsenate from aqueous solution by flotation*", Separation Science and Technology, vol. 31(6), pp. 769-785, August 2006.

[154] Pacheco A.C.C., Torem M.L., "*Influence of ionic strength on the removal of* As^{5+} *by adsorbing colloid flotation*", Separation Science and Technology, vol. 37(15), pp. 3599-3610, February 2007.

[155] Matis K.A., Papadoyannis I.N., Zouboulis A.I., "*Separation of germanium and arsenic from solutions by flotation*", International Journal of Mineral Processing, vol. 21(1-2), pp. 83-92, August 1987.

[156] Pan Z., Zhang L., Somasundaran P., "*Removal of arsenic from contaminated water by foam flotation*", European Journal of Mineral Processing & Environmental Protection, vol. 3(2), pp. 243-247, May 2003.

[157] Zamboulis D., Peleka E.N., Lazaridis N.K., Matis K.A., "*Metal ion separation and recovery from environmental sources using various flotation and sorption*

techniques", Journal of Chemical Technology and Biotechnology, vol. 86(3), pp. 335-344, March 2011.

[158] Matis K.A., Zouboulis A.I., Zamboulis D., Valtadorou A.V., "*Sorption of As(V) by goethite particles and study of their flocculation*", Water, Air, and Soil Pollution, vol. 111(1), pp. 297-316, April 1999.

[159] Nenov V., Zouboulis A.I., Dimitrova N., Dobtevsky I., "*As(III) removal from aqueous solutions using non-stoichiometric coprecipitation with iron(III) sulphate and filtration or flotation*", Environmental Pollution, vol. 83(3), pp. 283-289, 1994.

[160] Kordmostafapour F., Pourmoghadas H., Shahmansouri M.R., Parvaresh A., "*Arsenic removal by dissolved air flotation*", Journal of Applied Sciences, vol. 6(5), pp. 1153-1158, 2006.

[161] Matis K.A., Zouboulis A.I., Malamas F.B., Afonso M.D.R., Hudson M.J., "*Flotation removal of As(V) onto goethite*", Environmental Pollution, vol. 97(3), pp. 239-245, 1997.

[162] Mascolo M.C., Pei Y., Ring T.A., "*Room temperature coprecipitation synthesis of magnetite nanoparticles in a large pH window with different bases*", Materials, vol. 6(12), pp. 5549-5567, November 2013.

[163] Petcharoen K., Sirivat A., "*Synthesis and characterization of magnetite nanoparticles via the chemical co-precipitation method*", Materials Science and Engineering: B, vol. 177(5), pp. 421-427, March 2012.

[164] Xu J., Yang H., Fu W., Du K., Sui Y., Chen J., Zeng Y., Li M., Zou G., "*Preparation and magnetic properties of magnetite nanoparticles by sol-gel method*", Journal of Magnetism and Magnetic Materials, vol. 309(2), pp. 307-311, February 2007.

[165] Lemine O.M., Omri K., Zhang B., Mir L.E., Sajieddine M., Alyamani A., Bououdina M., "*Sol-gel synthesis of 8 nm magnetite (Fe_3O_4) nanoparticles and their magnetic properties*", Superlattices and Microstructures, vol. 52(4), pp. 793-799, October 2012.

[166] Haw C.Y., Mohamed F., Chia C.H., Radiman S., Zakaria S., Huang N.M., Lim H.N., "*Hydrothermal synthesis of magnetite nanoparticles as MRI contrast agents*", Ceramics International, vol. 36(4), pp. 1417-1422, May 2010.

[167] Daou T.J., Pourroy G., Begin-Colin S., Greneche J.M., Ulhaq-Bouillet C., Legare P., Bernhardt P., Leuvrey C., Rogez G., "*Hydrothermal synthesis of monodisperse magnetite nanoparticles*", Chemistry of Materials, vol. 18(18), pp. 4399-4404, September 2006.

[168] Liu Z.L., Wang X., Yao K.L., Du G.H., Lu Q.H., Ding Z.H., Tao J., Ning Q., Luo X.P., Tian D.Y., Xi D., "*Synthesis of magnetite nanoparticles in W/O microemulsion*", Journal of Materials Science, vol. 39(7), 2633-2636, April 2004.

[169] Ha N.T., Hai N.H., Luong N.H., Chau N., Chinh H.D., "*Effects of the conditions of the microemulsion preparation on the properties of Fe_3O_4 nanoparticles*", VNU Journal of Science, Natural Sciences and Technology, vol. 24, pp. 9-15, 2008.

[170] Maity D., Kale S.N., Kaul-Ghanekar R., Xue J.M., Ding J., "*Studies of magnetite nanoparticles synthesized by thermal decomposition of iron(III) acetylacetonate in tri(ethylene glycol)*", Journal of Magnetism and Magnetic Materials, vol. 321(19), pp. 3093-3098, October 2009.

[171] Chin S.F., Pang S.C., Tan C.H., "*Green synthesis of magnetite nanoparticles (via thermal decomposition method) with controllable size and shape*", Journal of Materials and Environmental Science, vol. 2(3), pp. 299-302, June 2011.

[172] Dang F., Enomoto N., Hojo J., Enpuku K., "*Sonochemical synthesis of monodispersed magnetite nanoparticles by using an ethanol-water mixed solvent*", Ultrasonics Sonochemistry, vol. 16(5), pp. 649-654, June 2009.

[173] Marchegiani G., Imperatori P., Mari A., Pilloni L., Chiolerio A., Allia P., Tiberto P., Suber L., "*Sonochemical synthesis of versatile hydrophilic magnetite nanoparticles*", Ultrasonics Sonochemistry, vol. 19(4), pp. 877-882, July 2012.

[174] Cabrera L., Gutierrez S., Menendez N., Morales M.P., Herrasti P., "*Magnetite nanoparticles: electrochemical synthesis and characterization*", Electrochimica Acta, vol. 53(8), pp. 3436-3441, March 2008.

[175] Fajaroh F., Setyawan H., Widiyastuti W., Winardi S., "*Synthesis of magnetite nanoparticles by surfactant-free electrochemical method in an aqueous system*", Advanced Powder Technology, vol. 23(3), pp. 328-333, May 2012.

[176] Carabante I., "*Arsenic (V) adsorption on iron oxide implications for soil remediation and water purification*", Doctoral thesis, Chemical Technology Division of Sustainable Process Engineering Department of Civil, Environmental and Natural Resources Engineering, Luleå University of Technology, SE- 971 87 Luleå Sweden, pp 1-54, October 2012.

[177] Khodabakhshi A., Amin M.M., Mozaffari M., "*Synthesis of magnetite nanoparticles and evaluation of its efficiency for arsenic removal from simulated industrial*

wastewater", Iranian Journal of Environmental Health Science & Engineering, vol. 8(3), pp. 189-200, June 2011.

[178] Yu Y.H., Chang S.C., Wu C.C., "*High arsenic adsorption capacity of sub-4 nanometer magnetite nanoparticles*", 2nd International Conference on Environmental Science and Technology IPCBEE, IACSIT Press, Singapore, vol. 6, pp. 109-113, 2011.

[179] Štefušová K., Václavíková M., Lovás M., Hredzák S., "*Use of magnetic filtration in waste water treatment*", Acta Montanistica Slovaca, vol. 17(1), pp. 81-84, January 2012.

[180] Turk T., Alp I., Deveci H., "*Adsorption of As(V) from water using nanomagnetite*", Journal of Environmental Engineering, vol. 136(4), pp. 399–404, April 2010.

[181] Chowdhury S.R., Yanful E.K., "*Arsenic removal from aqueous solutions by adsorption on magnetite nanoparticles*", Water and Environment Journal, vol. 25(3), pp. 429-437, September 2011.

[182] Chandra V., Park J., Chun Y., Lee J.W., Hwang I.C., Kim K.S., "*Water-dispersible magnetite-reduced graphene oxide composites for arsenic removal*", ACS Nano, vol. 4(7), pp. 3979–3986, July 2010.

[183] An B., Liang Q., Zhao D., "*Removal of arsenic(V) from spent ion exchange brine using a new class of starch-bridged magnetite nanoparticles*", Water Research, vol. 45(5), pp. 1961–1972, February 2011.

[184] Zheng Y.M., Lim S.F., Chen J.P., "*Preparation and characterization of zirconium-based magnetic sorbent for arsenate removal*", Journal of Colloid and Interface Science, vol. 338(1), pp. 22–29, October 2009.

[185] Chowdhury S.R., Yanful E.K., "*Arsenic and chromium removal by mixed magnetite-maghemite nanoparticles and the effect of phosphate on removal*", Journal of Environmental Management, vol. 91(11), pp. 2238-2247, November 2010.

[186] Hari P., Isley A., Medders G., Purser G., "*Kinetics of the remediation of arsenic-contaminated groundwater using nanoscale magnetite particles*", Materials Research Society Symposium Proceedings, vol. 1045, 2008.

[187] Zhang S., Li X.Y., Chen J.P., "*Preparation and evaluation of a magnetite-doped activated carbon fiber for enhanced arsenic removal*", Carbon, vol. 48(1), pp. 60–67, January 2010.

[188] Mishra A.K., Ramaprabhu S., "*Magnetite decorated multiwalled carbon nanotube based supercapacitor for arsenic removal and desalination of seawater*", The Journal of Physical Chemistry C, vol. 114(6), pp. 2583–2590, February 2010.

[189] Beker U., Cumbal L., Duranoglu D., Kucuk I., Sengupta A.K., "*Preparation of Fe oxide nanoparticles for environmental applications: arsenic removal*", Environmental Geochemistry and Health, vol. 32(4), pp. 291–296, August 2010.

[190] Parsons J.G., Lopez M.L., Peralta-Videa J.R., Gardea-Torresdey J.L., "*Determination of arsenic(III) and arsenic(V) binding to microwave assisted hydrothermal synthetically prepared Fe_3O_4, Mn_3O_4, and $MnFe_2O_4$ nanoadsorbents*", Microchemical Journal, vol. 91(1), pp. 100-106, January 2009.

[191] Singh S., Barick K.C., Bahadur D., "*Surface engineered magnetic nanoparticles for removal of toxic metal ions and bacterial pathogens*", Journal of Hazardous Materials, vol. 192(3), pp. 1539-1547, September 2011.

[192] Ohe K., Oshima T., Baba Y., "*Adsorption of arsenic using high surface area magnetites*", Environmental Geochemistry and Health, vol. 32(4), pp. 283-286, August 2010.

[193] Shipley H.J., Engates K.E., Guettner A.M., "*Study of iron oxide nanoparticles in soil for remediation of arsenic*", Journal of Nanoparticle Research, vol. 13(6), pp. 2387-2397, June 2011.

[194] Escudero C., Fiol N., Villaescusa I., Bollinger J.C., "*Arsenic removal by waste metal (hydr)oxide entrapped into calcium alginate beads*", Journal of Hazardous materials, vol. 164(2-3), pp. 533–541, May 2009.

[195] Yean S., Cong L., Yavuz C.T., Mayo J.T., Yu W.W., Kan A.T., Colvin V.L., Tomson M.B., "*Effect of magnetite particle size on adsorption and desorption of arsenite and arsenate*", Journal of Materials Research, vol. 20(12), pp. 3255-3264, December 2005.

[196] Dixit S., Hering J.G., "*Comparison of Arsenic(V) and Arsenic(III) Sorption onto Iron Oxide Minerals: Implications for Arsenic Mobility*", Environmental Science & Technology, vol. 37(18), pp. 4182–4189, September 2003.

[197] Shipley H.J., Khan A.T., Tomson M.B., "*Adsorption of arsenic to magnetite nanoparticles: effect of particle concentration, pH, ionic strength, and temperature*", Environmental Toxicology and Chemistry, vol. 28(3), pp. 509-515, March 2009.

[198] Hai N.H., Phu N.D., "*Arsenic removal from water by magnetic $Fe_{1-x}CoxFe_2O_4$ and $Fe_{1-y}Ni_yFe_2O_4$ nanoparticles*", VNU Journal of Science Mathematics– Physics, vol. 25, pp. 15-19, 2009.

[199] Chunming S., Puls R.W., "*Arsenate and arsenite sorption on magnetite: Relations to groundwater arsenic treatment using zerovalent iron and natural attenuation*", Water, Air, and Soil Pollution, vol. 193(1), pp. 65–78, September 2008.

[200] Pokhrel D., Viraraghavan T., "*Arsenic removal from an aqueous solution by modified A. niger biomass: Batch kinetic and isotherm studies*", Journal of Hazardous Materials, vol. 150(3), pp. 818-825, February 2008.

[201] Mondal P., Balomajumder C., Mohanty B., "*A laboratory study for the treatment of arsenic, iron, and manganese bearing ground water using Fe^{3+} impregnated activated carbon: Effects of shaking time, pH and temperature*", Journal of Hazardous Materials, vol. 144(1-2), pp. 420-426, June 2007.

[202] Zeng L., "*Arsenic adsorption from aqueous solutions on an Fe(III)-Si Binary oxide adsorbent*", Water Quality Research Journal Canada, vol. 39(3), pp. 267-275, April 2004.

[203] Bhaskar P.B., Gupta A.K., Ayoob S., Kandu S., "*Investigation of arsenic (V) removal by modified calcined bauxite*", Colloids and Surfaces A: Physicochemical and Engineering Aspects, vol. 281(1-3), pp. 237-245, June 2006.

[204] Tejedor-Tejedor M.I., Anderson M.A., "*Protonation of phosphate on the surface of goethite as studied by CTR-FTIR and electrophoretic mobility*", Langmuir, vol. 6(3), pp. 602-611, March 1990.

[205] Stumm W., Morgan J., "*Aquatic chemistry: an introduction emphasizing chemical equilibria in natural waters*", Wiley, New York, pp. 481-482, 1970.

[206] Katsoyiannis I.A., Zouboulis A.I., "*Removal of arsenic from contaminated water sources by sorption onto iron-oxide-coated polymeric materials*", Water Research, vol. 36, pp. 5141-5155, 2002.

[207] Shipley H.J., "*Magnetite nanoparticles for removal of arsenic from drinking water*", Doctorate thesis, Rice University, pp. 1-137, 2007.

[208] Dhoble R.M., Lunge S., Bhole A.G., Rayalu S., "*Magnetic binary oxide particles (MBOP): a promising adsorbent for removal of As(III) in water*", Water Research, vol. 45(16), pp. 4769–4781, October 2011.

[209] Sharma Y.C., Uma S., Upadhyay S.N., "*Removal of a cationic dye from wastewaters by adsorption on activated carbon developed from coconut coir*", Energy and Fuels, vol. 23(6), pp. 2983–2988, June 2009.

[210] Namdeo M., Bajpai S.K., "*Investigation of hexavalent chromium uptake by synthetic magnetite nanoparticles*", Electronic Journal of Environmental, Agicultural and Food Chemistry, vol. 7(7), pp. 3082-3094, January 2009.

[211] Tombacz E., Majzik A., Horvat Z.S., Illes E., "*Magnetite in aqueous medium: coating its surface and surface coated with it*", Romanian Reports in Physics, vol. 58(3), pp. 281-286, March 2006.

[212] Kundu S., Gupta A.K., "*As(III) removal from aqueous medium in fixed bed using iron oxide-coated cement (IOCC): experimental and modeling studies*", Chemical Engineering Journal, vol. 129(1-3), pp. 123-131, May 2007.

[213] Chakraborti A.K., Saha K.C., "*Arsenical dermatosis from tube well water in West Bengal*", Indian Journal of Medical Research, vol. 85, pp. 326-334, March 1987.

[214] World Health Organization (WHO), "*International standards for drinking-water*", WHO Press, Geneva, Switzerland, pp. 1-152, 1958.

[215] Food and Agriculuture Organization (FAO), "*Water quality guidelines for maximum crop production*", FAO/United Nations, 1985.

[216] United States Environmental Protection Agency (USEPA), "*National primary drinking water regulations, Arsenic and clarifications to compliance and new source contaminants monitoring*", Final rule, In Federal Register Part VIII, 40 CFR Parts 9, 141 and 142, pp. 6976-7066, January 2001.

[217] Shrestha R,K., Regmi D., Kafle B.P., "*Seasonal variation of arsenic concentration in ground water of Nawalparasi district of Nepal*", International Journal of Applied Sciences and Biotechnology, vol. 2(1), pp. 59-63, 2014.

[218] World Health Organization (WHO), "*International standards for drinking-water*", 2nd edition, WHO Press, Geneva, Switzerland, 1963.

[219] USA Today. Com, "*Arsenic in drinking water seen as threat*", August 2007.

[220] Park H., Myung N.V., Jung H., Choi H., "*As(V) remediation using electrochemically synthesized maghemite nanoparticles*", Journal of Nanoparticle Research, vol. 11(8), pp. 1981-1989, November 2009.

[221] Hinwood A., Bannister R., Shugg A., Sim M., "*Environmental arsenic in rural Victoria: an update*", Water Melbourne Then Artarmon, vol. 25, pp. 34-6, 1998.

[222] Caceras L.V., Grttner E.D., Cantreras R.N., "*Water recycling in arid regions: Chilean case*", Ambio, vol. 21(2), pp. 138-144, April 1992.

[223] British Geological Survey, "*Groundwater studies for arsenic contamination in Bangladesh*", *Phase I: Rapid investigation phase*, Final report, Newcastle upon Tyne: Mott MacDonald Ltd., S1-S12, 1999.

[224] British Geological Survey, "*Arsenic contamination of groundwater in Bangladesh*", Phase 2: editors: Kinniburgh DG, Smedley PL, Keyworth: British Geological Survey, (BGS technical report no. WC/00/19), pp. 231-53, 2001.

[225] Berg M., Tran H.C., Nguyeu T.C., Pham M.V., Scherteuleib R., Giger W., "*Arsenic contamination of groundwater and drinking water in Vietnam: a human health threat*", Environmental Science & Technology, vol. 35(13), pp. 2621-2626, July 2001.

[226] De Sastre M.S.R., Varillas A., Kirschbaum P., "*Arsenic content in water in the northwest area of Argentina. Arsenic in the environment and its incidence on health*", International Seminar Proceedings, Santiago: Universidad de Chile 91-9, 1992.

[227] Matschullat J., Borba R.P., Deschamps E., Figueiredo B.R., Gabrio T., Schwenk M., "*Human and environmental contamination in Iron Quadrangle, Brazil*", Applied Geochemistry, vol. 15(2), pp. 181-190, February 2000.

[228] Armienta M.A., Rodriguez R., Cruz O., "*Arsenic content in hair of people exposed to natural arsenic polluted groundwater in Zimapan Mexico*", Bulletin of Environmental Contamination and Toxicology, vol. 59(4), pp. 583-589, October 1997.

[229] Gomez-Arroyo S., Armienta M.A., Cortes-Eslava J., Villalobos-Pietrini R., "*Sister chromatid exchanges in Viciafaba induced by arsenic contaminated drinking water from Zimapan, Hidalgo, Mexico*", Mutatation Research/Genetic Toxicology and Environmental Mutagenesis, vol. 394(1-3), pp. 1-7, November 1997.

[230] Diaz-Barriga F., Santos M.A., Mejia J.J., Batres L., Yanez L., Carrizales L., Vera E., del Razo L.M., Cebrian M.E., "*Arsenic and cadmium exposure in children living near a smelter complex in San Luis Potosi, Mexico*", Environmental Research, vol. 62(2), pp. 242-250, August 1993.

[231] Grantham D.A., Jones J.F., "*Arsenic contamination of water wells in Nova Scotia*", Journal of American Water Works Association, vol. 69(12), pp. 653-657, December 1977.

[232] Samanta G., Chowdhury T.R., Mandal B.K., Chowdhury U.K., Basu G.K., Chanda C.R., Lodh D., Chakraborti D., "*Flow injection hydride generation atomic absorption spectrometery for determination of arsenic in water and biological samples from arsenic-affected districts of West Bengal, India and Bangladesh*", Michrochemical Journal, vol. 62(1), pp. 174-191, May 1999.

[233] Chakraborti D., Basu G.K., Biswas B.K., Chowdhury U.K., Rahman M.M., Paul K., Chowdhury T.R., Chanda C.R., Lodh D., "*Characterization of arsenic bearing sediments in Gangetic delta of West Bengal-India*", In: Chappell W.R., Abernathy C.O., Calderon R.L., editors, Arsenic exposure and health effects, Elsevier, Amsterdam, Lausanne, New York, Oxford, Tokyo, pp 27–52, 2001.

[234] Neriowlm, Pre-seminar proceedings from national seminar on arsenic and fluoride contamination in groundwater organized by North Eastern Regional Institute of Water and Land Management, Tezpur, Assam, pp. 1-10, 2004.

[235] Mukherjee A., Sengupta M.K., Hossain M.A., Ahamed S., Das B., Nayak B., Lodh D., Rahman M.M., Chakraborti D., "*Arsenic contamination in groundwater: A global perspective with emphasis on the Asian scenario*", Journal of Health, Population and Nutrition, vol. 24(2), pp. 142-163, June 2006.

[236] Southwick J.W., Western A.E., Beck M.M., Whitney T., Isaacs R., Petajan J., Hansen C.D., "*An epidemiological study of arsenic in drinking water in Millard county, Utah*", In: Leaderer W.H., Robert J.F., editors, Arsenic:industrial, biomedical, environmental perspectives, Van Nostrand Reinhold, New York, pp. 210-225, 1983.

[237] Pfeifer H.R, Zobrist J., "*Arsenic in drinking waters—also a problem in Switzerland*", EAWAG Newsletter, vol. 53, pp. 15- 17, 2002.

[238] Hsu J.C., Lin C.J., Liao C.H., Chen S.T., "*Evaluation of the multiple-ion competition in the adsorption of As(V) onto reclaimed iron-oxide coated sands by fractional factorial design*", Chemosphere, vol. 72(7), pp. 1049-1055, July 2008.

[239] Gupta A., Mohammed Y., Sankararmakrishnan N., "*Chitosan- and Iron-chitosan-coated sand filters: a cost-effective approach for enhanced arsenic removal*", Industrial & Engineering Chemistry Research, vol. 52(5), pp. 2066-2072, February 2013.

[240] Elwakeel K.J. "*Removal of arsenate from aqueous media by magnetic chitosan resin immobilized with molybdate oxoanions*", International Journal of Environmental Science and Technology, vol. 11(4), pp. 1051-1062, May 2014.

[241] Rahim M., Haris M.R.H.M., "*Application of biopolymer composites in arsenic removal from aqueous medium: a review*", Journal of Radiation Research and Applied Sciences, vol. 8(2), pp. 255-263, April 2015.

[242] Zhang K., Dwivedi V., Chi C., Wu J., "*Graphene oxide/ferric hydroxide composites for efficient arsenate removal from drinking water*", Journal of Hazardous Materials, vol. 182(1-3), pp. 162-168, October 2010.

[243] Kemp K.C., Seema H., Saleh M., Le H., Mahesh K., Chandra V., Kim K.S., *"Environmental applications using graphene composites: water remediation and gas adsorption*", Nanoscale, vol. 5(8), pp. 3149-3171, April 2013.

[244] Das G.K., Bonifacio C.S., Rojas J.D., Liu K., Benthem K.V., Kennedy L.M., "*Ultra-long magnetic nanochains for highly efficient arsenic removal from water*", Journal of Materials Chemistry A, vol. 2(32), pp. 12974-12981, August 2014.

[245] Nishida S., Takesoe S., Yamasaki Y., Nakahira A., "*Attempt of arsenic removal in wasted water by inorganic materials*", In: 14th International Conference on the properties of Water and Steam in Kyoto, Japan, pp. 387-390, 2004.

[246] Lagergren S., "*About the theory of so-called adsorption of soluble substance*", Kungliga Svenska Vetenskapsakademiens Handlingar, vol. 24(4), pp. 1–39, 1898.

[247] Ho Y.S., McKay G., "*The kinetics of sorption of divalent metal ions onto sphagnum moss peat*", Water Research, vol. 34(3), pp. 735-742, February 2000.

[248] Ho Y.S., McKay G., "*Kinetic models for the sorption of dye from aqueous solution by wood*", Process Safety and Environmental Protection, vol. 76(2), pp. 183–191, May 1998.

[249] Qiu H., Lu L.V., Pan B., Zhang Q., Zhang W., Zhang Q., "*Critical review in adsorption kinetic models*", Journal of Zhejiang University Science A, vol. 10(5), pp. 716-724, May 2009.

[250] Weber W.J., Morris J.C., "*Kinetics of adsorption on carbon from solution*", Journal of Sanitary Engineering Division, American Society Civil Engineering, vol. 89(1), pp. 31-60, 1963.

[251] Freundlich H.M.F.Z., "*Stoechiometrie und Verwandtschaftslehre*", Zeitschriftfuer Physikalische Chemie, vol. 57, pp. 385-470, 1906.

[252] Langmuir I., "*The adsorption of gases on plane surfaces of glass, mica and platinum*", Journal of American Chemical Society, vol. 40(9), pp. 1361-1403. September 1918.

[253] Wang X., Guo Y., Yang L., Han M., Zhao J., Cheng X., "*Nanomaterials as sorbents to remove heavy metal ions in wastewater treatment*" Journal of Environmental & Analytical Toxicology, vol. 2(7), pp. 154(1)–154(7), August 2012.

[254] Bulut Y., Gozubenli N., Aydin H., "*Equilibrium and kinetics studies for adsorption of direct blue 71 from aqueous solution by wheat shells*", Journal of Hazardous Materials, vol. 144(1-2), pp. 300-306, June 2007.

[255] Stat Trek, Statistics dictionary, "*Coefficient of determination*", Internet, Available: http://stattrek.com/statistics/dictionary.aspx?definition=coefficient of determination.

[256] Sokal R.R, Rohlf F.J., "*The principles and practice of statistics in biological research*", 3rd edition, W.H. Freeman and Company, New York, USA, pp. 1-871, 1995.

[257] Ren Z., Zhang G., Chen J.P., "*Adsorptive removal of arsenic from water by an iron-zirconium binary oxide adsorbent*", Journal of Colloid and Interface Science, vol. 358(1), pp. 230-237, June 2011.

[258] Kundu S., Gupta A.K., "*Adsorptive removal of As(III) from aqueous solution using iron oxide coated cement (IOCC): evaluation of kinetics, equilibrium and thermodynamic models*", Separation and Purification Technology, vol. 51(2), pp. 165–172, September 2006.

[259] Ranjan D., Talat M., Hasan S.H., "*Biosorption of arsenic from aqueous solution using agriculture residue rice polish*", Journal of Hazardous Materials, vol. 166(2-3), pp. 1050-1059, July 2009.

[260] Pandey P.K., Choubey S., Verma Y., Pandey M., Chandrashekhar K., "*Biosorptive removal of arsenic from drinking water*", Bioresource Technology, vol. 100(2), pp. 634–637, January 2009.

[261] Kaczala F., Marques M., Hogland W., "*Lead and vanadium removal from a real industrial wastewater by gravitational settling/sedimentation and sorption onto Pinussylvestris sawdust*", Bioresource Technology, vol. 100(1), pp. 235-243, January 2009.

[262] Fan T., Liu Y., Feng B., Zeng G., Yang C., Zhou M., Zhou H., Tan Z., Wang X., "*Biosorption of cadmium(II), zinc(II) and lead(II) by Penicillium simplicissimum: isotherms, kinetics and thermodynamics*", Journal of Hazardous Materials, vol. 160(2-3), pp. 655-661, December 2008.

[263] De Rome L., Gadd G.M., "*Copper adsorption by Rhizopus arrhizus, Cladosorium resinae and Penicillium italicum*", Applied Microbiology and Biotechnology, vol. 26(1), pp. 84-90, April 1987.

[264] Das B., Devi R.R., Umlong I.M., Borah K., Banerjee S., Talukdar A.K., "*Arsenic (III) adsorption on iron acetate coated activated alumina: thermodynamic, kinetics and equilibrium approach*", Journal of Environmental Health Science and Engineering, vol. 11(1), pp. 42(1)-42(10), December 2013.

[265] Singh A.P., Srivastava K.K., Shekhar H., "*Arsenic (III) removal from aqueous solutions by mixed adsorbent*", Indian Journal of Chemical Technology, vol. 16, pp. 136-141, March 2009.

[266] Lekic B.M., Markovic D.D., Rajakovic-Ognjanovic V.N., Yukic A.R., Rajakovic L.V., "*Arsenic removal from water using industrial by-products*", Journal of Chemistry, vol. 2013(1), pp. 121024(1)-121024(9), August 2013.

[267] Ergül B., Bektaş N., Öncel M.S., "*The use of manganese oxide minerals for the removal arsenic and selenium anions from aqueous solutions*", Energy and Environmental Engineering, vol. 2(5), pp. 103-112, 2014.

[268] Kuriakose S., Singh T.S., Pant K.K., "*Adsorption of As(III) from aqueous solution onto iron oxide impregnated activated alumina*", Water Quality Research Journal Canada, vol. 39(3), pp. 258-266, 2004.

[269] Yusof N.Z., Kassim M.A., Ismail R., Yusoff A.R.M., "*Development of simple and cost effective method for arsenic(III) removal*", Iranica Journal of Energy & Environment, vol. 5(3), pp. 287-294, August 2014.

[270] Danish M.I., Qazi I.A.,Zeb A., Habib A., Awan M.A., Khan Z., "*Arsenic removal from aqueous solution using pure and metal-doped titania nanoparticles coated on glass beads: adsorption and column studies*", Journal of Nanomaterials, vol. 2013(1), pp. 873694(1)- 873694(17), 2013.

[271] Luther S., Borgfeld N., Kim J., Parsons J.G., "*Removal of arsenic from aqueous solution: a study of the effects of pH and interfering ions using iron oxide nanomaterials*", Michrochemical Journal, vol. 101, pp. 30-36, March 2012.

[272] Lenoble C., Laclautre C., Deluchat V., Serpaud B., Bollinger J.C., "*Arsenic removal by adsorption on iron (III) phosphate*", Journal of Hazardous Materials, vol. 123(1-3), pp. 262-268, August 2005.

[273] United States Environmental Protection Agency (USEPA), "*Arsenic occurence in public drinking water supplies*", Rep. No. EPA-815-R-00-023,USEPA, Washington, pp. 156, December 2000.

[274] Nordstrom D.K., Archer D.G., "*Arsenic thermodynamic data and environmental geochemistry*", In: Cai Y., Braids O.C., editors, Biogeochemistry of environmentally important trace elements, Oxford University Press, Oxford, United Kingdom, pp. 1–25, 2003.

[275] Maji S.K., Pal M., Pal T., Adak A., "*Adsorption thermodynamic of arsenic on laterite soil*", Journal of Surface Science and Technology, vol. 23(3-4), pp. 161–176, 2007.

[276] Vaishya R.C., Gupta S.K., "*Modeling arsenic(V) removal from water by sulphate modified iron-oxide coated sand (SMIOCS)*", Separation Science and Technology, vol. 39(3), pp. 645-666, 2005.

[277] Zhang W., Singh P., Paling E., Delides S., "*Arsenic removal from contaminated water by natural iron ores*", Minerals Engineering, vol. 17(4), pp. 517-524, April 2004.

[278] Altundogan H.S., Altundogan S., Tumen F., Bildik M., "*Arsenic adsorption from aqueous solutions by activated red mud*", Waste Management, vol. 22(3), pp. 357-363, June 2002.

[279] Genc H., Tjell J.C., McConchie D., Schuiling O., "*Adsorption of arsenate from water using neutralized red mud*", Journal of Colloid Interface Science, vol. 264(2), pp. 327-334, August 2003.

[280] Yusof A.M., Malek N.A.N.N., "*Removal of Cr(VI) and As(V) from aqueous solutions by HDTMA-modified zeolite Y*", Journal of Hazardous Materials, vol. 162(2-3), pp. 1019-1024, March 2009.

[281] Fuhrman H.G., Bregnhoj H., McConchie D., "*Arsenate removal from water using sand-red mud columns*", Water Research, vol. 39(13), pp. 2944–2954, August 2005.

[282] Turk T., Alp I., Deveci H., "*Adsorption of As(V) from water using Mg-Fe-based hydrotalcite (FeHT)*", Journal of Hazardous Materials, vol. 171(1-3), pp. 665–670, November 2009.

[283] Myers L., "*Thermodynamics of adsorption*", In: Letcher T.M., editor, Chemical thermodynamics for industry, Royal Society of Chemistry, Cambridge, UK, pp. 243-252, 2004.

[284] Saha P., Chowdhury S., "*Insight into adsorption thermodynamics*", In: Tadashi M., editor, Thermodynamics, InTech Europe, pp. 349-364, January 2011.

[285] Ruthven D., "*Principles of adsorption and adsorption processes*", John Wiley & Sons, New York, 1984.

[286] Sekar M., Sakthi V., Rengaraj S., "*Kinetics and equilibrium adsorption study of lead(II) onto activated carbon prepared from coconut shell*", Journal of Colloid and Interface Science, vol. 279(2), pp. 307-313, November 2004.

[287] Bulut Y., Tez Z., "*Adsorption studies on ground shells of hazelnut and almond*", Journal of Hazardous Materials, vol. 149(1), pp. 35–41, October 2007.

[288] Al-Anber M.A., "*Thermodynamics approach in the adsorption of heavy metals*", In: Pirajain J.C.M., editor, Thermodynamics-interaction studies - solids, liquids and gases, InTech, Europe, pp. 1-918, November 2011.

[289] Han R., Lu Z., Zou W., Daotong W., Shi J., Jiujun Y., "*Removal of copper(II) and lead(II) from aqueous solution by manganese oxide coated sand: II. Equilibrium study and competitive adsorption*", Journal of Hazardous Materials, vol. 137(1), pp. 480–488, September 2006.

[290] Sumathi T., Alagumuthu G., "*Adsorption studies for arsenic removal using activated Moringa oleifera*", International Journal of Chemical Engineering, Vol. 2014, pp. 430417(1)-430417(6), March 2014.

[291] Bharathi K.S., Ramesh S.P.T., "*Fixed-bed column studies on biosorption of crystal violet from aqueous solution by Citrullus lanatus rind and Cyperus rotundus*", Applied Water Science, vol. 3(4), pp. 673–687, December 2013.

[292] Benefield L.D., Judkins J.F., Weand B.L., "*Process chemistry for water and wastewater treatment*", Prentice Hall Inc., New Jersey, 1982.

[293] Maji S.K., Kao Y.H., Wang C.J., Lu G.S., Wu J.J., Liu C.W., "*Fixed bed adsorption of As(III) on iron-oxide coated natural rock (IOCNR) and application to real arsenic-bearing groundwater*", Chemical Engineering Journal, vol. 203, pp. 285-293, September 2012.

[294] Maji S.K. Pal A., Pal T., Adak A., "*Modeling and fixed bed column adsorption of As(III) on laterite soil*", Separation and Purification Technology, vol. 56(3), pp. 284–290, September 2007.

[295] Nguyen V.L., Chen W.H., Young T., Darby J., "*Effect of interferences on the breakthrough of arsenic: rapid small scale column tests*", Water Research, vol. 45(14), pp. 4069–4080, August 2011.

[296] Wei Y.T., Zheng Y.M., Chen J.P., "*Uptake of methylated arsenic by a polymeric adsorbent: process performance and adsorption chemistry*", Water Research, vol. 45(6), pp. 2290–2296, March 2011.

[297] Yahaya N.K.E.M., Abustan I., Latiff M.F.P.M., Bello O.S., Ahmad M.A., "*Fixed-bed column study for Cu (II) removal from aqueous solutions using rice husk based activated carbon*", International Journal of Engineering & Technology, Vol. 11(1), pp. 186-190, February 2011.

[298] Gupta S., Babu B.V., "*Experimental investigations and theoretical modeling aspects in column studies for removal of Cr(VI) from aqueous solutions using activated tamarind seeds*", Journal of Water Resource and Protection, vol. 2(8), pp. 706-716, August 2010.

[299] Thomas H.C., "*Heterogeneous ion exchange in a flowing system*", Journal of American Chemical Society, vol. 66(10), pp. 1664-1666, October 1944.

[300] Yoon Y.H., Nelson J.H., "*Application of gas adsorption kinetics, I. A theoretical model for respirator cartridge service life*", American Industrial Hygiene Association Journal, vol. 45(8), pp. 509-516, August 1984.

LIST OF PUBLICATIONS

International Journals

1. **Sarita Kango**, Rajesh Kumar, (2016) "Low-cost magnetic adsorbent for As(III) removal from water: adsorption kinetics and isotherms", Environmental Monitoring and Assessment, 188:60 (14 pp.).
2. **Sarita Kango**, Rajesh Kumar, (2016) "Magnetite nanoparticles coated sand for arsenic removal from drinking water", Environmental Earth Sciences, 75:381 (12 pp.).

Conference Proceeding

1. **Sarita Kango**, Rajesh Kumar, (2015) "Magnetite nanoparticles coated glass wool for As(V) removal from drinking water", AIP Conference Proceeding, 1675:0300241-0300244.

Book Chapter

1. **Sarita Kango**, Rajesh Kumar, (2015) "Efficient removal of arsenic (III) from drinking water by Fe_3O_4 nanoparticles coated sand: Time dependent removal study", In: Nanotechnology: Novel Perspectives and Prospects (pp.), Publisher: Tata-McGraw Hill, New Delhi (India), Editors: Bhupinder Singh, Anupama Kaushik, S. K. Meheta, S. K. Tripathi.

Poster Presentations in Conferences

1. **Sarita Kango**, Rajesh Kumar, "Synthesis and characterization of magnetic adsorbent for arsenite removal from aqueous solution", Presented in 2nd National Conference on Multifunctional Advanced Materials (MAM-2014) held on 11-13 June, 2014 at Shoolini University, Solan, Himachal Pradesh, India.
2. **Sarita Kango**, Rajesh Kumar, "Kinetics study of As(III) removal from drinking water by magnetic adsorbent coated on glass wool", 2nd International Convention of Engineering and Management (ICEM) held on 4-5 April 2015 at JUIT Waknaghat, Solan, India.

3. **Sarita Kango**, Rajesh Kumar, “Effect of temperature on As(III) removal efficiency by using magnetite nanoparticles coated sand”, Presented in International Conference on Science: Engineering Scenario & Future Challenges (SESFC) held on April 11-12, 2016 at Hotel Inclover, Dharmshala, India.